NAVAL POSTGRADUATE SCHOOL
Monterey, California

THESIS

EXPERIMENTAL DEVELOPMENT OF TUBESIDE
HEAT TRANSFER CORRELATIONS FOR LAMINAR
FLOW WITH AND WITHOUT INSERTS

by

Joseph D. Guido

September 1992

Co-Advisor: Paul J. Marto
Co-Advisor: Stephen B. Memory

UNCLASSIFIED
_____
SECURITY CLASSIFICATION OF THIS PAGE

REPORT DOCUMENTATION PAGE	Form Approved OMB No. 0704-0188

1a. REPORT SECURITY CLASSIFICATION UNCLASSIFIED	1b. RESTRICTIVE MARKINGS

2a. SECURITY CLASSIFICATION AUTHORITY	3. DISTRIBUTION/AVAILABILITY OF REPORT
2b. DECLASSIFICATION/DOWNGRADING SCHEDULE	Approved for public release; distribution is unlimited.

4. PERFORMING ORGANIZATION REPORT NUMBER(S)	5. MONITORING ORGANIZATION REPORT NUMBER(S)

6a. NAME OF PERFORMING ORGANIZATION Naval Postgraduate School	6b. OFFICE SYMBOL (If applicable) 34	7a. NAME OF MONITORING ORGANIZATION Naval Postgraduate School

6c. ADDRESS (City, State, and ZIP Code) Monterey, California 93943-5000	7b. ADDRESS (City, State, and ZIP Code) Monterey, California 93943-5000

8a. NAME OF FUNDING/SPONSORING ORGANIZATION	8b. OFFICE SYMBOL (If applicable)	9. PROCUREMENT INSTRUMENT IDENTIFICATION NUMBER

8c. ADDRESS (City, State, and ZIP Code)	10. SOURCE OF FUNDING NUMBERS

	PROGRAM ELEMENT NO.	PROJECT NO.	TASK NO.	WORK UNIT ACCESSION NO.

11. TITLE (Include Security Classification)
EXPERIMENTAL DEVELOPMENT OF TUBESIDE HEAT TRANSFER CORRELATIONS FOR LAMINAR FLOW WITH AND WITHOUT INSERTS

12. PERSONAL AUTHOR(S)
Guido, Joseph D.

13a. TYPE OF REPORT Master's Thesis	13b. TIME COVERED FROM ____ TO ____	14. DATE OF REPORT (Yr., Mo., Day) 1992, June 17	15. PAGE COUNT 177

16. SUPPLEMENTARY NOTATION: The views expressed in this thesis are those of the author and do not reflect the official policy or position of the Department of Defense or the U.S. Government.

17.	COSATI CODES		18. SUBJECT TERMS (Continue on reverse if necessary and identify by block number)
FIELD	GROUP	SUB-GROUP	Laminar Flow, Tubeside Heat Transfer, Twisted Tape and HEATEX Inserts

19. ABSTRACT (Continue on reverse if necessary and identify by block number)
An experimental study of laminar flow heat transfer of an ethylene glycol/water mixture in an electrically heated horizontal tube using wire mesh (HEATEX) and twisted tape inserts was investigated. Twelve thermocouples, inserted in the tube wall at four longitudinal locations, enabled a mean inside experimental heat-transfer coefficient to be accurately measured. A constant wall heat flux boundary condition was placed on the wall by wrapping six 200 W flexible heater tapes tightly around the tube. The ethylene glycol/water mixture provided a coolant Reynolds number between 200-5000 and a Prandtl number between 30-140. Two smooth inside diameters and a roped tube profile were tested with and without the inserts. Heat-transfer correlations for tubes without inserts were developed and compared with theory for both thermally and hydrodynamically developing flow. Correlations were also developed for the two types of inserts. Nusselt numbers for fully developed flow were found to be a function of Reynolds and Prandtl numbers for the wire mesh insert and a function of tape twist ratio, Reynolds and Prandtl numbers for the twisted tape insert. Heat transfer enhancements of over 7 for the wire mesh insert and over 4 for the twisted tape insert at high Reynolds numbers were obtained over the empty tube. By using these correlations in conjunction with earlier obtained refrigerant condensation data (using the same tubes, inserts, and coolant), more accurate values of the outside condensation heat-transfer coefficients were obtained.

20. DISTRIBUTION/AVAILABILITY OF ABSTRACT [XX] UNCLASSIFIED/UNLIMITED [ ] SAME AS RPT. [ ] DTIC USERS	21. ABSTRACT SECURITY CLASSIFICATION Unclassified

22a. NAME OF RESPONSIBLE INDIVIDUAL Professor P.J. Marto	22b. TELEPHONE (Include Area Code) (408) 646-3382	22c. OFFICE SYMBOL MX

DD Form 1473, JUN 86   *Previous editions are obsolete.*   SECURITY CLASSIFICATION OF THIS PAGE

S/N 0102-LF-014-6603   UNCLASSIFIED

i

Approved for public release; distribution is unlimited.

EXPERIMENTAL DEVELOPMENT OF TUBESIDE HEAT TRANSFER CORRELATIONS FOR LAMINAR FLOW WITH AND WITHOUT INSERTS

by

Joseph D. Guido
Lieutenant Commander, United States Navy
B.S.N.E., University of Florida, 1981

Submitted in partial fulfillment of the
requirements for the degree of
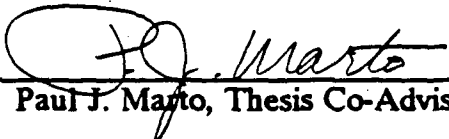
MASTER OF SCIENCE MECHANICAL ENGINEERING

from the

NAVAL POSTGRADUATE SCHOOL
September 1992

Author: _____
Joseph D. Guido

Approved by: _____
Paul J. Marto, Thesis Co-Advisor

_____
Stephen B. Memory, Thesis Co-Advisor

_____
Anthony J. Healey, Chairman
Department of Mechanical Engineering

ii

ABSTRACT

An experimental study of laminar flow heat transfer of an ethylene glycol/water mixture in an electrically heated horizontal tube using wire mesh (HEATEX) and twisted tape inserts was investigated. Twelve thermocouples, inserted in the tube wall at four longitudinal locations, enabled a mean inside experimental heat-transfer coefficient to be accurately measured. A constant wall heat flux boundary condition was placed on the wall by wrapping six 200 W flexible heater tapes tightly around the tube. The ethylene glycol/water mixture provided a coolant Reynolds number between 200-5000 and a Prandtl number between 30-140. Two smooth inside diameters and a roped tube profile were tested with and without the inserts. Heat-transfer correlations for tubes without inserts were developed and compared with theory for both thermally and hydrodynamically developing flow. Correlations were also developed for the two types of inserts. Nusselt numbers for fully developed flow were found to be a function of Reynolds and Prandtl numbers for the wire mesh insert and a function of tape twist ratio, Reynolds and Prandtl numbers for the twisted tape insert. Heat transfer enhancements of over 7 for the wire mesh insert and over 4 for the twisted tape insert at high Reynolds numbers were obtained over the empty tube. By using these correlations in conjunction with earlier obtained refrigerant condensation data (using the same tubes, inserts, and coolant), more accurate values of the outside condensation heat-transfer coefficients were obtained.

TABLE OF CONTENTS

vi

viii

LIST OF TABLES

LIST OF FIGURES

NOMENCLATURE

A	area, m^2
c_p	specific heat, J/kg K
D	diameter, m
Gz	Graetz number
h	heat transfer coefficient, W/m^2K
H	pitch for 180° rotation of tape
I	current, amps
k	thermal conductivity, $W/m\ K$
L	length, m
LMTD	log mean temperature difference
$\dot{m}$	mass flow rate, kg/s
Nu	Nusselt number
P	perimeter, m or Power, W
Pr	Prandtl number
$\dot{q}$	heat transfer rate, W
q''	heat flux, W/m^2
r	radius, m
R	electrical resistance, ohms
R_w	wall resistance, K/W

Re	Reynolds number
Re_s	Reynolds number for swirl flow
T	Temperature, K
t	fin thickness, m
U	overall heat transfer coefficient, $W/m^2 K$
u	velocity component in x direction, m/s
v	velocity component in y direction, m/s
V	velocity, m/s or Voltage, volts
x^*	dimensionless axial coordinate, (x/D)/(Re Pr)
y	twist ratio, H/D

Greek Symbols

δ	tape thickness, m or boundary layer thickness
ϵ	heat transfer enhancement ratio
μ	dynamic viscosity, kg/m s
ν	kinematic viscosity, m^2/s
ρ	density, kg/m^3

Subscripts

c	coolant or cross section
D	tube diameter
fd	fully developed
f	fin
h	hydrodynamically

HL	heated length
i	inside or inlet
lam	laminar
m	mean
o	outside or outlet
s	surface
sat	saturation
t	thermally
t/c	thermocouple
x	local
w	wall

I. INTRODUCTION

A. BACKGROUND

With the increasing complexity of shipboard weapons and combat systems used aboard United States Naval vessels, the need for more energy efficient, lightweight, and high capacity refrigeration, air conditioning, and chilled water systems has grown tremendously. One way to meet this need is to redesign the refrigeration condenser. In redesigning these condensers, changes in condenser tube material can be combined with various heat transfer enhancement methods to achieve a lighter weight, more efficient condenser tube.

Emphasis on refrigerant condensation research reached a much higher level of importance due to the pressing environmental issues of ozone depletion and global warming. In September 1987, an international conference was held in Montreal, Canada, in which 24 nations representing the United Nation's Environment Program (UNEP), signed the Montreal Protocol on Substances that Deplete the Ozone Layer. This agreement called for a near term freeze on the production and consumption of chlorofluorocarbons (CFCs), · the major contributor to ozone depletion [Ref. 1]. In August 1988, the Environmental Protection Agency (EPA) adopted the regulations of the Montreal Protocol under the Clean Air Act [Ref. 2]. These regulations required a freeze in both production and consumption of CFC-11,

12, 113, 114 and 115 at 1986 levels. The U.S. Navy currently uses CFC-12 and CFC-114 in its shipboard air conditioning and refrigeration systems. In June 1990 at a progress meeting held in London, England, UNEP delegates agreed to even larger reductions, calling for a 50% reduction by 1995, 85% reduction by 1997, and for CFCs to be totally phased out by the year 2000 [Ref. 3]. In the spring of 1992, President Bush moved up the CFC phase out deadline to 1995.

Because of the Navy's commitment to the CFC phase out policy and the increasing need for lighter weight, more efficient refrigeration systems, refrigerant condensation research has surfaced to the forefront of Naval Research.

B. REFRIGERANT CONDENSATION RESEARCH AT NPS

In order to examine heat transfer characteristics of various condenser tube designs and alternative refrigerants, a condenser/evaporator test platform was constructed at the Naval Postgraduate School. Construction was begun by Zebrowski [Ref. 4] and completed by Mabrey [Ref. 5] in 1988. The test platform, shown in Figure 1.1, consisted of an evaporator and a condenser section with an associated ethylene glycol/water mixture coolant system.

The evaporator section was designed so that in addition to supplying the refrigerant vapor to the condenser, it could also be utilized to conduct bundle boiling experiments. The condenser section consisted mainly of four instrumented condenser tubes and a series of auxiliary condenser coils used to control pressure in the apparatus. Details of design, construction and operation of the condenser/evaporator

test platform are provided by Zebrowski [Ref. 4], Mabrey [Ref. 5] and Mazzone [Ref. 6].

Unlike a typical vapor compression refrigeration system used aboard ships, the test platform at NPS lacked a compressor between the evaporator and the condenser. This compressor is normally required to increase the pressure (and hence temperature) of the refrigerant vapor sufficiently enough so that it can give up its latent heat to the ambient sea water, the primary coolant. Because there was no compressor in the NPS test platform, the condenser must operate at the saturation conditions of the evaporator. Therefore, a much colder coolant, a refrigerated ethylene glycol/water mixture, was needed to condense the vapor, leading to laminar flow conditions within the condenser tubes. This in turn leads to poor heat transfer due to a large inside thermal resistance.

The primary objective of the condensation experiments of Mabrey [Ref. 5] and Mazzone [Ref. 6] was to accurately determine outside heat transfer coefficients. Briefly, this was accomplished by first determining the heat transfer rate to the coolant by:

$$\dot{q} = \dot{m} \, c_p \, \Delta T \tag{1.1}$$

where $\dot{m}$ is the coolant mass flow rate and ΔT the coolant temperature rise.
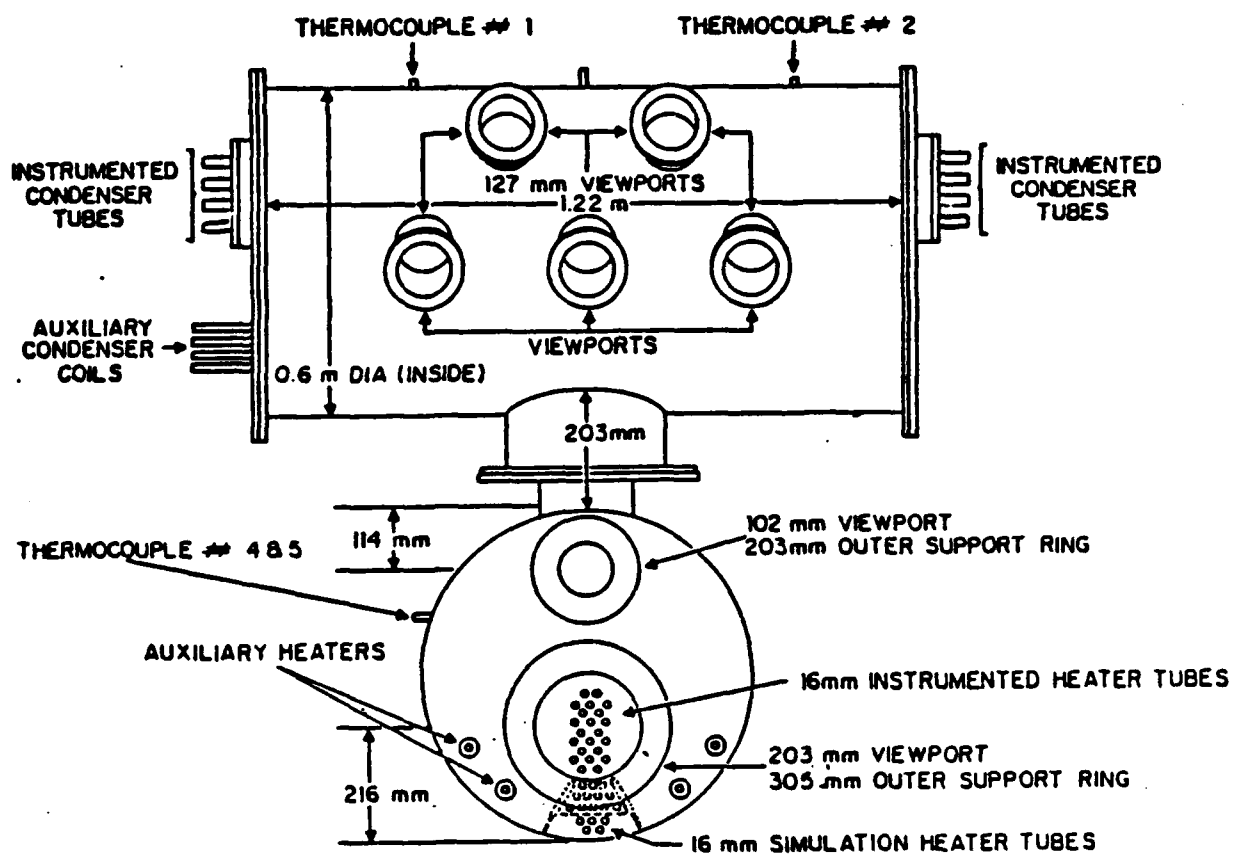
Figure 1.1 NPS Evaporator/Condenser Refrigeration Apparatus.

The overall heat transfer coefficient, U_o, could then be determined by:

$$U_o = \frac{\dot{q}}{A_o \, LMTD} \qquad (1.2)$$

where A_o is the outside surface area of the tube and LMTD is the log mean temperature difference, defined as:

$$LMTD = \frac{\Delta T}{\ln \left[\dfrac{T_{sat} - T_{in}}{T_{sat} - T_{out}} \right]} \qquad (1.3)$$

The overall heat transfer coefficient can also be thought of in terms of a sum of thermal resistances. The overall thermal resistance is given by:

$$\frac{1}{U_o A_o} = \frac{1}{h_o A_o} + R_w + \frac{1}{h_i A_i} \qquad (1.4)$$

The overall thermal resistance can be measured experimentally; the wall resistance, R_w, is known, and the inside resistance can be determined from a chosen correlation. Therefore, the outside heat transfer coefficient, h_o, can be calculated by:

$$h_o = \frac{1}{\dfrac{1}{U_o} - R_w A_o - \dfrac{1}{h_i} \left(\dfrac{A_o}{A_i} \right)} \qquad (1.5)$$

There is one major drawback to this method. As mentioned earlier, when laminar flow heat transfer conditions exist within the condenser tube, it leads to poor heat transfer performance and therefore represents the dominant thermal resistance within the condenser. This inside resistance then becomes the controlling factor in

5

the determination of the outside heat transfer coefficient. Indeed, if the inside resistance is a large proportion of the overall resistance, then the accuracy of the calculated outside heat transfer coefficient becomes uncertain. Therefore, the accuracy of the outside heat transfer coefficient relies heavily on an accurate correlation to determine h_i.

An alternative is to reduce the inside controlling resistance by augmenting the inside heat-transfer coefficient. Augmentation techniques for lowering the inside thermal resistance primarily focus on repeatedly bringing fresh fluid from the coolant bulk stream to the heated inside surface. This results in breaking up the thermal boundary layer and thereby reducing the thermal resistance. The technique utilized in the NPS condensation experiments to break up this thermal boundary layer made use of two types of inserts, a twisted tape insert and a wire mesh (HEATEX) insert. These inserts and their use will be discussed in more detail in later chapters.

The results of condensation experiments conducted by Mazzone [Ref. 6] show signs of inaccuracies related to the choice and accuracy of the inside heat transfer coefficient correlation. For example, in attempting to determine the outside heat transfer coefficient for a smooth tube with no insert, Mazzone found that the correlation used to determine the inside resistance yielded values that were greater than the actual measured overall resistance! Obviously, no sensible values of h_o could be determined. Similar problems existed (but to a lesser extent, due to the greatly reduced inside thermal resistance) when using various types of inserts. Mazzone concluded that "... laminar flow correlations for twisted tape, HEATEX, and no

6

insert conditions must be developed which have better accuracy than those used ... allowing for more accurate determination of outside heat transfer coefficients." Therefore, the determination of accurate inside heat transfer coefficients is paramount in the final outcome of the refrigeration condensation project.

C. OBJECTIVES

The main focus of this thesis was therefore to accurately determine inside heat transfer coefficients in support of refrigerant condensation experiments being conducted at NPS.

The specific objectives of this study were to:

1. Design and build a test apparatus to accurately determine inside heat transfer coefficients for the same tubes and inserts used in the condensation experiments.

2. Develop correlations for inside heat transfer coefficients under laminar flow conditions both with and without inserts.

3. Using the correlations mentioned above, reprocess existing condensation data to determine more accurate values of the outside heat transfer coefficients.

II. LITERATURE SURVEY

A. INTRODUCTION

Laminar fully developed and developing forced convection flows have been analyzed in great detail for various boundary conditions. The study of heat transfer in laminar flow through a closed duct was first made by Graetz [Ref. 7] in 1883 and later by Nusselt [Ref. 8] in 1910. An excellent and thorough study of the theoretical development (with both analytical and experimental solutions) for various laminar forced convection internal flow boundary conditions is given by Shah and London [Ref. 9].

This survey will be concerned with laminar flow heat transfer in fully developed and developing flows subjected to both a constant wall temperature and constant heat flux boundary condition. It will also summarize some of the augmentation techniques used to enhance tubeside laminar flow heat transfer and discuss the details involved when using twisted tape and wire mesh inserts to enhance inside heat transfer.

B. LAMINAR FLOW IN CIRCULAR DUCTS

1. Boundary Layers and Entrance Lengths

a. Hydrodynamic Boundary Layer

For laminar flow in a circular tube, fluid enters the tube with a uniform velocity as shown in Figure 2.1; but when the fluid particles make contact with the tube wall, viscous effects cause them to assume a zero velocity. These viscous effects, associated with shear stresses acting in planes parallel to the tube wall, tend to retard the motion of particles in adjoining fluid layers, causing a momentum boundary layer to develop. The momentum boundary layer thickness, δ, increases until its growth is stopped by symmetry at the tube centerline. The viscous effects then extend over the entire cross section of the tube. The flow is then said to be hydrodynamically fully developed. At this point, the fluid velocity distribution at a given cross section is independent of the axial distance, x (i.e., $\partial u/\partial x = 0$) [Refs. 9, 10, 11, 12].

The hydrodynamic entry length for laminar flow ($Re_D \leq 2300$) is defined as that region where the hydrodynamic boundary layer is developing and may be obtained from the approximation [Ref. 10]:

$$\left(\frac{X_{fd,h}}{D}\right)_{lam} \approx 0.05 Re_D \qquad (2.1)$$

This expression shows that for $Re_D = 2300$, the entrance length is 115 times the tube diameter, a considerable length for most experimental facilities.
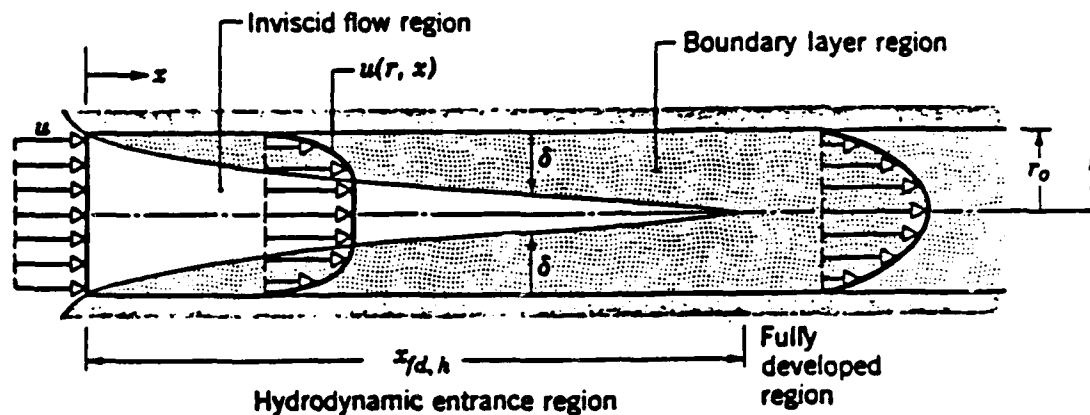
Figure 2.1 Laminar Hydrodynamic Boundary Layer Development in a Circular Tube (Courtesy [Ref. 10])

b. Thermal Boundary Layer

When a fluid with a uniform temperature distribution enters a circular duct with a wall temperature that is greater than the uniform fluid temperature, temperature gradients in the fluid develop and convective heat transfer occurs, as shown in Figure 2.2. The region of fluid where these temperature gradients exist is called the thermal boundary layer. The thermal boundary layer thickness, δ_t, grows until a dimensionless fluid temperature distribution is independent of x. The thermal boundary layer is then considered fully developed. This point is usually expressed in

10
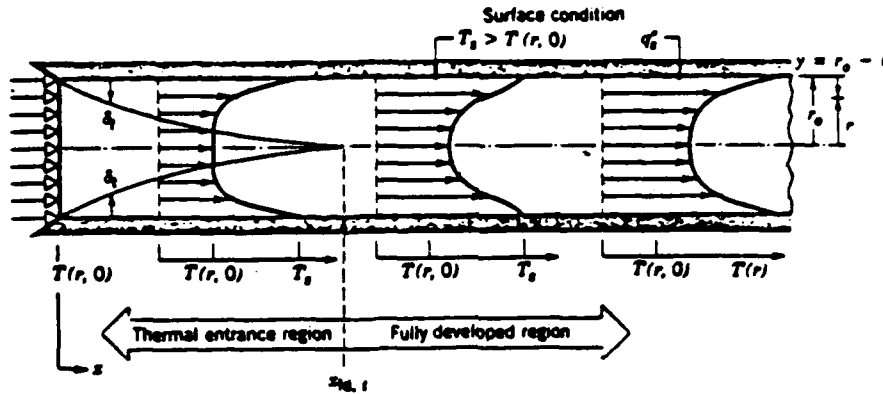
Figure 2.2 Thermal Boundary Layer Development in a Heated Circula. Tul (Courtesy of [Ref. 10])

terms of a non-dimensional temperature profile given by [R. 11]:

$$\frac{\partial}{\partial x} \left[\frac{T_s(x) - T(r,x)}{T_s(x) - T_m(x)} \right] = 0 \tag{2.2}$$

where T_s is the tube surface temperature, T is the local fluid temperature, and T_m is the mean temperature of the fluid over the cross section of the tube. The exact shape of the fully developed temperature profile is dependent upon the boundary conditions imposed, either a uniform surface temperature or constant heat flux.

For laminar flow, the thermal entry length may be expressed as the following [Ref. 10]:

$$\left(\frac{X_{fd,t}}{D} \right) \approx 0.05 Re_D Pr \tag{2.3}$$

It should be noted that the rate of development of the velocity and temperature profiles in the entry region depend upon the fluid Prandtl number. For

11

$Pr = 1$, both velocity and temperature profiles develop at the same rate. However, for $Pr > 1$, the hydrodynamic boundary layer develops more rapidly than the thermal boundary layer ($X_{fd,h} < X_{fd,t}$). For very large Prandtl number ($Pr > 100$), $X_{fd,h}$ is so much smaller than $X_{fd,t}$ that it is reasonable to assume that a fully developed velocity profile exists throughout the thermal entry region. [Refs. 9, 10, 11, 12]

2. Fully Developed Flow

Fully developed laminar flow of an incompressible fluid through a circular duct exists when both the thermal and velocity profiles are fully developed. Two boundary conditions must now be addressed, that of a uniform wall temperature and constant wall heat flux.

For these conditions, the general form of the energy equation in cylindrical coordinates for an incompressible fluid having constant properties (with no heat generation and neglecting body forces, pressure gradients and viscous dissipation), is given by [Ref. 11]:

$$u \frac{\partial T}{\partial x} + v \frac{\partial T}{\partial r} = \frac{\alpha}{r} \frac{\partial}{\partial r} \left(r \frac{\partial T}{\partial r} \right) \tag{2.4}$$

It can be shown that for these two cases, the energy equation reduces to the following differential equations,

Constant Wall Heat Flux: $\quad \dfrac{1}{r} \dfrac{\partial}{\partial r} \left(r \dfrac{\partial T}{\partial r} \right) = \dfrac{u}{\alpha} \left(\dfrac{dT_m}{dx} \right) \tag{2.5}$

12

Uniform Wall Temperature: $\dfrac{1}{r}\dfrac{\partial}{\partial r}\left(r\dfrac{\partial T}{\partial r}\right)=\dfrac{u}{\alpha}\left(\dfrac{T_s-T}{T_s-T_m}\right)\left(\dfrac{dT_m}{dx}\right)$ (2.6)

For the constant wall heat flux boundary condition, Kays [Ref. 11] solves the differential equation (equation 2.5) for a fully developed velocity and temperature profile and expresses the Nusselt number as:

$$Nu = \frac{hD}{k} = 4.364 \qquad (2.7)$$

Note that for this specified case, the heat transfer coefficient, h, depends only on the thermal conductivity, k, and the tube diameter, D.

A solution to the uniform wall temperature case is more complex, and involves evaluating the infinite series solution to the differential equation (equation 2.6) for the hydrodynamically developed, thermally developing flow situation. In evaluating the series solution, the resulting asymptotic Nusselt number is given by [Ref. 11]:

$$Nu = 3.657 \qquad (2.8)$$

This result is 16% less than the solution for the constant wall heat flux boundary condition. The asymptotic values in equations 2.7 and 2.8 are shown in Figure 2.3. Note that the inverse of the Graetz number is equivalent to the dimensionless axial distance x^*.

3. Entry Length Problem

The solution to the energy equation for the entry region is far more difficult to obtain because velocity and temperature vary both axially and radially. There are two entry length problems to be considered, a combined entry length, where both temperature and velocity profiles develop simultaneously, and the thermal entry length problem, where the thermal conditions develop in the presence of a fully developed velocity profile. This latter case would exist if the place at which heat transfer begins is preceded by an unheated starting length, a situation that exists in most experimental facilities. It should be noted that for $Pr << 1$ (i.e., liquid metals), the thermal boundary layer would develop faster than the hydrodynamic boundary layer. However, this case has little practical application and is therefore rarely considered in the literature.

Solutions have been obtained for both entry length conditions mentioned above [Refs. 9, 10, 11, 12] and these results are also presented in Figure 2.3. The Nusselt number is plotted against a dimensionless axial coordinate x^* (the inverse of the Graetz number) given by:

$$x^* = \frac{x/D}{Re_D Pr} \qquad (2.9)$$

Fully developed conditions are reached at $x^* \approx 0.05$ where the solutions for the thermal entry length converge with those for the combined entry length. For $x^* > 0.05$, the two types of entry length asymptotically reach the fully developed solutions

14

of 4.36 and 3.66 for the constant wall heat flux and uniform wall temperature boundary conditions respectively.
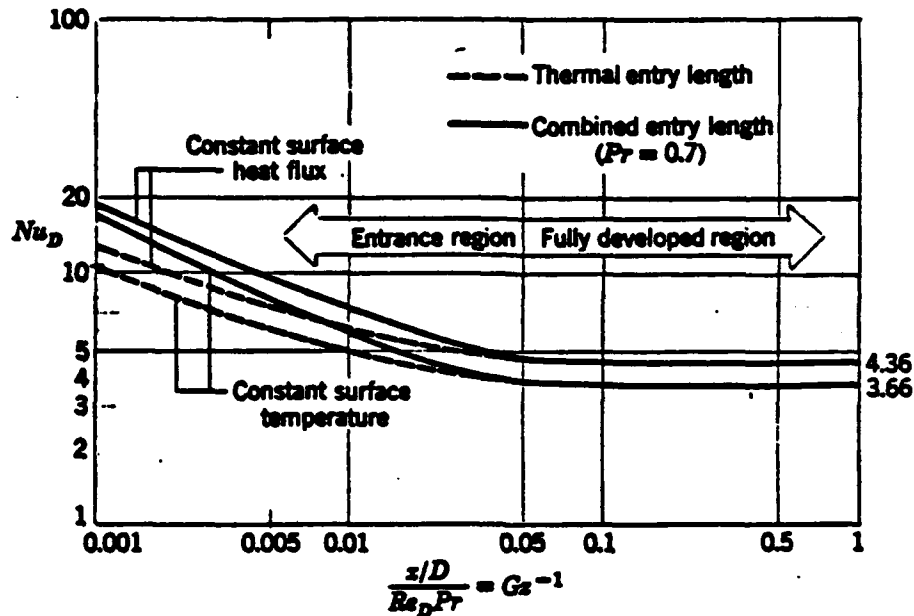
Figure 2.3 Local Nusselt Number Obtained from Entry Length Solutions for Laminar Flow in a Circular Tube (Courtesy [Ref. 10])

a. *Thermal Entry Region - Uniform Wall Temperature*

The thermal entry length problem, first studied by Graetz in 1883 and later by Nusselt in 1910, is more commonly known as the *Graetz Problem*. They considered an incompressible fluid with constant properties flowing through a circular tube having a fully developed laminar velocity profile and a developing laminar temperature profile subjected to a uniform wall temperature. Shah and London [Ref. 9] present a numerically derived infinite series solution to the *Graetz Problem*.

15

A more useful correlation presented by Incropera and Dewitt [Ref. 10] for the uniform wall temperature thermal entry length problem was developed by Hausen and is of the form:

$$Nu_m = 3.66 + \frac{0.0668(D/L)Re_D Pr}{1 + 0.04[(D/L)Re_D Pr]^{2/3}} \qquad (2.10)$$

This correlation was used by Mazzone [Ref. 6] in his refrigerant condensation experiments to predict the average inside heat transfer coefficient for a smooth tube without any type of insert.

Shah and London [Ref. 9] present a more complete set of correlations derived from experimental data for heat exchanger tubes in laminar flow for local (Nu_x) and mean (Nu_m) Nusselt numbers based on various x^* ranges. The correlations for local Nusselt number are given by:

$$\begin{aligned}
Nu_x &= 1.077(x^*)^{-1/3} - 0.7 & & for\ x^* \leq 0.01 \\
Nu_x &= 3.657 + 6.874(10^3 x^*)^{-0.488} e^{-57.2x^*} & & for\ x^* > 0.01
\end{aligned} \qquad (2.11)$$

and for mean Nusselt numbers by:

$$\begin{aligned}
Nu_m &= 1.615(x^*)^{-1/3} - 0.7 & & for\ x^* \leq 0.005 \\
Nu_m &= 1.615(x^*)^{-1/3} - 0.2 & & for\ 0.005 < x^* < 0.03 \\
Nu_m &= 3.657 + \frac{0.0499}{x^*} & & for\ x^* \geq 0.03
\end{aligned} \qquad (2.12)$$

The reader is reminded that both the Hausen correlation and the Shah and London correlations presented above are for a thermally developing flow with a fully developed velocity profile subjected to a uniform wall temperature.

16

b. Thermal Entry Region - Constant Wall Heat Flux

For the thermal entry length problem under a constant wall heat flux boundary condition, Shah and London [Ref. 9] present several numerical solutions but recommend the following approximate equations for the local Nusselt number:

$$
\begin{aligned}
Nu_x &= 1.302(x^*)^{-1/3} - 1 & &\text{for } x^* \leq 5 \times 10^{-5} \\
Nu_x &= 1.302(x^*)^{-1/3} - 0.5 & &\text{for } 5 \times 10^{-5} \leq x^* \leq 1.5 \times 10^{-3} \qquad (2.13) \\
Nu_x &= 4.364 + 8.68(10^3 x^*)^{-0.506} e^{-41 x^*} & &\text{for } x^* \geq 1.5 \times 10^{-3}
\end{aligned}
$$

Shah and London also recommend the following approximate equations for the mean Nusselt number:

$$
\begin{aligned}
Nu_m &= 1.953(x^*)^{-1/3} & &\text{for } x^* \leq 0.03 \\
Nu_m &= 4.364 + \frac{0.0722}{x^*} & &\text{for } x^* > 0.03
\end{aligned}
\qquad (2.14)
$$

The above two sets of equations are for a thermally developing, hydrodynamically developed flow subjected to a constant wall heat flux.

c. Combined Entry Length

As discussed earlier, the rate at which the temperature and velocity profiles develop is dependent upon the Prandtl number. At medium to high Prandtl numbers (Pr > 100), the velocity profile develops much more rapidly than the temperature profile and a fully developed velocity profile assumption is valid; for such conditions the equations given above should be used.

For 1 < Pr < 100, however, a fully developed velocity profile is no longer a valid assumption and a combined entry length solution must be developed.

17

Again, Shah and London [Ref. 9] present a comprehensive study of various solutions to the combined entry length problem, including two solutions for local Nusselt numbers developed by Churchill and Ozoe [Ref 13], the first, for a uniform wall temperature:

$$\frac{Nu_x + 1.7}{5.357\{1 + [(388/\pi)x^*]^{-8/9}\}^{3/8}} = \left[1 + \left(\frac{\pi/(284x^*)}{\{1 + (Pr/0.0468)^{2/3}\}^{1/2}\{1 + [(388/\pi)x^*]^{-8/9}\}^{3/4}}\right)^{4/3}\right]^{3/8} \quad (2.15)$$

and the second, for a constant wall heat flux:

$$\frac{Nu_x + 1}{5.364\{1 + [(220/\pi)x^*]^{-10/9}\}^{3/10}} = \left[1 + \left(\frac{\pi/(115.2x^*)}{\{1 + (Pr/0.0207)^{2/3}\}^{1/2}\{1 + [(220/\pi)x^*]^{-10/9}\}^{3/5}}\right)^{5/3}\right]^{3/10} \quad (2.16)$$

From the preceding paragraphs, it can be seen that the subject of laminar flow forced convection in circular ducts has been studied in great detail yielding both analytical and experimental results. The reader is referred to Shah and London [Ref. 9] and Kays and Crawford [Ref. 11] for a more complete and thorough review of this subject.

C. AUGMENTATION TECHNIQUES TO ENHANCE TUBESIDE HEAT TRANSFER

1. General Introduction

As discussed earlier, when laminar flow heat transfer occurs within tubes, it usually represents the dominant thermal resistance in a heat exchanger. These large resistances result in low inside heat transfer coefficients. In recent years, the requirement for more efficient heat exchangers has stimulated considerable interest in techniques to augment or enhance tubeside heat transfer.

The various methods to enhance tubeside heat transfer can be classified into two categories, passive and active techniques. Passive techniques involve no external energy (except increased pump work) to produce the necessary enhancement. Passive techniques are divided into the following methods:

1. Internally finned tubes (longitudinal or spiral fins) designed to increase the inside heat transfer surface area.

2. Surface roughness techniques aimed at agitating flow rather than increasing heat transfer surface area.

3. Swirl flow techniques which involve the use of inlet vortex generators, periodically spread propellers or twisted tape inserts designed to cause enhancement by creating a rotating and/or secondary flow.

4. Displaced promoters which alter the fluid flow near the surface by the use of inserts such as wire mesh, static mixer elements, rings or disks.

5. Coolant additives designed to increase the conductivity of the coolant.

6. Compound techniques that involve more than one of the above mentioned methods.

Active techniques utilize an external energy source to promote the required augmentation. These techniques include: (1) mechanical aids, (2) heated surface vibration, (3) fluid pulsation, (4) electrostatic fields, and (5) suction or injection.

All of the above techniques are aimed at creating turbulence in the relatively slow moving or stagnant boundary layer fluid by displacing this fluid from the heateu surface and mixing it with the bulk fluid. Essential in all of these techniques is a balance between increased heat transfer rate and increased pumping power requirements/costs. Bergles and Joshi [Ref. 14] present an excellent review of augmentation techniques and compare heat transfer data taken at low Reynolds number flow subjected to both uniform wall temperature and constant wall heat flux.

Of particular interest to this thesis are two passive techniques, the swirl flow technique using twisted tape inserts and the displaced promoter technique using wire mesh inserts. These two methods of enhancement of tubeside heat transfer are discussed in more detail in the following sections.

2. Heat Transfer Enhancement with Twisted Tape Elements

Among the most common swirl flow augmentation techniques is the use of twisted tape inserts. The tapes usually consist of a thin stainless steel, brass or copper strip which is the width of the inside diameter of the tube. The tapes are twisted by clamping one end to an overhead, attaching weights to the other end and then twisting to the desired specifications [Ref. 15]. Enhancement occurs not only

20

due to the increased path length of flow, but also due to secondary flow effects and fin effects caused by tape contact with the inside tube wall.

Analytical studies of twisted tape inserts by Date and Singham [Ref. 16] suggest that swirl flows improve heat transfer by as much as a factor of 70; however, no experimental data have confirmed their unrealistically large predictions. The first experimental work of swirl flow using twisted tapes was conducted by Hong and Bergles [Ref. 15]. Their primary objective was to develop experimentally based correlations for predicting heat transfer coefficients for laminar flow of water and ethylene glycol in an electrically heated tube (heated length of 1.22 m, inside diameter of 10.2 mm) with two sizes of twisted tape inserts. They showed that the Nusselt number was independent of axial location, suggesting that fully developed conditions existed. Therefore, the mean Nusselt number should take the form:

$$Nu_m = f(Re_s, Pr, y).$$ (2.17)

Re_s is the Reynolds number for the swirl flow given by:

$$Re_s = \frac{4\dot{m}}{\pi \mu (D_i - 4\delta)}$$ (2.18)

and δ is the tape thickness. The twist ratio, y, is defined as:

$$y = \frac{H}{D_i}$$ (2.19)

21

where H is the pitch for a 180° twist of the tape. Hong and Bergles then combined Re_s and y as a single parameter and came up with the following correlation for values of $Re_s/y > 10$:

$$Nu_m = 0.383 Pr^{0.35} (Re_s/y)^{0.622} \tag{2.20}$$

For values of $Re_s/y < 10$, the following correlation was obtained:

$$Nu_m = 5.172\{1 \cdot 5.484 \times 10^{-3} Pr^{0.7} (Re_s/y)^{1.25}\}^{0.5} \tag{2.21}$$

It should be noted that all fluid properties in equations 2.20 and 2.21 should be evaluated at the bulk fluid temperature. One additional important observation was made by Hong and Bergles regarding tube wall temperature. They found a significant variation of temperature at one axial location with two different tape orientations at that position of 90° and 120°, suggesting that the temperature profile was related to the tape orientation. Hong and Bergles concluded that for a fully developed flow, inside heat transfer coefficients depend on twist ratio and could be improved by a factor of two or three over an empty tube. These conclusions were confirmed by later studies of Saha et. al. [Ref. 17] and Marner and Bergles [Ref. 18].

3. **Heat Transfer Enhancement with Wire Mesh (HEATEX) Elements**

The use of wire mesh inserts to promote inside heat transfer falls into the displaced promoter technique mentioned earlier. One such wire mesh insert was commercially developed by CAL-GAVIN Limited (UK) and called "HEATEX."

This HEATEX insert consists of a central wire core on which a series of wire loops or petals are attached. The petals are attached to the core at an inclined angle that face the oncoming fluid flow. Ideally, each petal makes contact with the tube wall in the form of an arc, thereby maximizing disturbance of fluid along the tube wall. In addition to the boundary layer disturbance, radial mixing occurs caused by repeated redistribution and mixing of fluid through the mesh of loops near the tube axis [Ref. 19]. Various wire loop densities and nominal diameters are available, depending on the application.

Initial studies by Gough et. al. [Ref. 19] with HEATEX inserts suggest enhancements of a factor greater than ten times that of a similar tube with no insert. Additional experiments were conducted by Oliver and Aldington [Ref. 20] in which a correlation was determined:

$$Nu = 0.232 Re^{0.54} Pr^{0.46} \qquad (2.22)$$

It must be remembered, however, that this correlation is for a specific loop density and nominal diameter HEATEX element.

The two types of HEATEX mixing elements supplied by CAL-GAVIN (nominal diameters of 13.26 and 10.16 mm) did not match the loop densities of previous studies; therefore new correlations needed to be developed. Mazzone [Ref. 6] developed correlations for these inserts from limited data supplied by CAL-GAVIN. For the 13.26 mm and 10.16 mm elements, these correlations were respectively:

23

$$Nu = 0.226 Re^{0.65} Pr^{0.46} \quad (13.26mm) \tag{2.23}$$

and

$$Nu = 0.063 Re^{0.76} Pr^{0.46} \quad (10.16mm) \tag{2.24}$$

Since these correlations were developed from a very limited amount of data taken under conditions that did not exactly match that of Mazzone's condensation experiments, they were always subject to inaccuracy. Therefore, the need for more accurate correlations under the exact conditions used in the condensation experiments are required.

III. EXPERIMENTAL APPARATUS

A. SYSTEM OVERVIEW

The test apparatus utilized is shown in Figures 3.1 and 3.2. The apparatus is a closed loop, low pressure system utilizing an ethylene glycol/water mixture as the coolant. The coolant is circulated by a centrifugal pump from a supply tank, through a reducing manifold and flowmeter into the test section. Coolant is then returned to the supply tank via a return header.

The test section consisted of an inlet and outlet thermocouple well/mixing chamber to measure inlet and outlet coolant temperatures and the test tube itself. The tube was instrumented with twelve thermocouples (embedded in the tube wall) to determine inside wall temperatures. A constant heat flux boundary condition was achieved using a series of flexible electrical heating elements wrapped around the tube. Monitoring the system as well as data acquisition and data processing were provided by a Hewlett-Packard microcomputer and Data Acquisition System.

Figure 3.1 Primary and Secondary Coolant Systems.
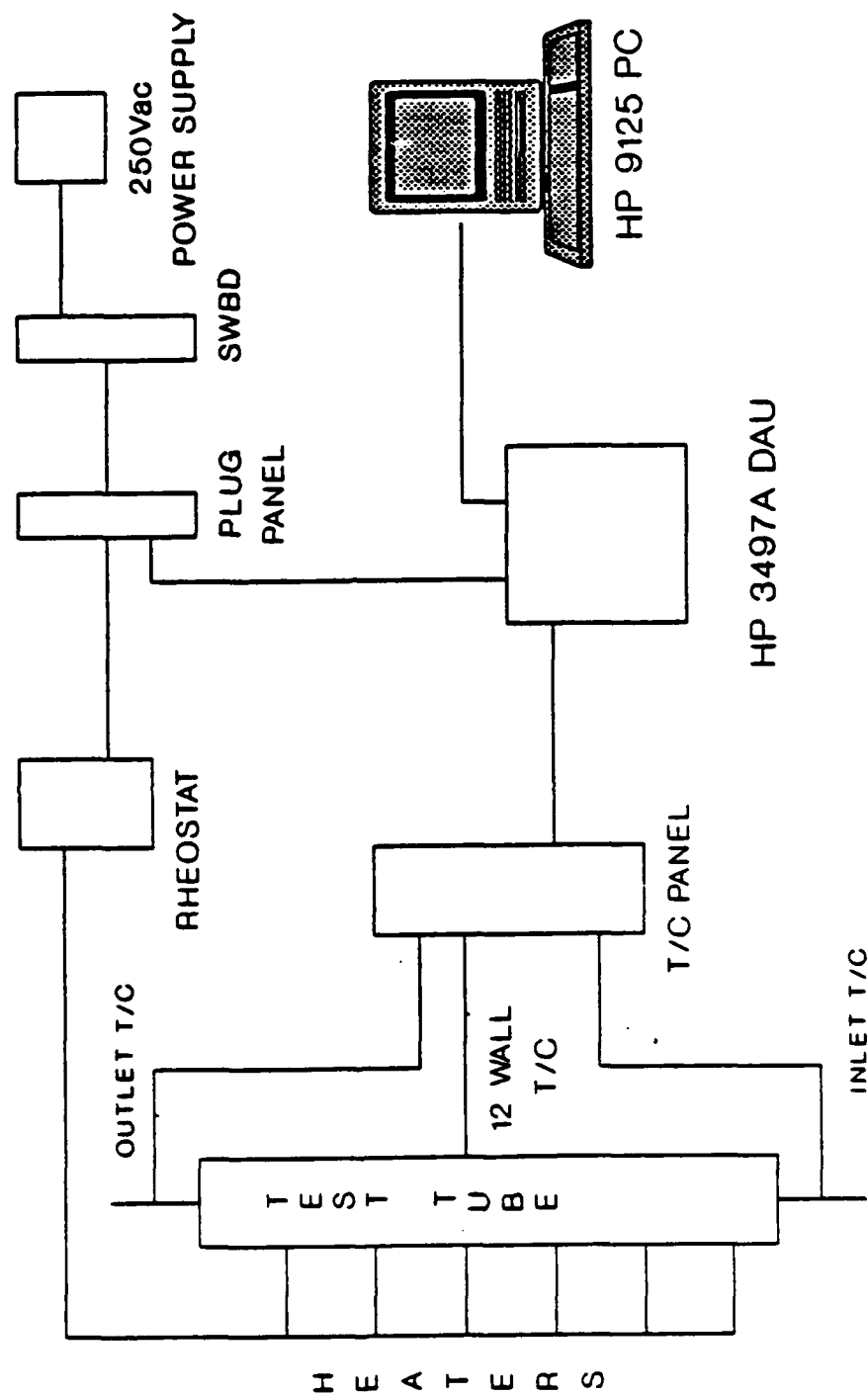
Figure 3.2 Data Acquisition and Control Systems.

B. TUBES AND INSERTS TESTED

1. Tubes Tested

Three types of tubes were utilized in the experiments, a copper smooth tube, a copper/nickel externally finned tube, and a copper/nickel corrugated or roped tube. These tubes correspond to the tubes utilized in the refrigerant condensation experiments of Mabrey [Ref. 5] and Mazzone [Ref. 6].

The smooth copper tube provided a baseline set of experimental data which were then compared with previous experimental and theoretical work for the inside heat transfer coefficient conducted by Shah and London [Ref. 9] for no insert, Oliver and Aldington [Ref. 20] for the HEATEX insert, and Hong and Bergles [Ref. 15] for the twisted tape insert.

The Cu/Ni finned tube provided a smaller inside diameter to be used in these comparisons. Note that the fins play little part in the experiments. The wall thermocouples were buried in the tube wall and were used to measure the inside wall temperature, which had a smooth bore. Consequently, for the purposes of these experiments, the tube behaved like a smooth copper tube with a different internal diameter.

The final tube tested was a Cu/Ni corrugated (or roped) tube, commercially referred to as a "Korodense" tube. The tube was manufactured and provided by Wolverine Tube Company of Decatur, Al. All tube dimensions and specifications were taken from the Wolverine Technical Bulletin No. 4020 [Ref.

21]. Figure 3.3 is a schematic of the Korodense tube. Tube specifications for all three tubes are listed in Table E.1 of Appendix E.
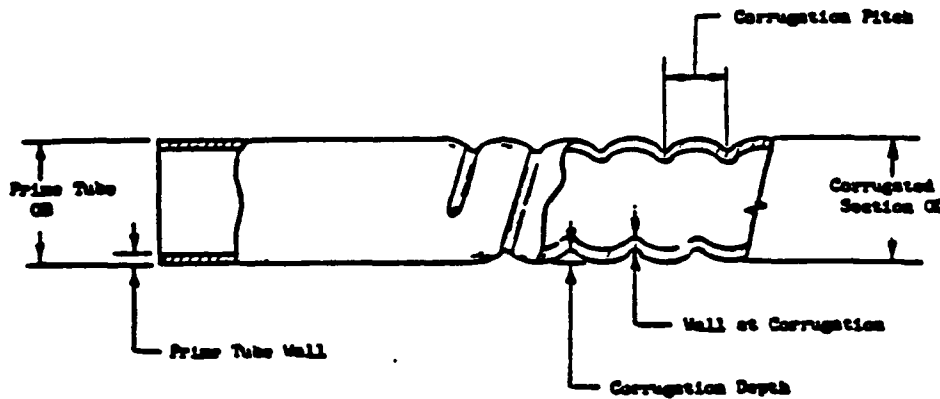
Figure 3.3 Wolverine Korodense Tube (Courtesy [Ref. 21])

2. Insert Elements Tested

Two types of insert mixing elements were utilized in this investigation, a twisted tape insert and a wire mesh insert commercially referred to as a "HEATEX" tube insert. In both cases, two sizes were required due to the two different tube inside diameters used.

The twisted tape inserts were made of a strip of brass 0.559 mm thick and either 10.16 mm or 13.26 mm wide. The tapes were manufactured in the NPS Mechanical Engineering machine shop by clamping them to the overhead, attaching a weight to the opposite end, and twisting them to the desired twist ratio. A twist ratio of 3 and 4 corresponding to the two respective tube inside diameters were manufactured. Once installed in the tube, the edges of the tape should ideally have been in contact with the tube wall.

The second type of insert used was a commercially available product referred to as HEATEX radial mixing elements. These elements were supplied by Cal Gavin of Birmingham, U.K. They are manufactured from stainless steel and consist of a central wire core onto which a series of wire loops or petals are attached. Each petal was inclined at an angle facing the oncoming flow. The outside diameter of the elements were slightly oversized for the tube, ensuring that close contact with the tube wall in the form of an arc, rather than a point, was achieved. As with the twisted tape elements, different diameter HEATEX elements were needed, 13.26 mm used in the smooth and Korodense tubes and the other 10.15 mm for the Cu/Ni finned tube. Figure 3.4 shows both the twisted tape and HEATEX inserts.
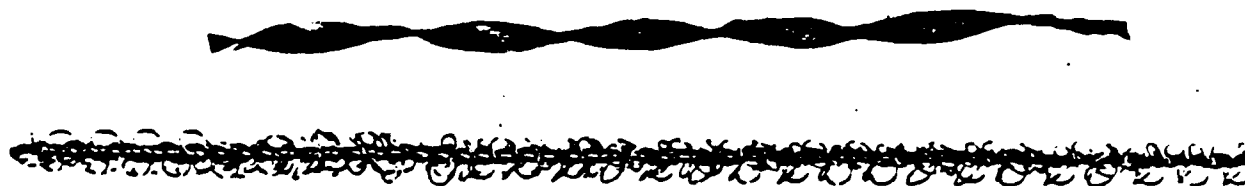
Figure 3.4 Twisted Tape and HEATEX Inserts

C. COOLANT SYSTEM

1. Primary Coolant System

An ethylene glycol/water mixture (54/46% by weight) was stored in a 1.5 m³ insulated supply tank. The mixture was circulated through the primary system by a 1½ hp, constant speed, centrifugal pump. The coolant was discharged from the pump via a 76 mm diameter PVC pipe to a manifold where it was reduced to a 15.9 mm diameter Tygon flexible tube. A rotameter type flowmeter with a ball valve at its entrance was used to control the flow rate through the system. Flowmeter calibration results are discussed in Appendix A.

Flow entered the test section through a 90° bend which housed the thermocouple well and exited through a mixing chamber/thermocouple well combination (see Figure 3.1). Prior to entering the exit mixing chamber, the coolant passed through a 10 cm length of flexible tubing containing a high density wire mesh. This wire mesh, in conjunction with the mixing chamber, served to minimize radial temperature variations and provide a uniform outlet coolant temperature. The flow then exited the test section through more flexible tubing to a manifold and return PVC header, suspended above the apparatus, and back to the coolant supply tank.

2. Secondary Coolant System

In order to achieve a wide range of Reynolds number, coolant inlet temperatures were varied from -10°C to +20°C. This was accomplished by a secondary coolant system comprised of a 28 kW (8 ton) external refrigeration system.

31

A 30 gpm, .75 hp centrifugal pump continuously circulated coolant between the supply tank and a chiller barrel where it was cooled to the desired temperature. Temperature was maintained by a thermostatically controlled solenoid valve at the discharge side of the chiller barrel. This system allowed for a range of coolant temperatures between -20°C and ambient to be selected while maintaining the coolant inlet temperature approximately constant (±2°C) during each run.

D.   INSTRUMENTATION AND TEST SECTION

1.   Instrumentation

All temperature measurements were made using copper/constantan type-T teflon coated thermocouples and were previously calibrated by Mabrey [Ref. 5]. The inlet coolant temperature was measured by a single thermocouple while the outlet coolant temperature was measured by two thermocouples located immediately after the mixing chamber.

Each test tube was fitted with twelve wall thermocouples to determine the average inside wall temperature. Thermocouples were placed at four different longitudinal positions along the axis of the tube. Three thermocouples at each location were spread evenly around the tube at 120°C intervals. Figure 3.5 shows a typical tube with the exact longitudinal and nodal thermocouple locations. Actual longitudinal locations varied slightly for each tube and are given in Table E.1 as x/D_i where x is the length from the start of the heated length to the thermocouple location and D_i in the inside diameter of the tube. The two extreme longitudinal

32

locations of the thermocouples corresponded to the beginning and end of the "effective" condensing length of the tubes being used in the condensation experiments of Mabrey [Ref. 5] and Mazzone [Ref. 6].

INSTRUMENTED TUBE

POS 1	POS 2	POS 3	POS 4
15.2cm	55.9cm	96.5cm	137.2cm

L_T = 1.52m   Do = 15.88mm
L_H = 1.42m   Di = 13.26mm
L/D = 105.6   Dt/c = 14.36mm
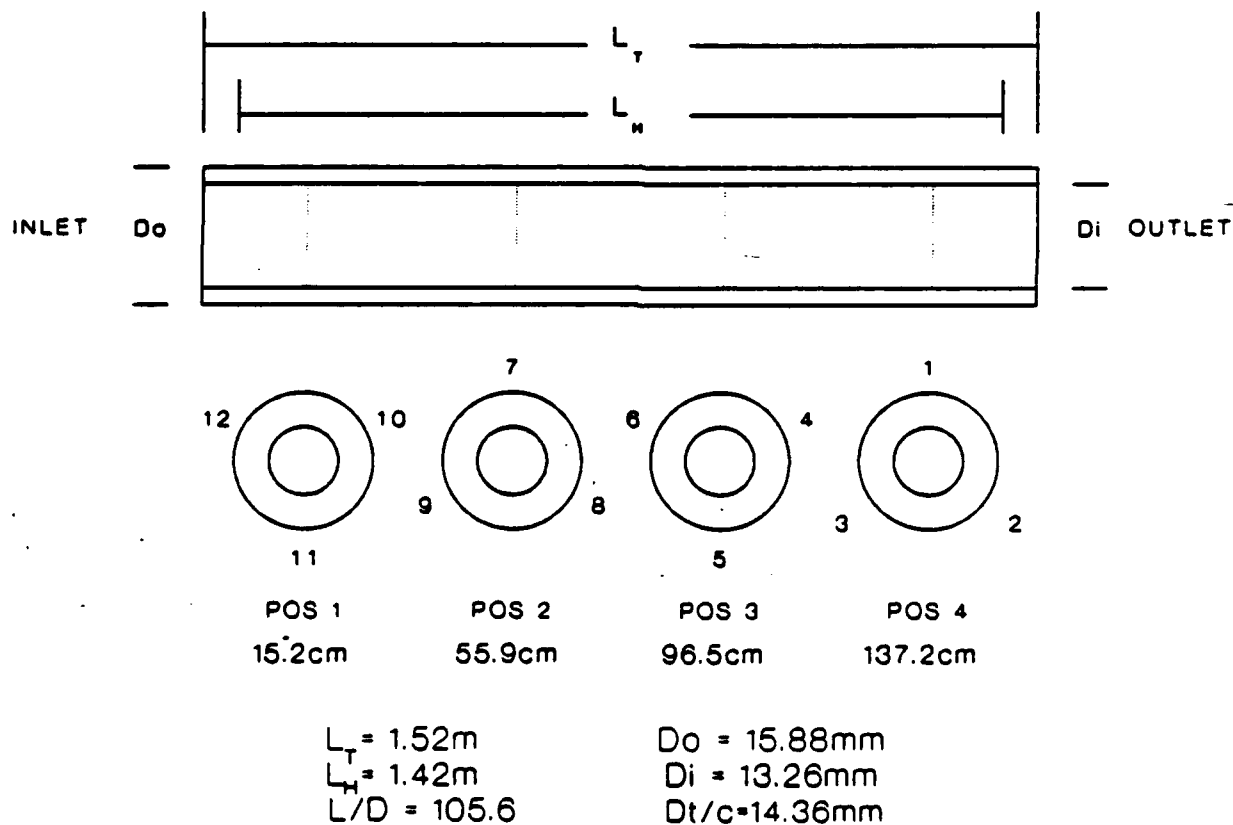
Figure 3.5 Instrumented Tube

2. Thermocouple Attachment Method

In order to attach the thermocouples to the wall of the tube, short longitudinal grooves were cut at each location. These longitudinal grooves were cut to a depth of ½ the tube wall thickness. It was decided that a thermocouple embedded within the tube wall vice being attached to the surface would lead to a more accurate tube wall temperature and minimize the effect of direct contact heating from the heating elements. Thermocouples were then placed in these grooves and either soldered in place or tack welded and covered with a liquid metal epoxy. Different methods for attaching and covering the thermocouples were used for each tube based on the tube material and configuration (discussed below).

In the case of the smooth copper tube, the thermocouples were silver soldered in place and the remainder of the groove then covered with silver solder. Since the tubes were copper, this was relatively easy to accomplish. Care was taken to ensure that the thermocouple remained in contact with the tube wall and that no air pockets were created (which would cause an additional large resistance to heat flow). Also, great care was taken to prevent any melting of the teflon insulation past the thermocouple joint. This condition could have caused an electrical contact between the two wires of the thermocouple prior to the tube wall, leading to an unrealistically high observed wall temperature.

A different method was required to attach the thermocouples to the copper/nickel finned tube due not only to the external fins but also the 10% nickel content. Initially, a small diameter hole was machined into the tube to minimize fin

damage (rather than cutting a longitudinal groove). Since the thermocouple was to be embedded half way into the tube wall, this hole proved to be relatively deep. Also, because of the nickel content of these tubes, the preheat temperature required to ensure that the silver solder would adhere to the tube wall was much higher. These higher required temperatures and the hole depth caused a significant amount of the thermocouple teflon insulation to be melted, allowing for potential contact between the thermocouple wires at some point other than the tube wall. This technique was therefore abandoned in favor of the longitudinal groove method. However, thermocouple insulation was again being destroyed due to the higher required preheat temperatures. An alternative solder, soft solder, with lower preheat and melting temperatures, was therefore used. The final combination of longitudinal grooves and soft solder was successful.

For the copper/nickel Korodense tube, the groove and soft solder method was again tried. Initial tests in the apparatus showed wall temperatures at one longitudinal position varying by as much as 15°C. On closer examination of the thermocouple connections (using a magnifying glass), it was revealed that insulation damage was evident on over half of the thermocouples. Several more attempts at the groove and soft solder method were tried, all leading to the same results.

A third method utilizing a tack welding machine (acquired and adapted for our use) was tried. Thermocouples were tack welded into the bottom of the groove resulting in no damage to the insulation and a liquid steel epoxy was used to fill the remainder of the groove, providing additional strength and protection to the

connection. This final method proved to be the most successful and is recommended for use in any follow-up experiments.

3. Test Section

In order to achieve a constant heat flux, each tube was tightly wrapped with six silicone rubber flexible electrical heating elements rated at 240 V, 200 W each. Each strip was 2.5 cm wide and 50.6 cm long. The heating elements were connected in parallel to a 240 Vac power supply via a plug panel and power switchboard. Power to the six heaters was controlled by a STACO, 240 Vac, 23.5 kVa rheostat (see Figure 3.2).

To minimize heat loss from the heater to ambient, the tube was wrapped in a 20 mm thick neoprene type insulation. This type of insulation proved to be extremely effective giving a negligible heat loss. It also provided insulation against heat influx from ambient at the colder coolant inlet temperatures. Actual heat loss and heat influx experiments and their results are discussed in more detail in Appendices B and C. All other tubing and PVC piping was wrapped in similar type insulation.

The whole test section was then placed in a restraining stand which minimized outside vibration effects and ensured that each tube remained horizontal and in the same relative position (to the remainder of the apparatus) for each experiment.

E. DATA ACQUISITION AND CONTROL SYSTEM

A Hewlett-Packard 9125 microcomputer (MC) was used to control a Hewlett-Packard 3497A Automatic Data Acquisition Unit (DAU) (see Figure 3.2). The DAU read the output from the twelve tube wall thermocouples and three coolant thermocouples (one inlet and two outlet). Additional channels were assigned to sense heater input voltage and current at the plug panel. The voltage was converted to heater power using the heater resistance and the calibration discussed in Appendix D.

Thermocouple readings were made in microvolts which were converted to temperatures (along with the heat flux calculations) using the data reduction program. The data reduction program, DRPSING, will be discussed in more detail in a later chapter. All temperatures, power, and heat flux measurements were monitored using the MC and DAU. DAU channel assignments are listed in Table 3.1.

TABLE 3.1 DATA ACQUISITION UNIT CHANNEL ASSIGNMENTS

CHANNEL NO.	MEASURED QUANTITY
1	Thermocouple Pos 1
2	Thermocouple Pos 2
3	Thermocouple Pos 3
4	Thermocouple Pos 4
5	Thermocouple Pos 5
6	Thermocouple Pos 6
7	Thermocouple Pos 7
8	Thermocouple Pos 8
9	Thermocouple Pos 9
10	Thermocouple Pos 10
11	Thermocouple Pos 11
12	Thermocouple Pos 12
13	Tube Inlet
14, 15	Tube Outlet
25	Input Current
29	Input Voltage

IV. EXPERIMENTAL PROCEDURES

A. CALIBRATION EXPERIMENTS

Several calibration experiments were required prior to performing the main experiments. Figure 4.1 depicts a typical tube being tested. The primary heat source is from the heating elements ($\dot{q}_{tape}$). However, to complete the heat balance on the system, several other heat sources and heat sinks needed to be accounted for. The first experiment conducted was to determine the amount of heat being lost from the heating elements to the atmosphere vice going to the coolant. Heat loss experiments are discussed in Appendix B.

The second experiment was to account for two additional potential heat sources: heat leakage into the coolant from ambient ($\dot{q}_{leak}$) and frictional temperature rise ($\dot{q}_{fric}$). Approximately 8 cm at either end of the tube, along with the flexible tubing section prior to the thermocouple wells, were not covered by the heating elements. Since coolant inlet temperatures were primarily below ambient temperature, a potential for heat leakage to the coolant from ambient existed. Also, because of these cold inlet temperatures, frictional heating could exist, especially when using the various inserts. Heat leakage into the system and frictional effects were considered together as one heat influx. These experiments were conducted with the heater tapes turned off; any temperature rise was then monitored using the inlet

39

and outlet thermocouples. Appendix C discusses the experiments conducted to determine this part of the heat balance equation. As mentioned earlier, the test section and all other tubing were insulated to minimize these effects.
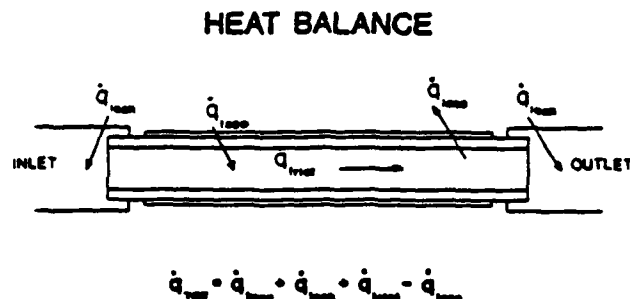
HEAT BALANCE

Figure 4.1 Heat Balance.

B. PROCEDURES FOR DETERMINATION OF INSIDE HEAT TRANSFER RATE

1. General Procedures

Each tube utilized in this study was tested with no insert and the appropriate twisted tape and HEATEX inserts corresponding to the tube inside diameter. For each insert condition, four nominal coolant inlet temperatures, -10°C, 0°C, +10°C and +20°C were chosen to increase the range of experimental Reynolds and Prandlt numbers that could be attained. To check that heat flux variations did not affect the results, data were taken at heat fluxes of 10 kW/m² and 15 kW/m² for each inlet temperature. For each insert, coolant inlet temperature and heat flux setting, coolant velocity was varied between 0.2 m/s and 1.4 m/s. Since the inside diameter of the Cu/Ni finned tube was smaller than the other two tubes, higher

40

coolant velocities of up to 2.4 m/s could be attained. A matrix of the individual data runs and data file names is shown in Table 4.1.

With the tube installed and all calibration experiments completed, the experiments to determine the inside heat transfer coefficient were conducted. Since flowmeter settings for specific coolant velocities were based upon the inlet coolant temperature, the system was initially operated at a 100% flowmeter setting with no power to the heating elements for 15 minutes. This allowed the inlet thermocouple well to stabilize. Once the desired inlet coolant temperature was reached and maintained, power to the heating elements was set to the predetermined heat flux setting for that data run (10 or 15 kW/m²). The flowmeter was then adjusted to achieve the desired coolant velocity based upon flowmeter calibration results (discussed in Appendix A). Flow was maintained for approximately 10 minutes to ensure steady state equilibrium conditions prior to taking data.

TABLE 4.1 DATA FILE NAMES

TEMP(C)/ q'(kw/m²)	Cu Smooth Tube			Cu/Ni Finned Tube			Cu/Ni Korodense Tube		
	No Insert	Twisted Tape	HEATEX	No Insert	Twisted Tape	HEATEX	No Insert	Twisted Tape	HEATEX
20/10	SMNI04	.	SMHX04	CFNI04 (+15)	CFT01 (+15)	CFHX01 (+15)	KDNI01	KDTT01	KDHX01
20/15.	SMNI04	.	SMHX04	CFNI04 (+15)	CFTT01 (+15)	CFHX01 (+15)	KDNI01	KDTT01	KDHX01
10/10	SMNI03	SMTT01	SMHX01	CFNI01	CFTT02	CFHX02	KDNI02	KDTT02	KDHX02
10/15	SMNI03	SMTT01	SMHX01	.	CFTT02	CFHX02	KDNI02	KDTT02	KDHX02
0/10	SMNI02	SMTT02	SMHX02	CFNI03	CFTT03	CFHX03	KDNI03	KDTT03	KDHX03
0/15	SMNI02	SMTT02	SMHX02	CFNI03	CFTT03	CFHX03	KDNI03	KDTT03	KDHX03
-10/10	SMNI01	SMTT03	SMHX03	CFNI02	CFTT04	CFHX04	KDNI04	KDTT04	KDHX04
-10/15	SMNI01	SMTT03	SMHX03	CFNI02	CFTT04	CFHX04	KDNI04	KDTT04	KDHX04

Velocities were increased from 0.2 m/s to 1.4 m/s in steps of 0.2 m/s and then decreased from 1.3 m/s to 0.3 m/s in similar steps. This method of increasing on even values and decreasing on odd values was done not only to determine if any hysteresis effects existed (i.e., a difference in the increasing and decreasing data), but also to ultimately increase the number of data points acquired. Also, since data were immediately plotted (as Nu_m versus Re), the method allowed for an easy determination as to whether a data point had reached a steady state condition.

Inlet and outlet coolant temperatures, tube wall temperatures, heat flux and heating element power settings were all continuously monitored using the computer program DRPSING in conjunction with the Data Acquisition System discussed earlier (DRPSING is listed in Appendix G). Individual data runs for each tube and insert condition were conducted in a similar manner.

2. Specific Experiments

a. Copper Smooth Tube

The first tube tested was the copper smooth tube. This tube was chosen to provide a baseline set of data needed for validation of system performance and for comparison with data acquired using other tubes. It should also be noted that two complete independent sets of data covering all insert conditions and inlet temperatures were taken over a period of two weeks. Data from both sets were compared and found to be in very good agreement ($\pm 2\%$); this validated the repeatability of data obtained from the system under the same conditions.

The initial intention for all tubes was to start with a given insert at the highest coolant inlet temperature, take data at each of the heat flux settings and then proceed to the next coolant temperature. Once one insert was completed, the system could then be shut down and the insert changed. This procedure would then be repeated for all three insert conditions. However, the coolant supply tank and coolant system were used concurrently for other experiments which required the coolant temperature to be -20°C. Since it took approximately 36-48 hours for the coolant temperature to increase from -10°C to +20°C (the sump was not fitted with a heater), only the copper smooth tube was done in this way. The method for the other two tubes is discussed below.

b.   Cu/Ni Externally Finned Tube

The second tube tested was the Cu/Ni finned tube. For a given inlet temperature and tube insert, the same procedure as with the copper smooth tube was used. However, rather than decreasing coolant temperature with the same insert, the coolant temperature was maintained and the insert changed until all three of the insert conditions were completed for a given inlet temperature. Once all the data for a given inlet temperature had been taken, the supply tank temperature was decreased to the next inlet temperature condition. It took only about one hour for the secondary coolant system to decrease the temperature by 10°C. Since it was a relatively short task to change inserts, the 36 to 48 hour waiting period required to raise coolant temperatures back to +20°C between insert changes was eliminated.

43

It should be noted that for the Cu/Ni finned tube, the highest nominal inlet temperature attained was only +15°C vice +20°C. Colder than normal ambient temperatures existed preventing supply tank temperatures from reaching +20°C. Also, due to the smaller inside diameter, coolant velocities could be varied between 0.3 m/s and 2.4 m/s.

c.   *Cu/Ni Korodense Tube*

The same procedure used with the finned tube was also used with the Korodense tube. In addition, another test was conducted with this tube. It was noted that larger than normal wall temperature variations existed at one longitudinal location when using the two inserts. It was suspected that the point of contact between the insert and tube wall was directly below a thermocouple position causing a higher wall temperature at that point. To verify this, the system was shut down by securing the coolant pump and the heating elements so that the flowmeter and power settings remained exactly the same. The outlet end of the tube was opened and the insert moved downstream by approximately 2 cm. The system was then closed and the coolant flow and power to the heating elements restored. Wall temperature variations still existed but were significantly less. This procedure was repeated several times with similar results.

V. DATA REDUCTION

A. AVERAGE INSIDE HEAT TRANSFER COEFFICIENT

The main objective of the data reduction scheme was to determine the average inside heat transfer coefficient ($\bar{h}_i$). This in turn was used to determine a mean Nusselt number (for the whole heated length of the tube) to be used as the basis for establishing the desired correlations.

To accomplish this task, the Data Acquisition Unit discussed in Chapter III made use of the computer program DRPSING. A listing of the program is given in Appendix E. The program allowed the user to monitor information from the instrumentation attached to the apparatus, acquire and then process the data to determine the desired output. In doing this, the user would select the tube and insert condition as well as the nominal coolant inlet temperature for that particular data run. The desired coolant velocity was then selected. Based on the actual measured coolant inlet temperature, coolant mixture properties and flowmeter calibration results (see Appendix A), the appropriate flowmeter setting (as a %) was calculated and set on the flowmeter.

The program then monitored coolant inlet and outlet temperatures, the twelve wall thermocouple temperatures and the actual measured heat flux and power settings. Once all readings reached a steady state condition (approximately 10 min.),

the user could terminate the display session and acquire data for that coolant velocity setting.

The DAU measures emf from the thermocouples and then converts these values to temperatures using the temperature calibration equation developed by Mabrey [Ref. 5]. Heater power was determined by measuring the voltage at the plug panel and calculating the power based on heater resistance and the power calibration contained in Appendix D.

The twelve wall thermocouples (placed axially and radially) were used to minimize the uncertainty in determining the average inside wall temperature. These twelve wall temperatures were averaged and corrected (to account for the depth of burial using a simple conduction calculation) to determine the average inside wall temperature, $\bar{T}_{wi}$.

The physical and thermodynamic properties of the ethylene glycol/water mixture (density, dynamic viscosity, thermal conductivity, heat capacity) were determined using equations and figures from Cragoe [Ref. 22] and Gallant [Ref. 23] and correlated by Mabrey [Ref. 5]. From these quantities, the coolant mass flow rate was calculated by:

$$\dot{m} = V_c \rho_c A_i \qquad (5.1)$$

where A_i is the inside cross sectional area of the tube and V_c is the set coolant velocity. The coolant Reynolds number, Re_D was calculated by:

46

$$Re_D = \frac{V_c D_i \rho_c}{\mu_c} \qquad (5.2)$$

where D_i is the inside diameter of the tube. The dimensionless distance (x^*) in the flow direction is calculated as:

$$x^* = \frac{x/D_i}{Re_D Pr} \qquad (5.3)$$

where x is the axial distance from the beginning of the heated length.

To determine the heat transfer rate to the coolant, several factors were considered. The basic equation to determine the heat transfer rate is given by:

$$\dot{q} = \dot{m} c_p \Delta T \qquad (5.4)$$

where ΔT is the measured coolant temperature rise along the tube. The temperature rise required is that for the actual heated length of the tube that is subjected to the constant heat flux condition, ΔT_{HL}. To determine ΔT_{HL} from ΔT, corrections have to be made to account for heat loss, heat leakage and heat transferred to the unheated ends. Figure 5.1 depicts a typical tube and the correction terms considered in the heat balance.

The overall ΔT is first corrected for heat loss to the ambient, ($\dot{q}_{loss}$) and heat leakage into the system, ($\dot{q}_{leak}$). The heat leakage term consisted of any temperature rise due to the influx of heat from ambient as well as that caused by frictional effects. Appendix D discusses the experiments conducted to determine both this heat loss and heat leakage correction.

47

TEMPERATURE RISE CORRECTIONS
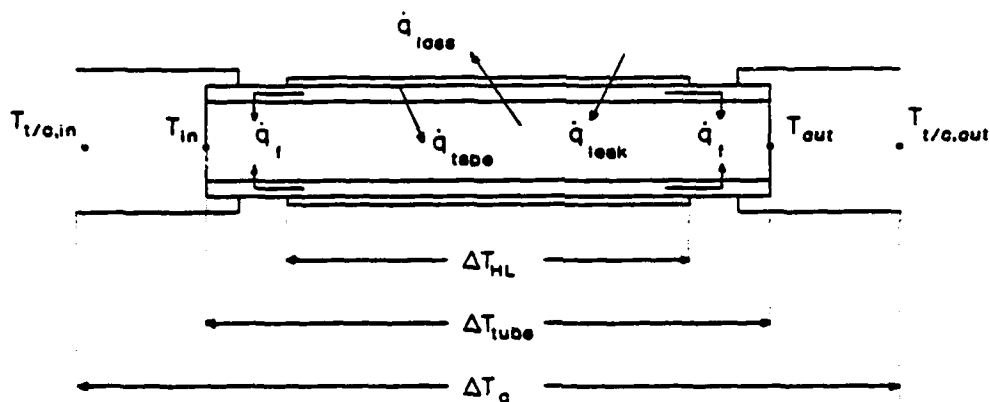
Figure 5.1 Temperature Rise Corrections.

To take account of the heat transferred to the coolant from the unheated ends, the heat transfer rate to the coolant over the entire length of the tube (heated and unheated) is first calculated. The average heat transfer coefficient can then be determined by:

$$\overline{h}_i = \frac{\dot{q}_{HL}}{A_i LMTD} \qquad (5.5)$$

where A_i is the inside surface area based on the heated length (L_H) and LMTD is the log mean temperature difference defined as:

At this point in the calculation, however, the heat transfer rate to the coolant from the heated length alone ($\dot{q}_{HL}$) is not known. Since the heating elements did not

48

$$LMTD = \frac{T_{out} - T_{in}}{\ln\left[\dfrac{T_{wi} - T_{in}}{T_{wi} - T_{out}}\right]} \tag{5.6}$$

cover the entire length of the tube, account must be taken of heat added to the coolant from the unheated lengths at the inlet and outlet of the tube. This was accomplished by considering these ends as annular fins. An adiabatic fin tip and outer wall boundary condition was applied and the heat transfer from the fins, $\dot{q}_f$ (as given by Incopera and Dewitt [Ref. 10]), determined from:

)

$$\dot{q}_f = \sqrt{\overline{h}_i P k A_c}\;\; \theta_b \tanh m L_f$$

where L_f = fin length

P = fin perimeter = πDi

A_c = fin cross sectional area

$$= \frac{\pi}{4}(D_o^2 - D_1^2)$$

$\theta_b = \overline{T}_{wi} - T_{in}$ (for inlet fin)

$= \overline{T}_{wi} - T_{out}$ (for outlet fin)

$$m = \left[\frac{h_i P}{k A_c}\right]^{0.5}$$

49

The fin calculation requires a known average inside heat transfer coefficient ($\bar{h}_i$).
Therefore, an initial estimate of $\bar{h}_i$ is calculated by:

$$\bar{h}_i = \frac{\dot{q}_{tube}}{A_i LMTD} \qquad (5.8)$$

where $\dot{q}_{tube}$ is known. The amount of heat that passes through the unheated ends is
then calculated using the fin correction above. The heat transfer rate to the coolant
from the heated length ($\dot{q}_{HL}$) is then calculated by:

$$\dot{q}_{HL} = \dot{q}_{tube} - \dot{q}_f \qquad (5.9)$$

A new average inside heat transfer coefficient ($\bar{h}_i$) can then be calculated using
equation 5.5 and an iteration process carried out until convergence to a final average
inside heat transfer coefficient is reached.

An additional correction for the Cu/Ni finned tube is needed to account for the
change in inside diameter of the smooth ends (needed to fit through the tube sheet
in the condenser). The heat transfer coefficient based on the smaller inside diameter
corresponding to the finned portion of the tube is what ultimately is desired. As
shown in Figure 5.2, the heated length extended beyond the smaller diameter section.
To correct for this, the annular fin correction discussed earlier was applied to
determine the temperatures at the inlet and outlet of the heated length. The coolant
temperature rise along the heated length was assumed to be linear, and therefore the
temperature rise along the smooth larger inside diameter lengths (L_1 and L_2) could
be determined by the simple ratio:

$$\Delta T_1 = \frac{L_1 \Delta T_{HL}}{L_{HL}} \quad and \quad \Delta T_2 = \frac{L_2 \Delta T_{HL}}{L_{HL}} \tag{5.10}$$

where L_{HL} is the heated length of the tube and ΔT_{HL}, the temperature rise along the heated length. These corrections were then added or subtracted from the corrected finned inlet and outlet temperatures.

Cu/Ni EXTERNALLY FINNED TUBE TEMPERATURE RISE CORRECTIONS
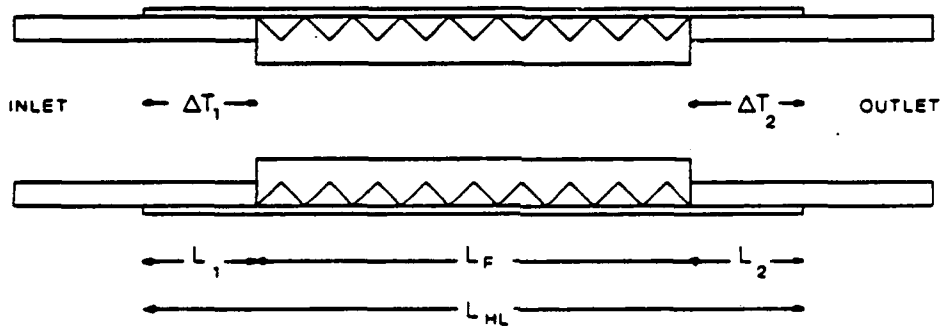
Figure 5.2 Cu/Ni Finned Tube Temperature Rise Corrections.

With the average inside heat transfer coefficient known, the mean Nusselt number can be determined by:

$$Nu_m = \frac{\bar{h}_i D_i}{k} \tag{5.11}$$

where k is the thermal conductivity of the ethylene glycol/water mixture.

The experimentally determined mean Nusselt number was then compared to various theoretical and experimental correlations, based on the insert condition. These correlations were discussed earlier but are briefly mentioned here.

For the no insert condition, the data were compared to two theoretical correlations, the Hausen correlation [Ref. 10] given by:

$$Nu_m = 3.66 + \frac{0.0668(D/L)Re_D Pr}{1 + 0.0\cdot[(D/L)Re_D Pr]^{2/3}} \qquad (5.12)$$

and the Shah and London correlation [Ref. 9] given by:

$$Nu_m = 1.93(x^*)^{-1/3} \qquad (5.13)$$

The reader is reminded that the Hausen correlation is for a uniform wall temperature boundary condition and was used in Mazzone's condensation experiments [Ref. 6]. The Shah and London correlation is for a constant wall heat flux condition. It should also be noted that equation 5.13 is used since x^* for the test section was always less than 0.03.

For the twisted tape insert the experimental mean Nusselt number was compared to the correlation developed by Hong and Bergles [Ref. 15]:

$$Nu_m = 0.383Pr^{0.35}(Re_s/y)^{0.622} \qquad (5.14)$$

Equation 5.14 is used because values for Re_s/y were always greater than 10.

For the HEATEX insert, the data were compared to the two correlations developed by Mazzone [Ref. 6]. For the 13.26 mm inside diameter tube, the equation is given by:

$$Nu_m = 0.226 Re^{0.65} Pr^{0.46} \qquad (5.16)$$

and for the 10.16 mm inside diameter tube by:

$$Nu_m = 0.063 Re^{0.76} Pr^{0.46} \qquad (5.16)$$

B. ADDITIONAL TUBE LENGTHS

In addition to the above calculations for the entire tube length, mean Nusselt numbers for three additional tube "lengths" could be determined. This was accomplished by sectioning the heated length of the tube into four cells as shown in Figure 5.3. Each cell contained one longitudinal thermocouple position. Three additional tube lengths were then determined by adding cell lengths together. The first length, L_1, consisted of cell 1 alone, L_2 consisted of cells 1 and 2 and L_3 consisted of cells 1, 2 and 3. The fourth length was actually the entire heated length as previously discussed.

The coolant temperature rise along the heated length of the tube was assumed to be linear. The correction to the wall heat flux to account for variation in electrical resistance with temperatures was assumed to be negligible. Therefore, the temperature rise along each cell could be determined by:

SECTIONED TUBE
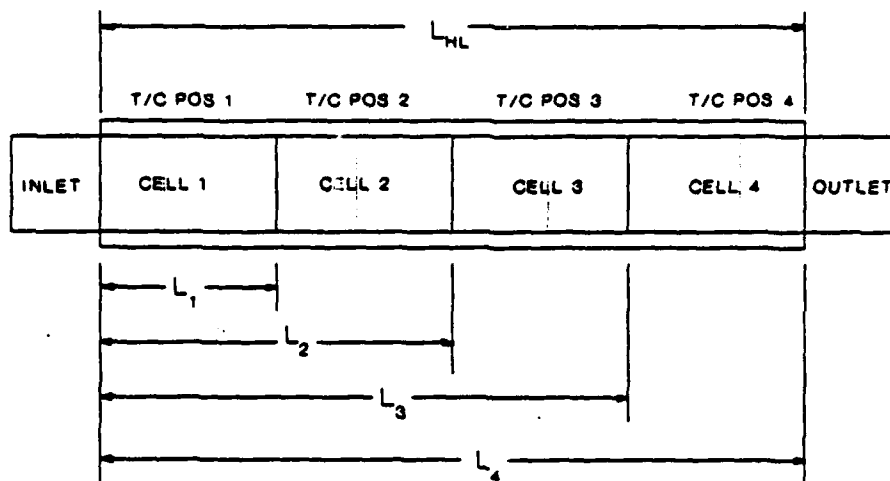
Figure 5.3 Additional Tube Lengths.

$$\Delta T_{cell} = \frac{\Delta T_{HL}}{4} \tag{5.17}$$

Average inside wall temperatures were based on the thermocouples within that tube "length." Therefore, the temperature rise, heat flux and average inside wall temperatures were all known for each tube length. Applying the same calculation method as before, the mean Nusselt number for these three additional tube "lengths" could be calculated.

This adaption to the program was not done until after the smooth tube experiments had been completed; however, this extra data were taken for the remaining two tubes.

C. LOCAL NUSSELT NUMBERS

The program was also adapted to determine local inside heat transfer coefficients at the four axial thermocouple positions. Corrections discussed earlier to determine the temperatures at the inlet and outlet of the heated length were first accounted for. Exact thermocouple longitudinal positions were entered into the program as L/D ratios so that a local x^* could also be calculated. Again, the temperature rise along the heated length was assumed to be linear; therefore, the bulk coolant temperature at the particular thermocouple position could be determined by the simple ratio method discussed earlier (equation 5.10).

The local heat transfer coefficient, h_{xi}, was then determined by:

$$h_{xi} = \frac{q''}{T_{wi} - T_c} \qquad (5.13)$$

where $\bar{T}_{wi}$ is the average inside wall temperature based on the three thermocouples at that position and T_c is the bulk coolant temperature at that position. The local Nusselt number was then given by:

$$Nu_x = \frac{h_{xi} D_i}{k} \qquad (5.19)$$

The local Nusselt number for all four thermocouple positions was then determined.

For the smooth tube experiments, local Nusselt numbers were calculated only for position 1. The program was later adapted to include local calculations at positions 2, 3, and 4 for the Cu/Ni finned tube and Korodense tube.

55

VI. RESULTS AND DISCUSSION

A. GENERAL

The experimental heat transfer results are initially presented in terms of the mean Nusselt and Reynolds numbers for all insert conditions. From these graphs, it can be seen how the Nusselt number is inlet temperature dependent, indicating the need for a Prandtl number (raised to an exponent) in the final correlation. However, although not specifically shown, the data shows no dependence on the heat flux setting. In addition, the Nu vs. Re graphs for the no insert condition show when a transition to turbulent flow occurs.

The heat transfer results are then compared to existing correlations based upon the insert condition. For the no insert condition, the Nusselt number is plotted against x^* (dimensionless x coordinate). Note that for a given tube, L/D is constant and x^* varies due to Re and Pr changes. The data are then compared to the Hausen [Ref. 10] correlation (equation 2.10) and the Shah and London [Ref. 9] correlation (equation 2.14). Recall that the Hausen correlation is for a uniform wall temperature boundary condition and was used by Mazzone [Ref. 6] in the refrigerant condensation experiments. Since the present data were taken under a constant heat flux boundary condition, comparison with the Shah and London correlation was also required. The twisted tape insert data are compared to the correlation developed by

Hong and Bergles [Ref. 15] (equation 2.20) which was also used by Mazzone. The HEATEX insert data are compared to the two correlations developed from the limited data received from CAL-GAVIN by Mazzone (equations 2.27 and 2.28).

Correlations are developed for each tube and insert condition based upon a least squares linear regression. An r-squared value, a measure of the accuracy of the least squares curve fitting to the data, is used to determine the uncertainty of the correlation. The correlations and the corresponding r-squared values are summarized in Table 6.1. Note that the 0.2 m/s and 0.3 m/s data were eliminated prior to developing all correlations due to the high degree of uncertainty in these data points.

TABLE 6.1 SUMMARY OF CORRELATIONS

SUMMARY OF CORRELATIONS

	NO INSERT	TWISTED TAPE	HEATEX
SMOOTH TUBE	Nu = 4.137Xstar^-0.234 r-sq = 71.9%	Nu = .512Pr^.35(Res/y)^.568 r-sq = 99.5%	Nu = .184Pr^.46Re^.641 r-sq = 98.9%
EXT FINNED TUBE	Nu = 1.84Xstar^-0.341 r-sq = 93.0%	Nu = .148Pr^.35(Res/y)^.687 r-sq = 96.7%	Nu = .126Pr^.46Re^.657 r-sq = 95.9
KORODENSE TUBE	Nu = 2.047Xstar^-0.326 r-sq = 89.2%	Nu = .569Pr^.35(Res/y)^.498 r-sq = 98.9%	Nu = .282Pr^.46Re^.499 r-sq = 94.3%

B. SMOOTH TUBE

1. Smooth Tube - No Insert

The first tube tested was the copper smooth tube with no insert. Heat transfer data is presented in Figure 6.1 in terms of the Nusselt number as a function of Reynolds number for each nominal inlet temperature. The first thing to notice is the sudden increase in Nu at a Re number of about 2300. This is indicative of a change from laminar to transition flow where the heat transfer is greatly increased due to improved mixing. This contradicts Mazzone's [Ref. 6] assumption of a transition to turbulence occurring at Re > 4000. The data in the transition region was primarily for the +20°C and +10°C nominal inlet temperatures. Figure 6.1 also shows distinct groupings of data at given inlet temperatures, indicating a Prandtl number effect. These groupings are shown more clearly in Figure 6.2 which represent data under laminar flow conditions only (Re ≤ 2300) and Figure 6.3 for data in the transition region only (Re > 2300).

To develop a useful heat transfer correlation, the mean Nusselt number is plotted as a function of x* in Figure 6.4. Recall that x* can be determined by:

$$x^* = \frac{L/D}{Re_D Pr} \qquad (2.9)$$

For a given tube, L/D is a fixed quantity. Therefore, for a given Prandtl number (essentially fixed inlet temperature), x* is dependent only upon the Reynolds number.

58

Figure 6.4 also shows a comparison of the experimental data with the Hausen correlation (equation 2.10) for a uniform wall temperature (used by Mazzone) and the Shah and London correlation (equation 2.14) for a constant heat flux. The Hausen correlation appears to significantly underestimate the heat transfer coefficient found in the present experimental data, i.e., the present experimental data indicate a lower inside thermal resistance. This is consistent with Mazzone's [Ref. 6] results in that the Hausen correlation was predicting larger inside resistances than the overall measured resistance. However, it must always be remembered that the Hausen correlation is for a uniform wall temperature boundary condition and this would indeed lead to lower heat-transfer coefficients.

The data also fall slightly above (but parallel to) that predicted by the Shah and London correlation. Due to the constant heat flux boundary condition used by Shah and London, one may expect better agreement (as seen). However, the fact that the data fall slightly above can be attributed to secondary flow induced by the apparatus inlet conditions (90° bend due to the thermocouple well). Also, as before, a departure from laminar flow can be seen in Figure 6.4. Since the transition data forms two distinct lines (+20°C and +10°C), it indicates that x^* is not a good correlating parameter for transitional flow.

After removal of the transitional flow data, a correlation was developed based upon the form of the Shah and London correlation. The resulting present

correlation for the mean Nusselt number for laminar flow with no insert is given by:

$$Nu_m = 4.137(x^*)^{-0.234} \qquad (6.1)$$

Equation 6.1 and the Hausen correlation, equation 2.10, are both shown in Figure 6.5 with the present laminar flow data. The general form of Figure 6.5 is explained by the fact that at low x^* (high Re) the heat transfer is improved due to slightly better mixing. As x^* increases (coolant velocity decreases), the heat transfer decreases.

Figure 6.5 also shows a high degree of scatter in the data. Initially, it was thought that this scatter was due to the flow not being hydrodynamically fully developed. However, it is seen to be more pronounced at large x^*. Recall that for a given nominal inlet temperature, large x^* represents a low Reynolds number. For a low Reynolds number, the hydrodynamic entry length (given by $X/D = 0.05Re$) is the shortest. Also, since we are dealing with relatively large Prandtl numbers (30-140), the assumption that the velocity profile is fully developed throughout the thermal entry region should be fairly valid. Therefore, it is felt that this scatter is not due to the flow being hydrodynamically undeveloped.

This scatter is believed to be due to the effects of the different inlet temperatures, indicating that x^* is not an ideal correlating parameter. That is to say, the Prandtl number exponent needs to be adjusted to account for the different inlet temperatures. It should also be noted that due to the high degree of detail in Figure

6.5, the scatter appears more pronounced. However, in Figure 6.4 with larger scale increments, the scatter seems minimal.

2. Smooth Tube - Twisted Tape

Results for the smooth tube with a twisted tape insert are shown in Figures 6.6 and 6.7. A definite Prandtl number dependence can be seen in Figure 6.6 where the mean Nusselt number is presented as a function of Reynolds number. Following the guidance of Hong and Bergles [Ref. 15] the dimensionless parameters Re_s and y were combined as one parameter Re_s/y and the mean Nusselt number and Prandtl number were combined as $Nu/Pr^{0.35}$. The final correlation shown in Figure 6.7 is:

$$Nu_m = 0.512 Pr^{0.35} (Re_s/y)^{0.568} \qquad (6.2)$$

This correlation is in close agreement with the Hong and Bergles correlation (equation 2.20). The slight differences can be attributed to differences in the experimental apparatus (including the insert itself) and the possible existence of secondary flows. Figure 6.7 shows little inlet temperature dependence, indicating that the Prandtl number exponent of 0.35 is probably fairly accurate. Furthermore, there is little experimental data scatter, giving increased confidence in this correlation.

3. Smooth Tube - HEATEX Insert

HEATEX insert results for a smooth tube are shown in Figures 6.8 and 6.9. Again, on a Nu vs. Re basis, it can be seen from Figure 6.8 that there is a definite dependence on the inlet temperature. Using the same form as the

61

correlation of Oliver and Aldington [Ref. 20], the resulting correlation for the mean Nusselt number is:

$$Nu_m = 0.164 Pr^{0.46} Re^{0.641} \tag{6.3}$$

This is compared in Figure 6.9 to the correlation developed and used by Mazzone (equation 2.23). It is clearly evident that Mazzone's correlation underpredicts the inside thermal resistance and therefore gives a larger inside heat transfer coefficient. Again, Figure 6.9 shows little dependence on inlet temperature indicating that the Prandtl number exponent is fairly accurate. Comparisons of the enhancement in heat transfer gained by the use of HEATEX and twisted tape insert, over the no insert condition are given section F of this chapter.

SMOOTH TUBE - NO INSERT
Nu vs Re
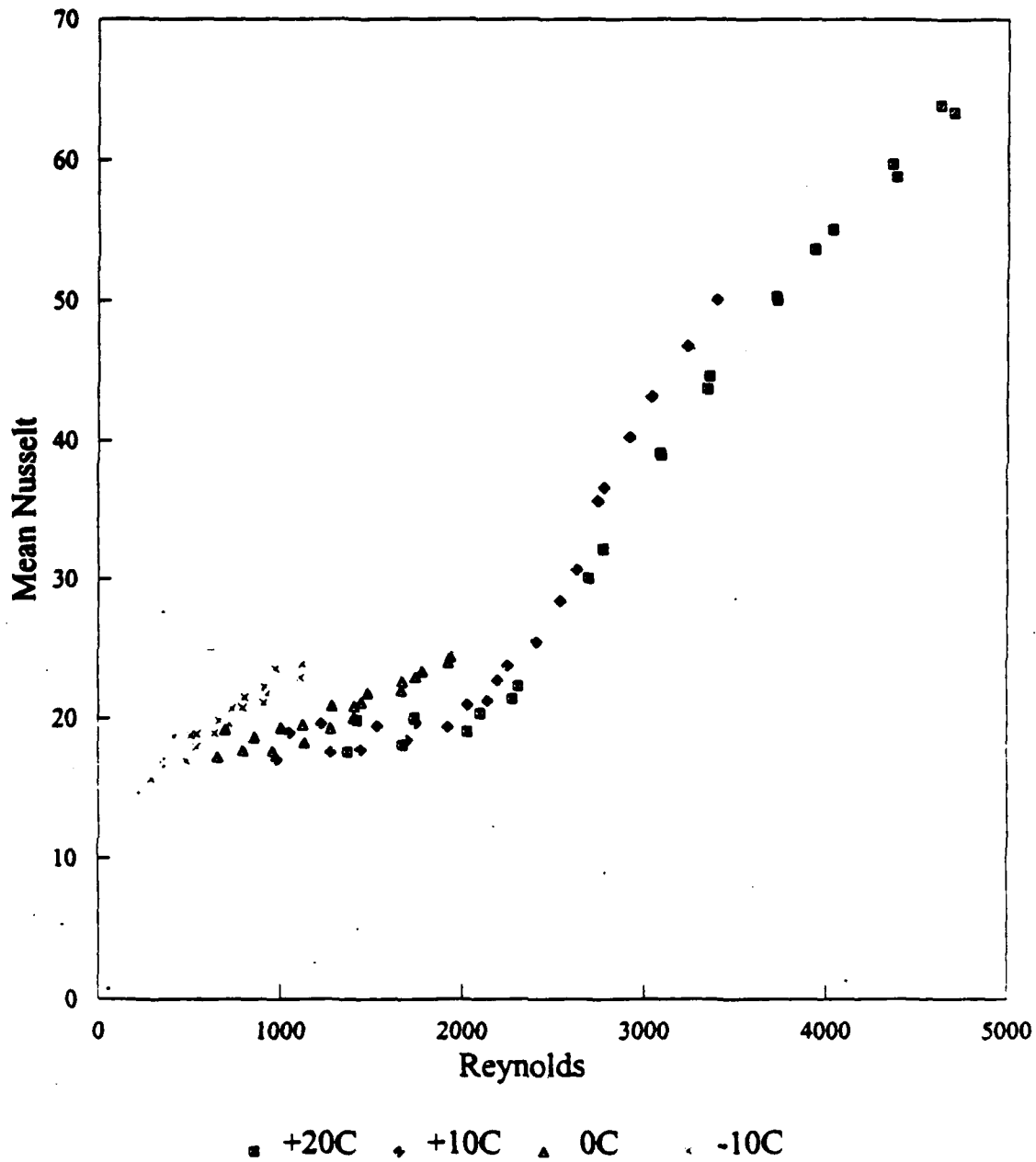
Figure 6.1 Smooth tube - No insert (Nu$_m$ vs. Re) results.

SMOOTH TUBE - NO INSERT
LAMINAR FLOW
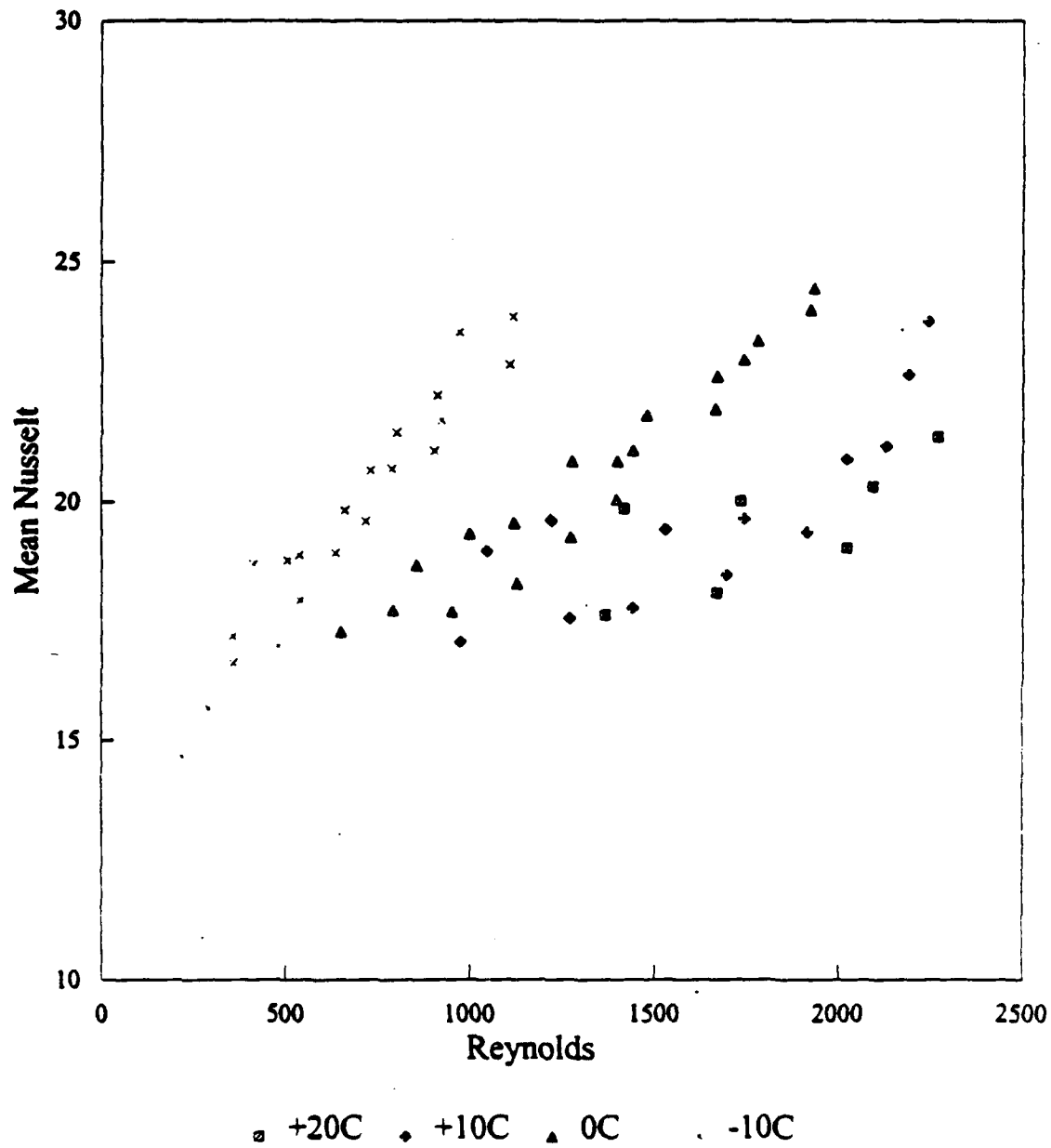
Figure 6.2 Smooth tube - No insert (Nu$_m$ vs. Re) laminar flow results.

64

SMOOTH TUBE - NO INSERT
TRANSITIONAL FLOW
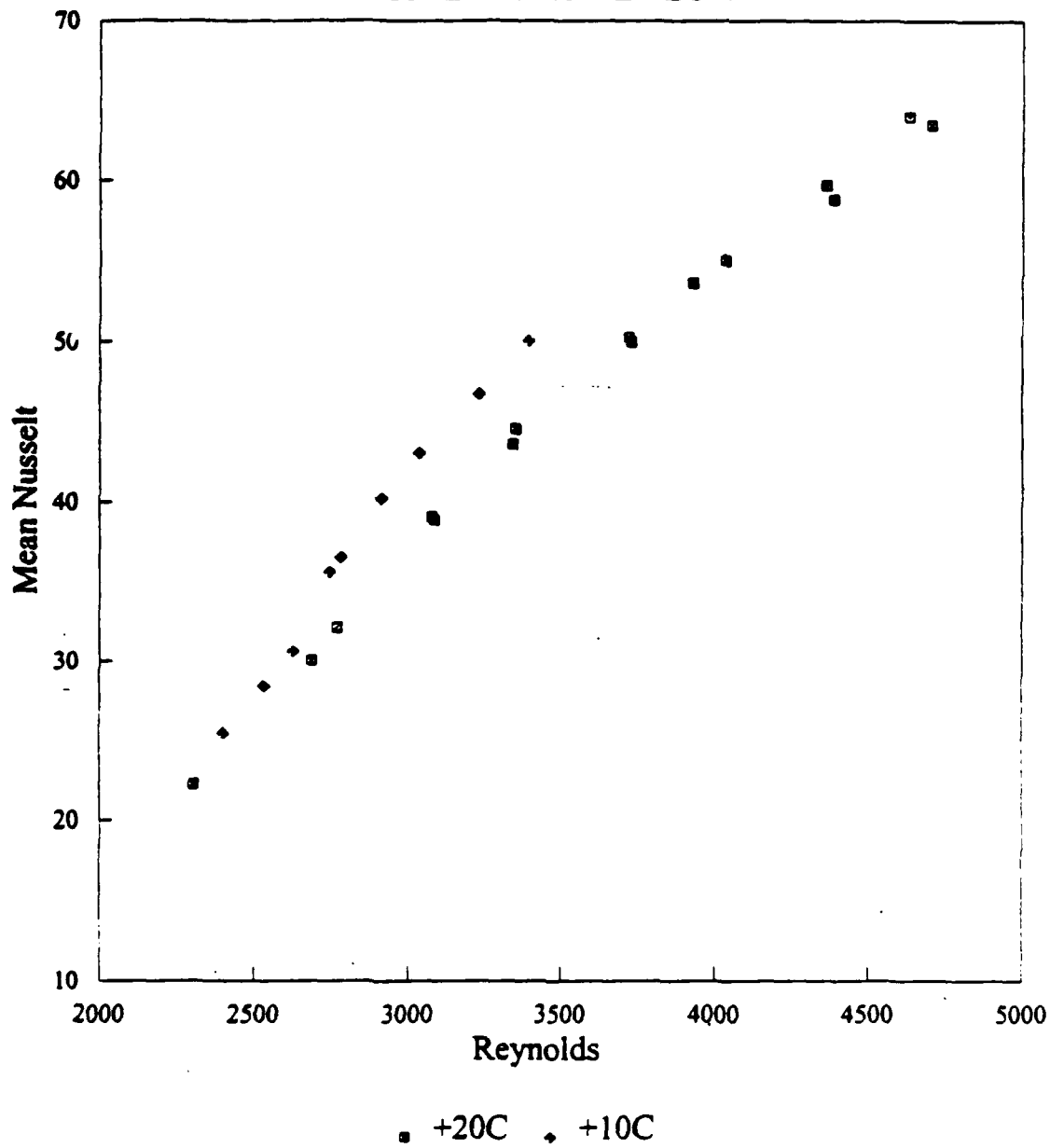
Figure 6.3 Smooth tube - No insert (Nu_m vs. Re) transitional flow results.

SMOOTH TUBE - NO INSERT

Nu vs Xstar
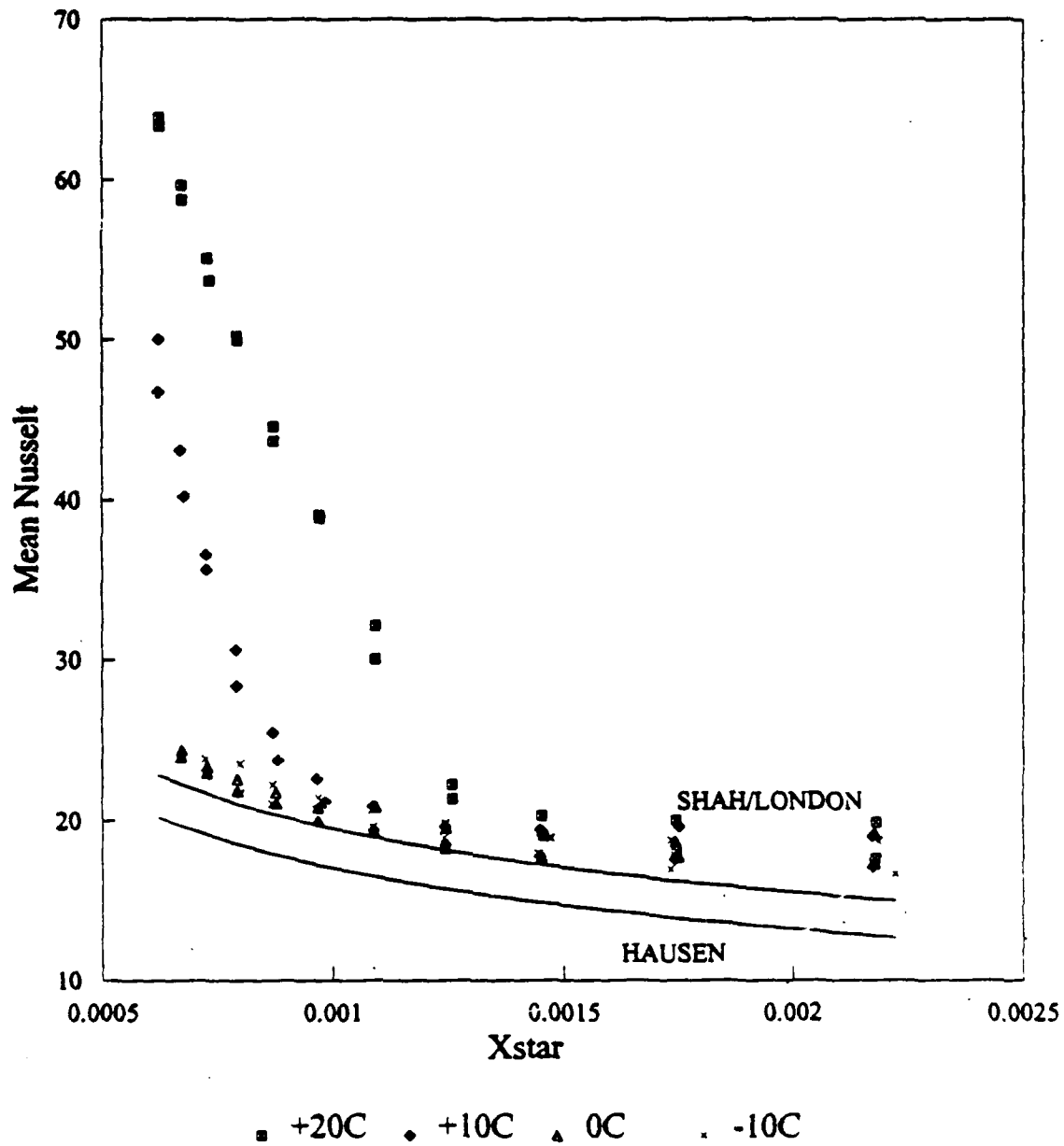
Figure 6.4   Smooth tube - No insert (Nu_m vs. x^*) results.

SMOOTH TUBE - NO INSERT
LAMINAR FLOW

Nu = 4.14Xstar^-0.234

HAUSEN

▪ +20C   ✦ +10C   ▲ 0C   . -10C

Nu vs Xstar
SMNIXNULAM
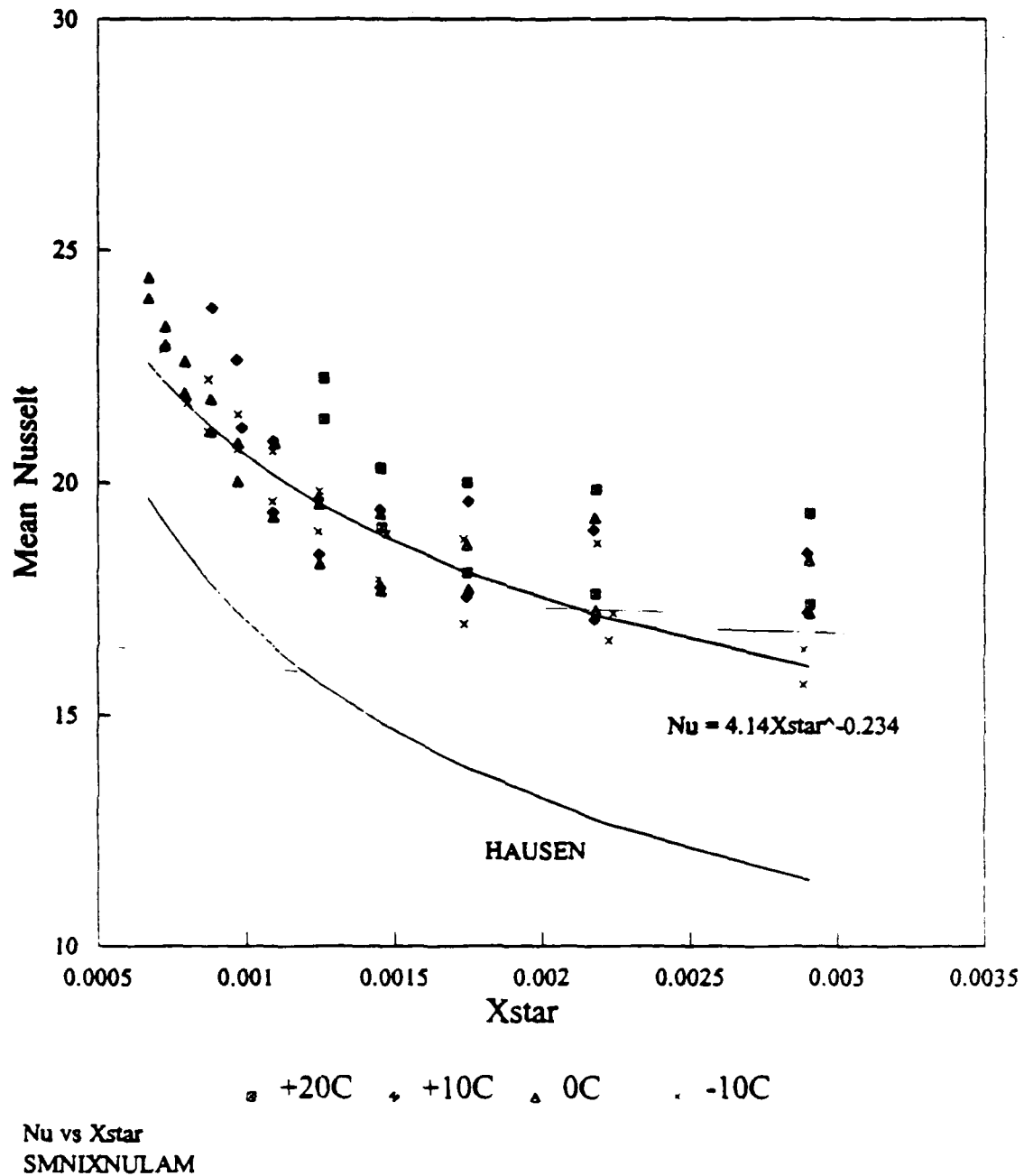
Figure 6.5 Smooth tube - No insert laminar flow correlation results.
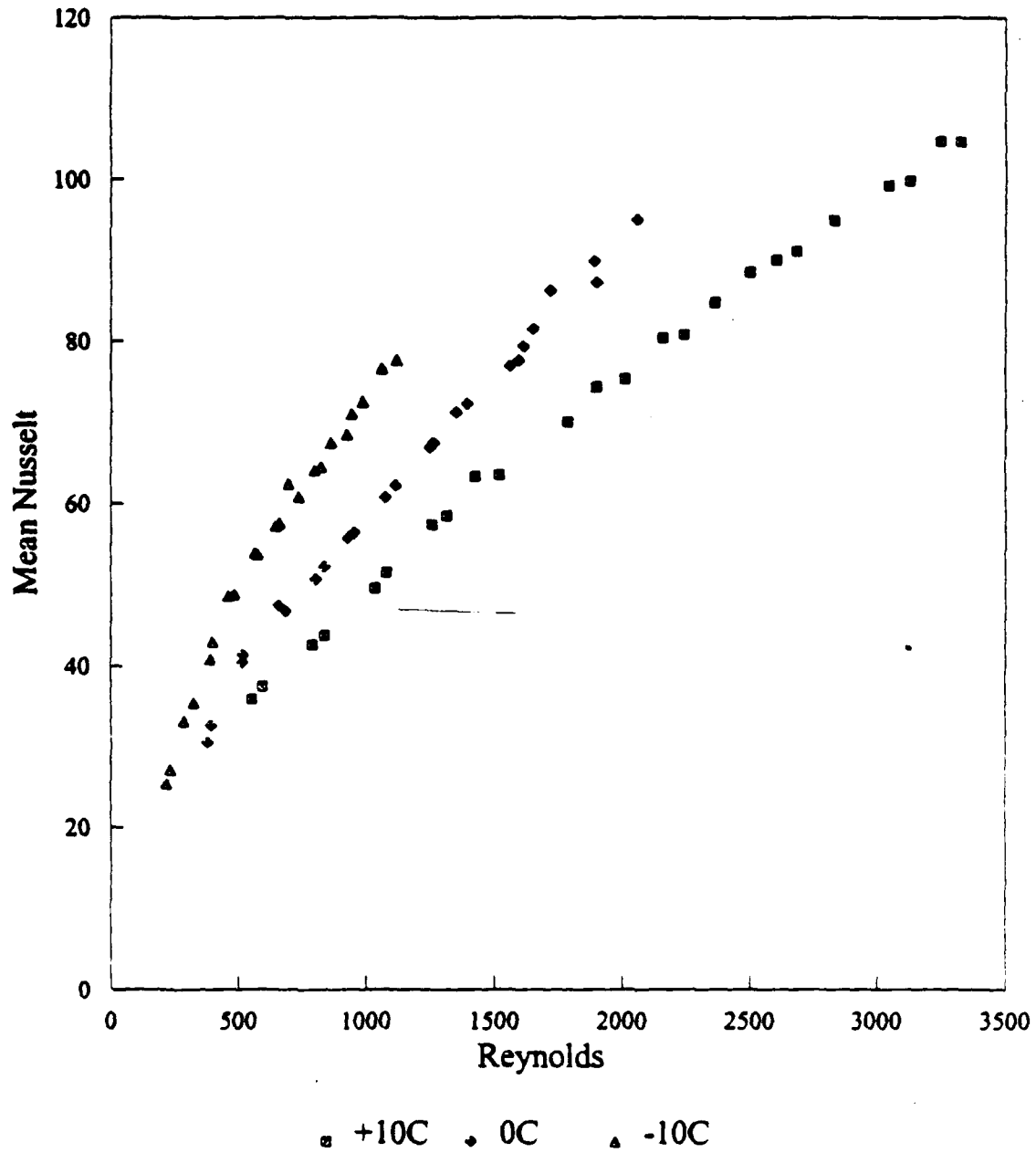
Figure 6.6 Smooth tube - Twisted tape (Nu$_m$ vs. Re) results.

SMOOTH TUBE - TWISTED TAPE
(Nu/Pr^.35) vs (Res/y)

$Nu = 0.383Pr^{0.35}(Res/y)^{0.622}$

$Nu = 0.512Pr^{0.35}(Res/y)^{0.568}$

Res/y

Nu/Pr^.35
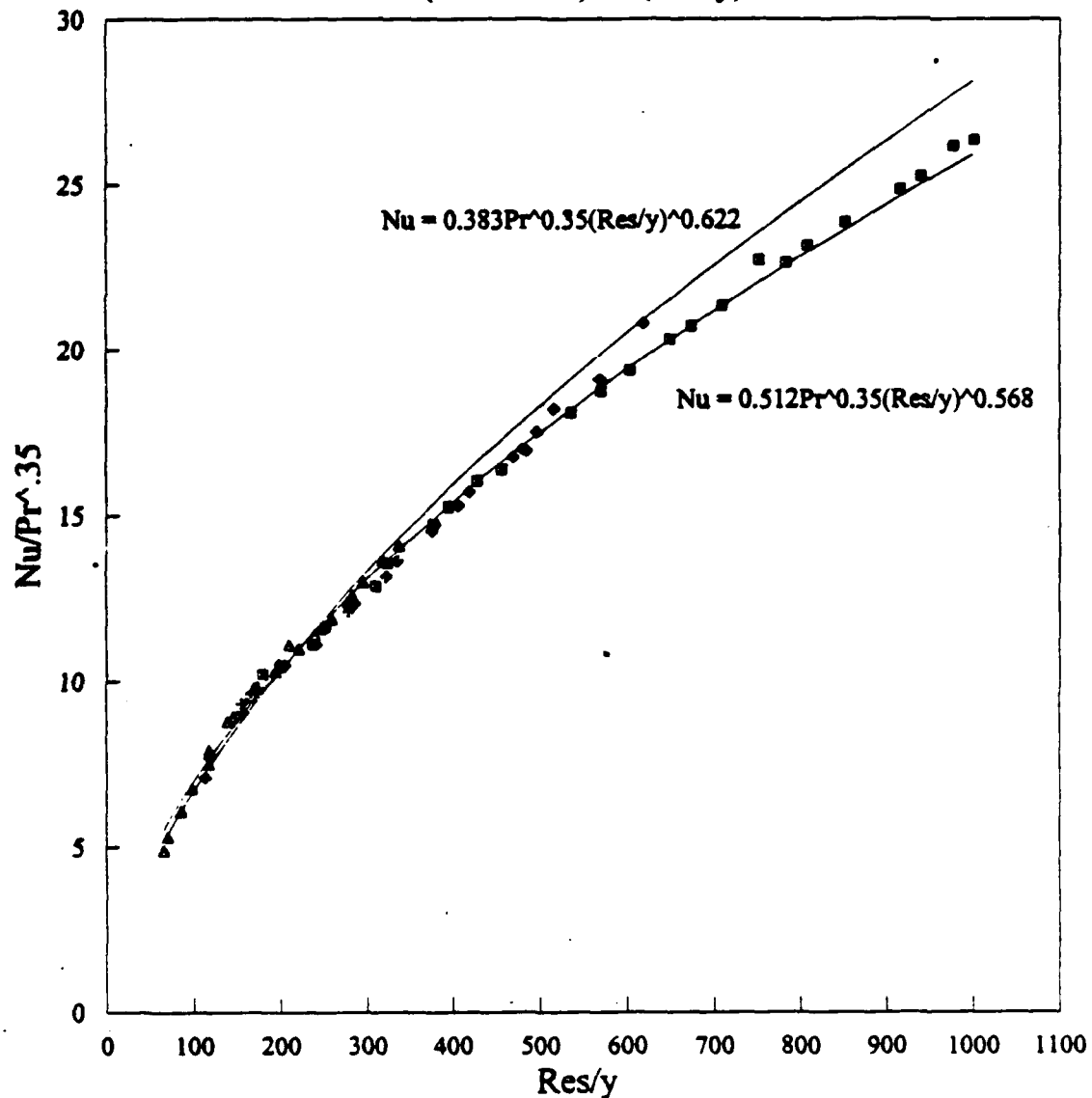
◼ +10C   ◆ 0C   △ -10C

Res = (ṁDi)/(Asμ) , y = H/Di
SMTTNUPR

Figure 6.7 Smooth tube - Twisted tape correlation results.

69

Figure 6.8 Smooth tube - HEATEX (Nu$_m$ vs. Re) results.

SMOOTH TUBE - HEATEX
(Nu/Pr^.46) vs Re

Nu = 0.226Pr^0.46Re^0.65

Nu = 0.164Pr^0.46Re^0.641

Nu/Pr^.46

Reynolds

■ +20C ◆ +10C ▲ 0C × -10C
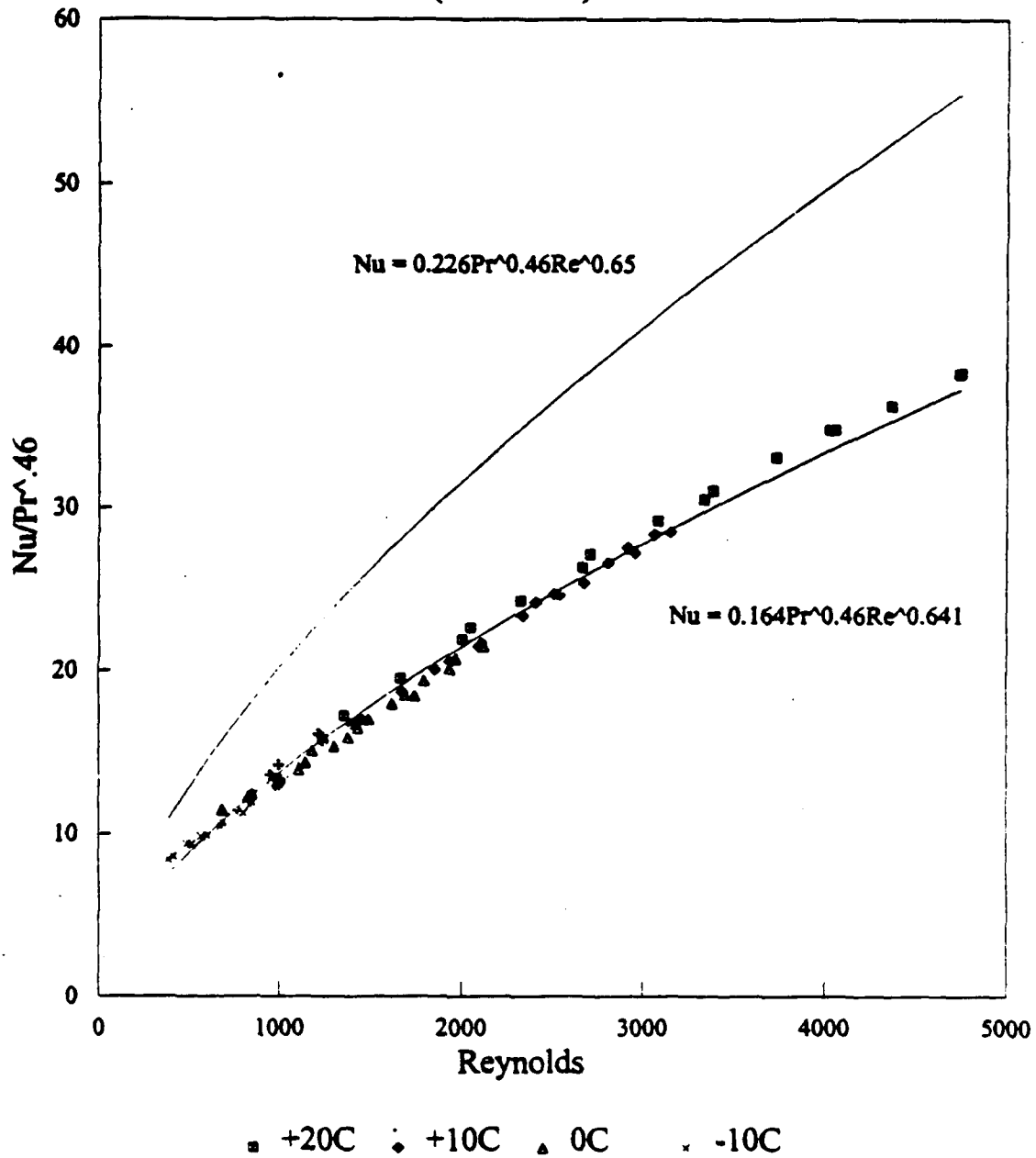
SMHXNUPR

Figure 6.9 Smooth tube - HEATEX correlation results.

C. CU/NI EXTERNALLY FINNED TUBE

1. Cu/Ni Finned Tube - No Insert

The second tube tested was the Cu/Ni externally finned tube. Recall that this tube has a smaller inside smooth diameter than the smooth tube (10.15 mm vs. 13.26 mm). The no insert results for the mean Nusselt number as a function of Reynolds number are shown in Figure 6.10 and in more detail in Figures 6.11 and 6.12 for laminar and transitional flows, respectively. It can be seen that a slightly higher Reynolds number (Re $\approx$ 2700) for the departure from laminar flow exists for this tube. Again, the dependence on inlet temperature is clearly evident.

The data are compared to the Hausen correlation (equation 2.10) and the Shah and London correlation (equation 2.14) in Figure 6.13. As expected, the Hausen correlation again underpredicts the inside heat transfer coefficient. However, the laminar flow data is in closer agreement with the Shah and London correlation than they were for the smooth tube. This can be attributed to the different diameter affecting the thermal boundary layer development. The resulting correlation for the laminar flow mean Nusselt number is shown in Figure 6.14 and is given by:

$$Nu_m = 1.84 (x^*)^{-0.341} \tag{6.4}$$

The same conclusions about data scatter can be drawn as for the smooth tube results, although in general the scatter seems to be less.

2. Cu/Ni Finned Tube - Twisted Tape Insert

Figures 6.15 and 6.16 show the results for the Cu/Ni finned tube using a twisted tape to enhance tubeside heat transfer. The inlet temperature dependence in Figure 6.15 seems to be reduced, but still evident. The form of the correlation was again that of Hong and Bergles' correlation. It was developed in the same manner as for the smooth tube and is given by:

$$Nu_m = 0.148 Pr^{0.35} (Re_a/y)^{0.687} \qquad (6.5)$$

The data and resulting correlation are compared to the Hong and Bergles correlation (equation 2.20) in Figure 6.16 where the latter is seen to overpredict the mean Nusselt number. This difference can be attributed to several factors. A small diameter tube with a larger diameter smooth entrance length could cause severe secondary flows. Also, because of the smaller diameter tube a different size twisted tape (twist ratio, y=3) was used, which had a slightly looser fit than the tape used with the smooth tube. Additionally, Prandtl number effects need to be investigated more closely, as Figure 6.16 shows a definite trend with inlet temperature.

3. Cu/Ni Finned Tube - HEATEX Insert

Data for the Cu/Ni finned tube using the HEATEX insert are presented in Figures 6.17 and 6.18. Figure 6.17 (Nu vs. Re) again shows a dependence of the data on the coolant inlet temperature. Since the HEATEX element used for this tube was a smaller diameter (10.16 mm) with a different loop density than that used for the smooth tube, a new correlation needed to be developed. Again, using the

73

form of the correlation proposed by Oliver and Aldington, the final proposed correlation is given by:

$$Nu_m = 0.126 Pr^{0.46} Re^{0.657} \qquad (6.6)$$

The data and resulting correlation are compared to the correlation developed by Mazzone (equation 2.24) for this insert in Figure 6.18. It can be seen that Mazzone's correlation is adequate for predicting the inside heat transfer coefficients at low Reynolds number (Re < 1400), where both correlations merge. However, at higher Reynolds numbers, Mazzone's correlation overpredicts the present experimental data. The differences in the two correlations are primarily due to the limited amount of data available to Mazzone when developing his correlation. Furthermore, the data he used were taken on a different experimental facility (by the manufacturers). As seen before, the data shown in Figure 6.18 still indicate a dependence on inlet temperature and hence the value of 0.46 for the Prandtl number exponent needs to be reinvestigated and optimized.

Cu/Ni FINNED TUBE - NO INSERT
Nu vs Re
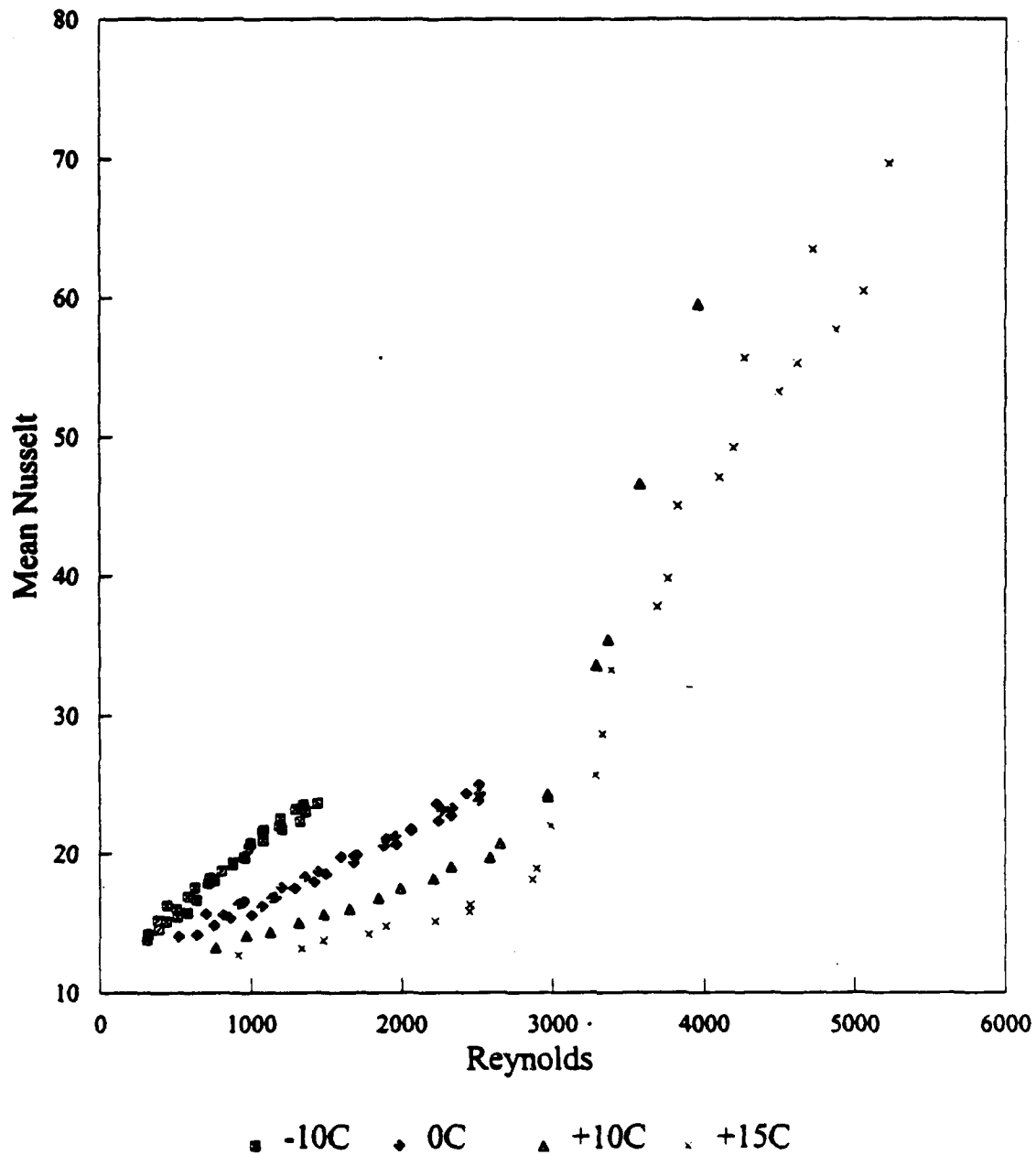
CFNINURE

Figure 6.10 Cu/Ni externally finned tube - No insert (Nu$_m$ vs. Re) results.

Figure 6.11 Cu/Ni externally finned tube - No insert (Nu_m vs. Re) laminar flow results.

Cu/Ni FINNED TUBE - NO INSERT
TRANSITIONAL FLOW
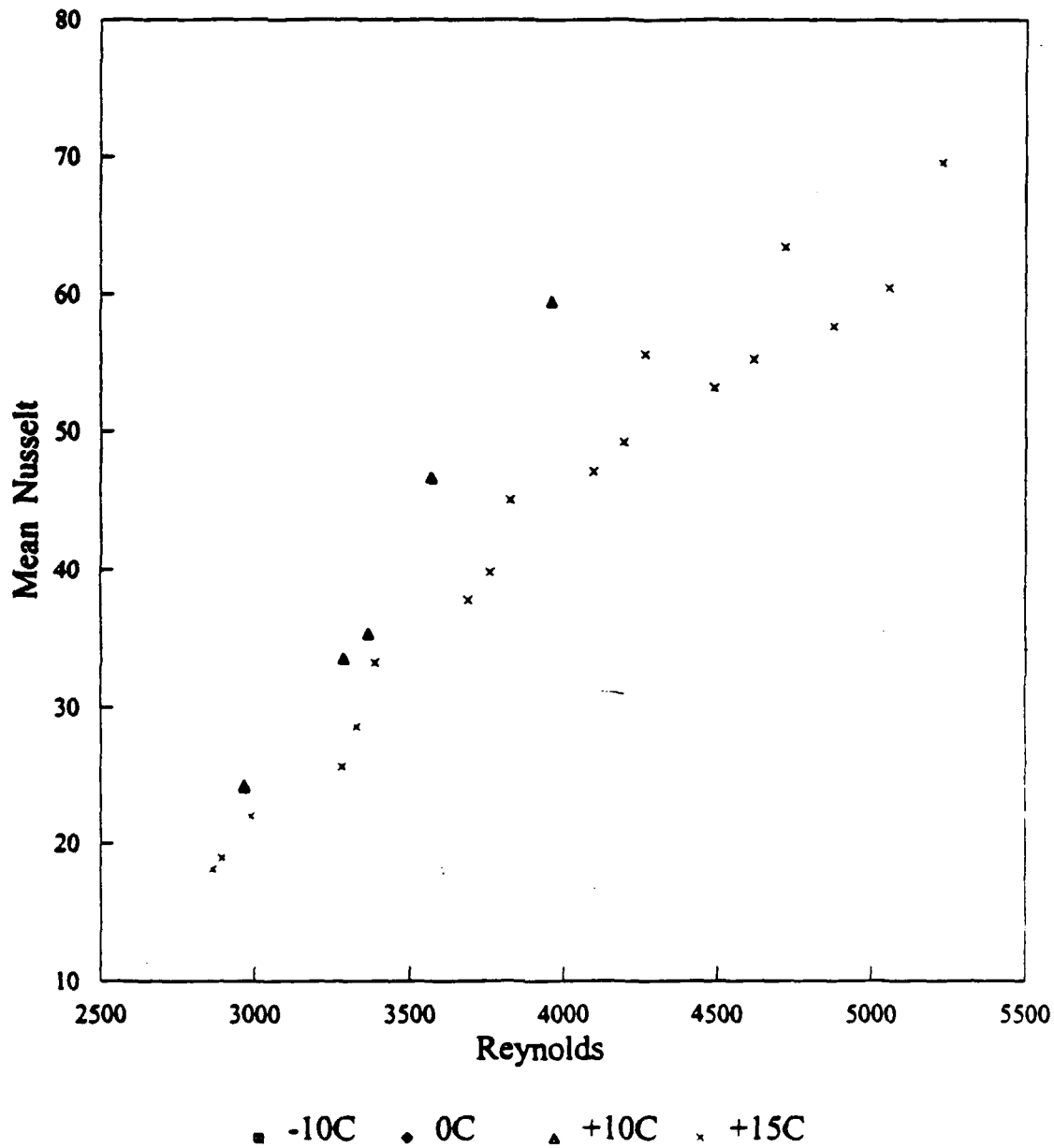
Figure 6.12 Cu/Ni externally finned tube - No insert (Nu_a vs. Re) transitional flow results.

Cu/Ni FINNED TUBE - NO INSERT
Nu vs Xstar
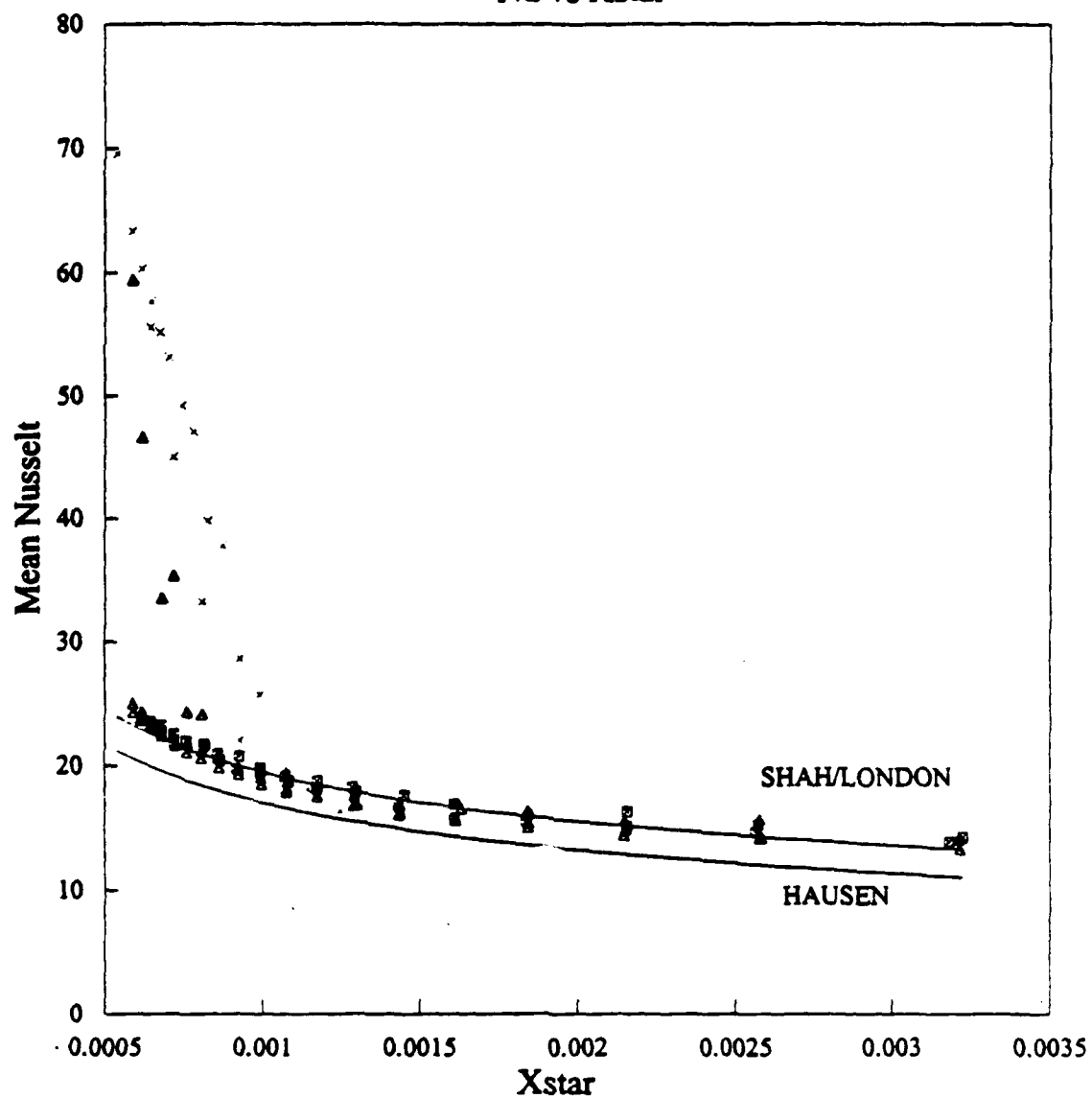
Figure 6.13 Cu/Ni externally finned tube - No insert (Nu_m vs. x^*) results.

Cu/Ni FINNED TUBE - NO INSERT
LAMINAR FLOW

$Nu = 1.84Xstar^{-0.341}$

HAUSEN

Mean Nusselt

Xstar

▣ -10C ◆ 0C ▲ +10C · +15C

Nu vs Xstar
CFNIXNUL
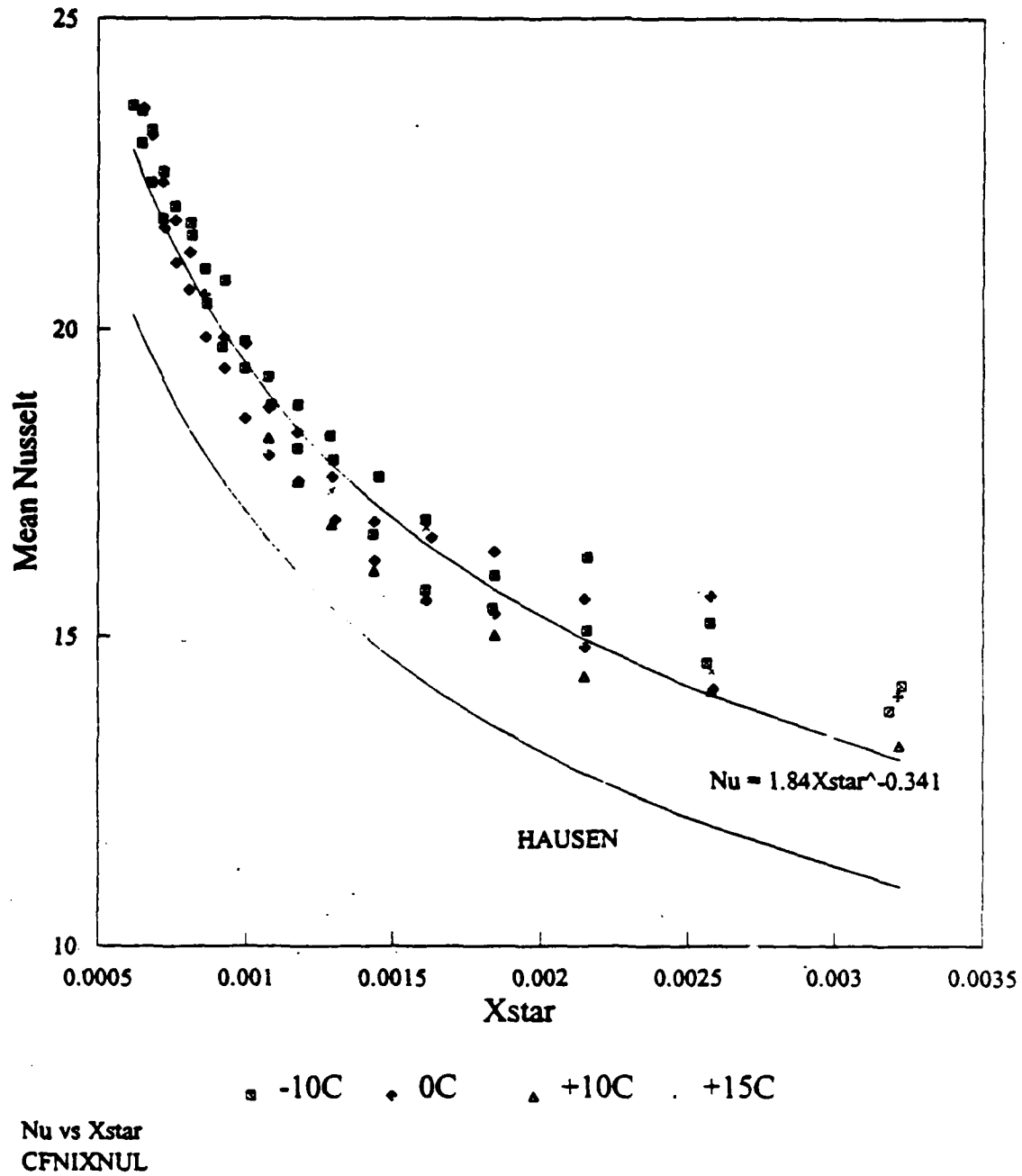
Figure 6.14 Cu/Ni externally finned tube - No insert laminar flow correlation results.

Figure 6.15 Cu/Ni externally finned tube - Twisted tape (Nu_m vs. Re) results.

Cu/Ni FINNED TUBE - TWISTED TAPE
(Nu/Pr^.35) vs (Res/y)

$Nu = 0.383Pr^{0.35}(Res/y)^{0.622}$

$Nu = 0.148Pr^{0.35}(Res/y)^{0.687}$
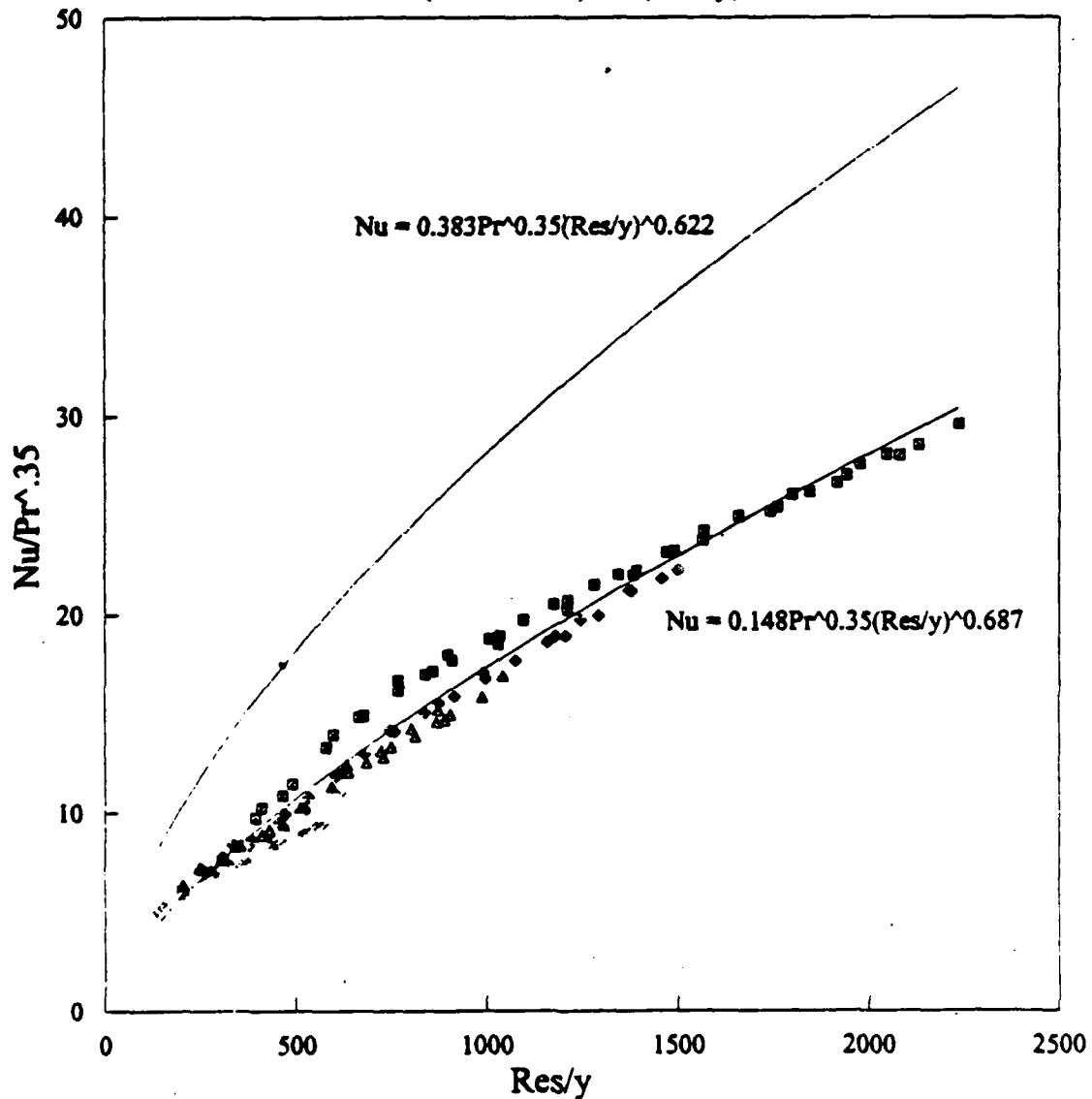
■ +15C   ◆ +10C   ▲ 0C   ·. -10C

Res = (ṁDi)/(Asμ), y = H/Di
CFTTNUPR

Figure 6.16 Cu/Ni externally finned tube - Twisted tape correlation results.

Cu/Ni FINNED TUBE - HEATEX
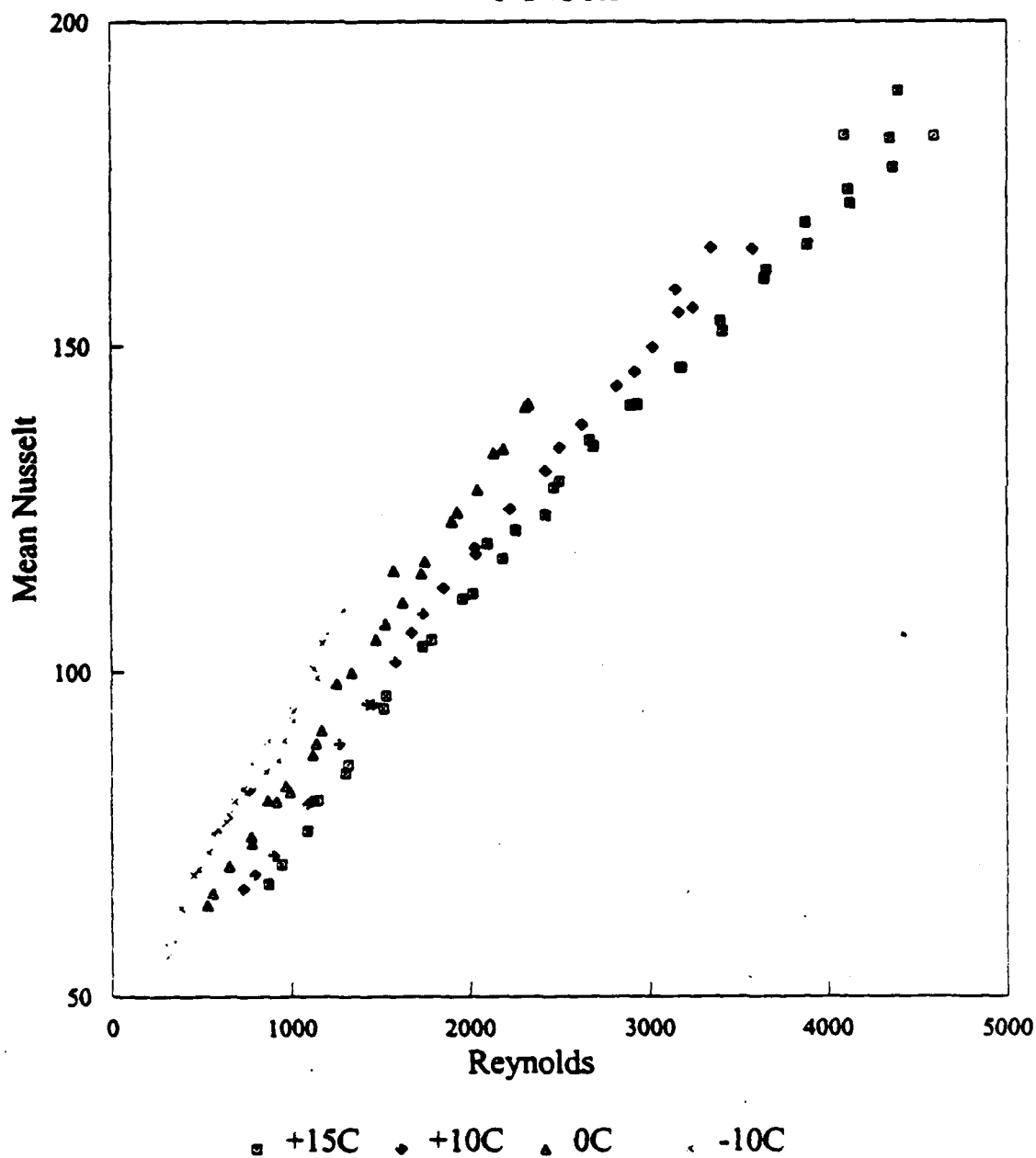
Nu vs Re

Figure 6.17 Cu/Ni externally finned tube - HEATEX (Nu_m vs. Re) results.

CFHXNURE

82

Cu/Ni FINNED TUBE - HEATEX
(Nu/Pr^.46) vs Re
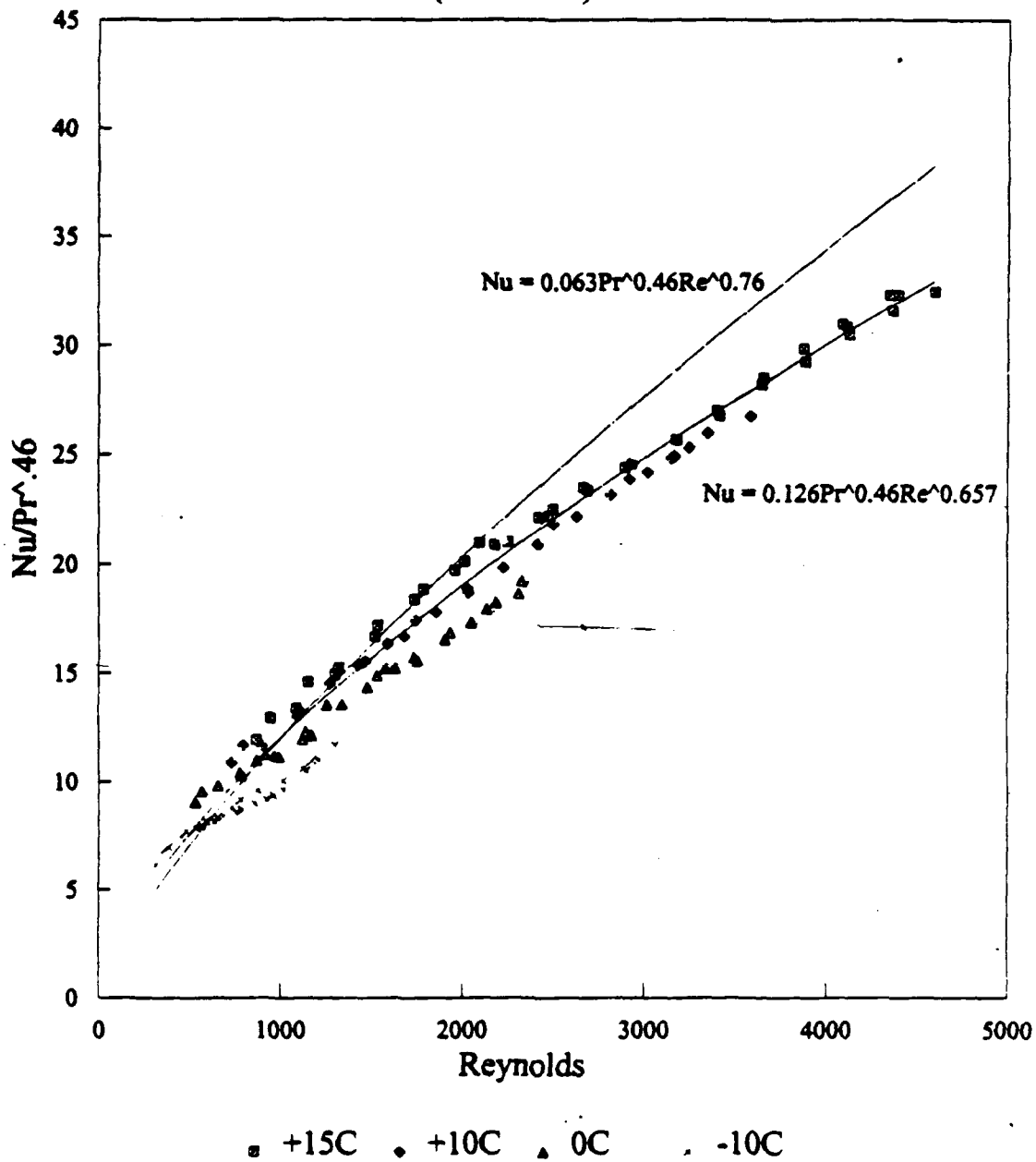
Figure 6.18 Cu/Ni externally finned tube - HEATEX correlation results.

D. KORODENSE TUBE

1. Korodense Tube - No Insert

The final tube tested was the Korodense tube. This tube was first tested with no insert. The results for the mean Nusselt number as a function of Reynolds number are shown in Figure 6.19 and in more detail for laminar and transitional flow in Figures 6.20 and 6.21, respectively. As was seen in the smooth tube case, a transition to turbulent flow occurred at a Reynolds number of approximately 2300.

Figure 6.22 compares the data to Hausen's correlation (equation 2.10) and the Shah and London correlation (equation 2.14). As before, the transitional flow data are seen as two distinct lines for data taken at +20°C and +10°C nominal inlet temperatures. Under laminar flow conditions, the data are seen to fall very closely to Shah and Londons' correlation, but significantly above Hausen's correlation. This was also found for the other two tubes. This result was expected since a mildly corrugated wall is not good in enhancing laminar flow and the tube behaves essentially like a smooth tube. Significant enhancement for Korodense tubes is not expected until $Re_D > 10^4$ [Ref. 21].

The resulting correlation for laminar flow data is shown on Figure 6.23 and given by:

$$Nu_m = 2.05(x^*)^{-0.326} \tag{6.7}$$

The Hausen correlation (equation 2.10) used by Mazzone again under predicts the present measured inside heat transfer coefficient. It was expected that the mean

Nusselt number would be the same (or maybe slightly higher) as for the smooth tube case for the reasons already mentioned. However, the Korodense data fall slightly below the smooth tube data and closer to Shah and Londons' smooth tube correlation (equation 2.14). No explanation can be given for this result. Data scatter explanations given for the other tubes also apply for the Korodense tube.

2. Korodense Tube - Twisted Tape Insert

The results for the Korodense tube with a twisted tape insert are shown in Figures 6.24 and 6.25. The same twisted tape that was used for the smooth tube was used for the Korodense tube. Note that the Korodense tube nominal inside diameter (13.35 mm) is slightly larger than the smooth tube inside diameter (13.26 mm). This small difference in inside diameters (together with corrugation in the Korodense tube) led to a looser fit for the twisted tape insert.

The mean Nusselt number as a function of Reynolds number is shown in Figure 6.24 which again clearly indicates the inlet temperature dependence. The data were again correlated using the form of Hong and Bergles' correlation. The present data were compared to their correlation (equation 2.20) in Figure 6.25. The correlation developed for the present data is:

$$Nu_m = 0.569 Pr^{0.35} (Re_j/y)^{0.498} \qquad (6:8)$$

This correlations falls below the Hong and Bergles correlation (equation 6.20) as well as for the smooth tube. This result is thought to be primarily due to the looser fit of the twisted tape inside the Korodense tube. The corrugations also leave areas of no

contact between the tape and the inside wall of the tube. Stagnant flow or even air bubbles may form in these gaps, especially at low Reynolds numbers, causing an interruption of the swirled flow. The thermal boundary layer, therefore, is not as efficiently mixed as in the smooth tube. For these reasons, lower inside heat transfer coefficients than those assumed by Mazzone should be expected.

3. Korodense Tube - HEATEX Insert

The last tube-insert condition tested was the Korodense tube with the HEATEX insert. The same HEATEX insert used for the smooth tube was used here. Figure 6.26 shows the mean Nusselt number as a function of Reynolds number and again shows an inlet temperature dependence. The resulting correlation for the present data is given by:

$$Nu_m = 0.282 Pr^{0.46} Re^{0.499} \tag{6.9}$$

The data and this correlation are compared with the correlation Mazzone used (equation 2.23) in Figure 6.27. It is evident that Mazzone's chosen correlation overpredicts the inside heat transfer coefficient significantly. This again is thought to be primarily due to the incomplete mixing of the thermal boundary layer caused by non-contact regions existing between the tube wall and HEATEX petals.
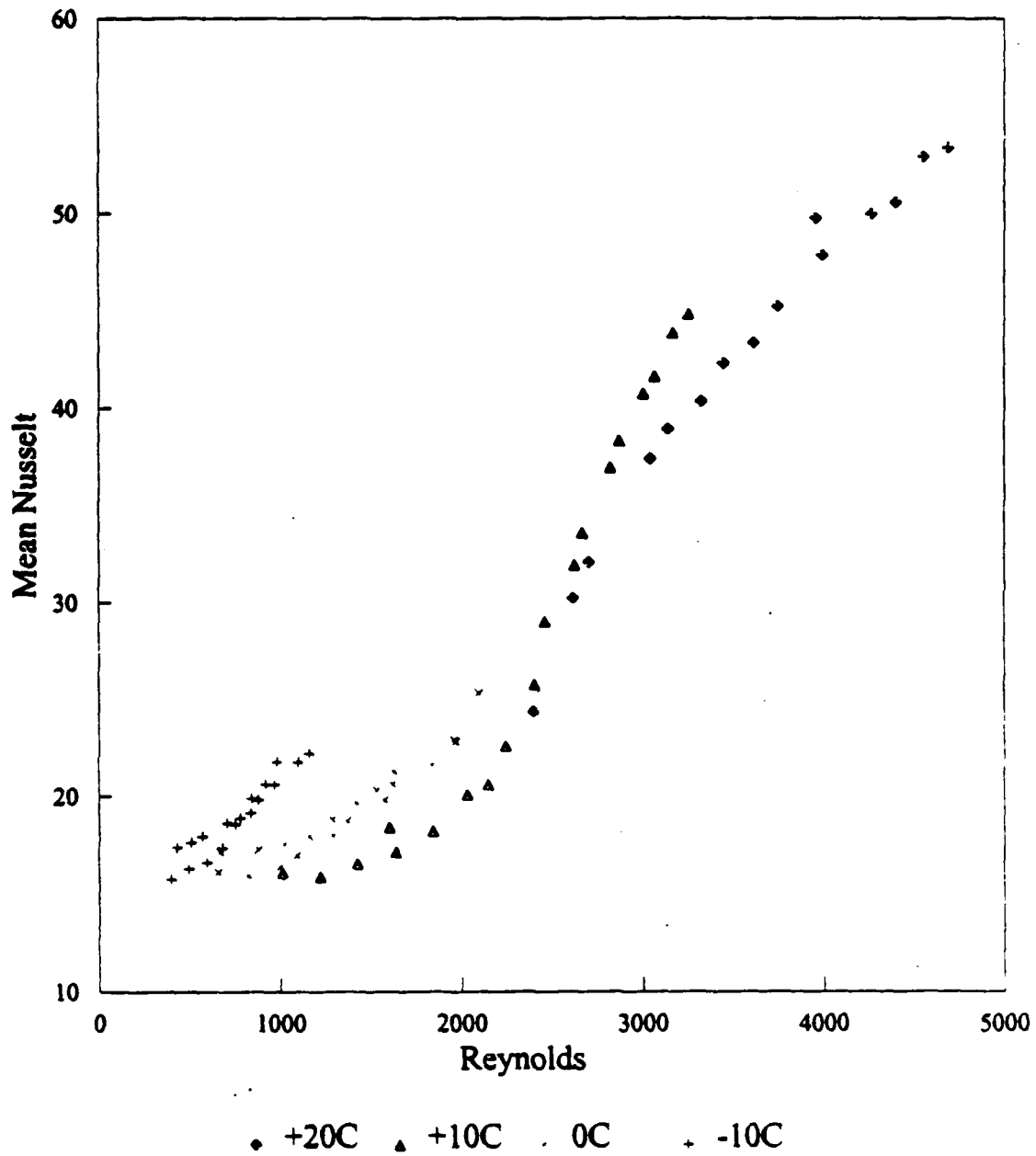
KORODENSE TUBE - NO INSERT
Nu vs Re

Figure 6.19 Korodense tube - No insert (Nu_m vs. Re) results.

87
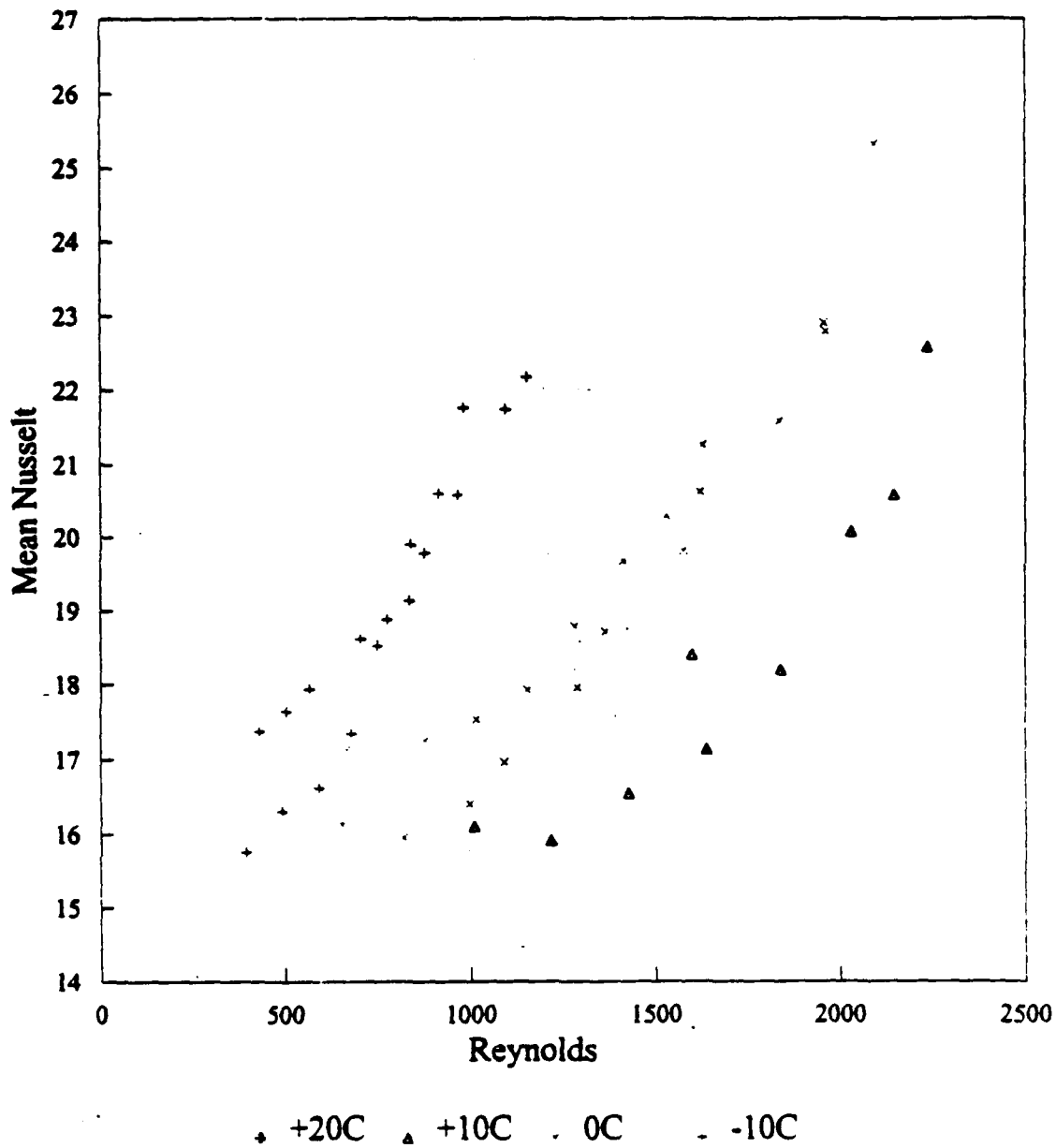
KORODENSE TUBE - NO INSERT
LAMINAR FLOW

Figure 6.20 Korodense tube - No insert (Nu_m vs. Re) laminar flow results.

KORODENSE TUBE - NO INSERT
TRANSITIONAL FLOW

+20C ♦   +10C ▲   0C   -10C +
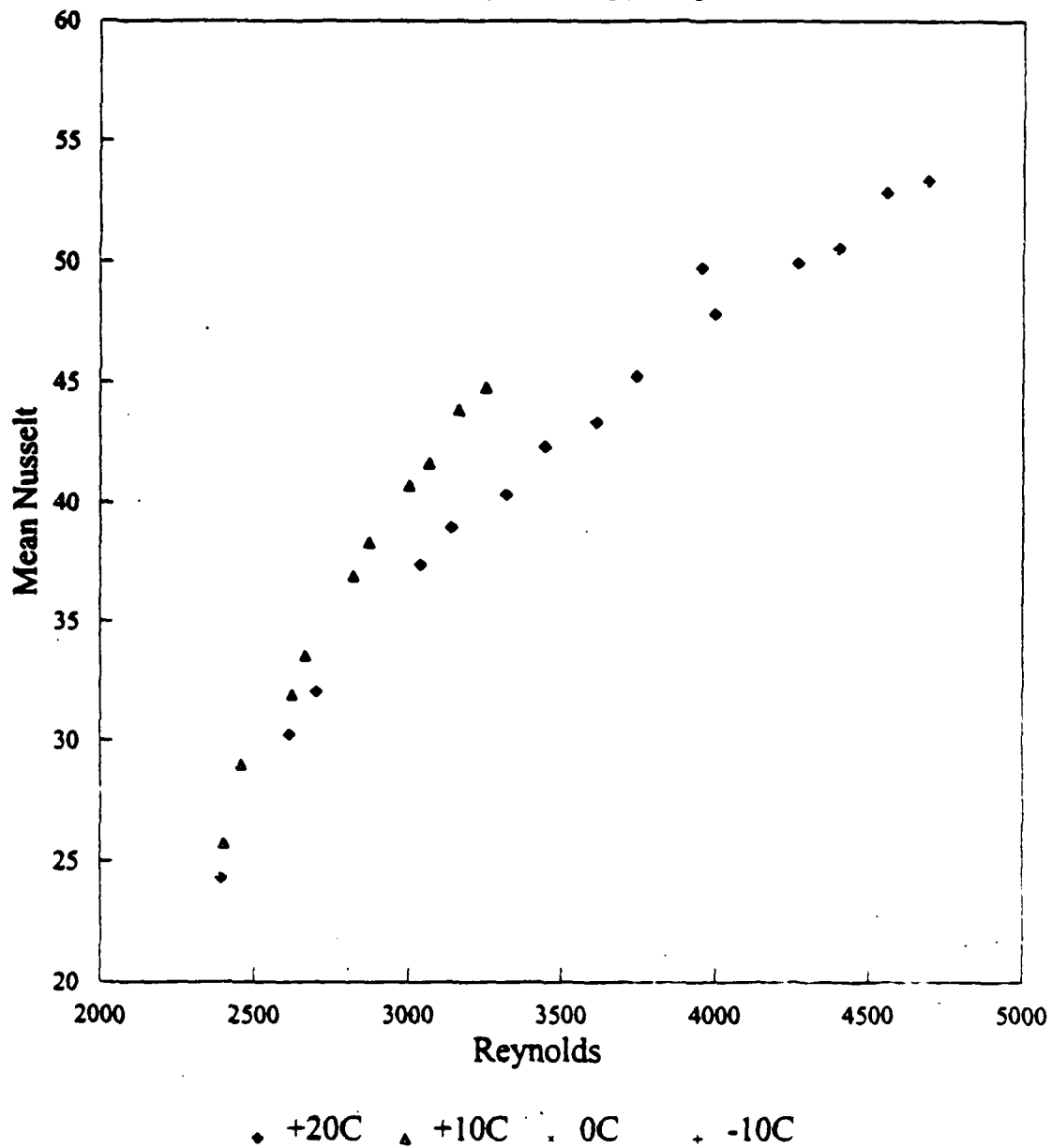
Nu vs Re
KDNINURETRAN

Figure 6.21 Korodense tube - No insert (Nu_m vs. Re) transitional flow results.

KORODENSE TUBE - NO INSERT
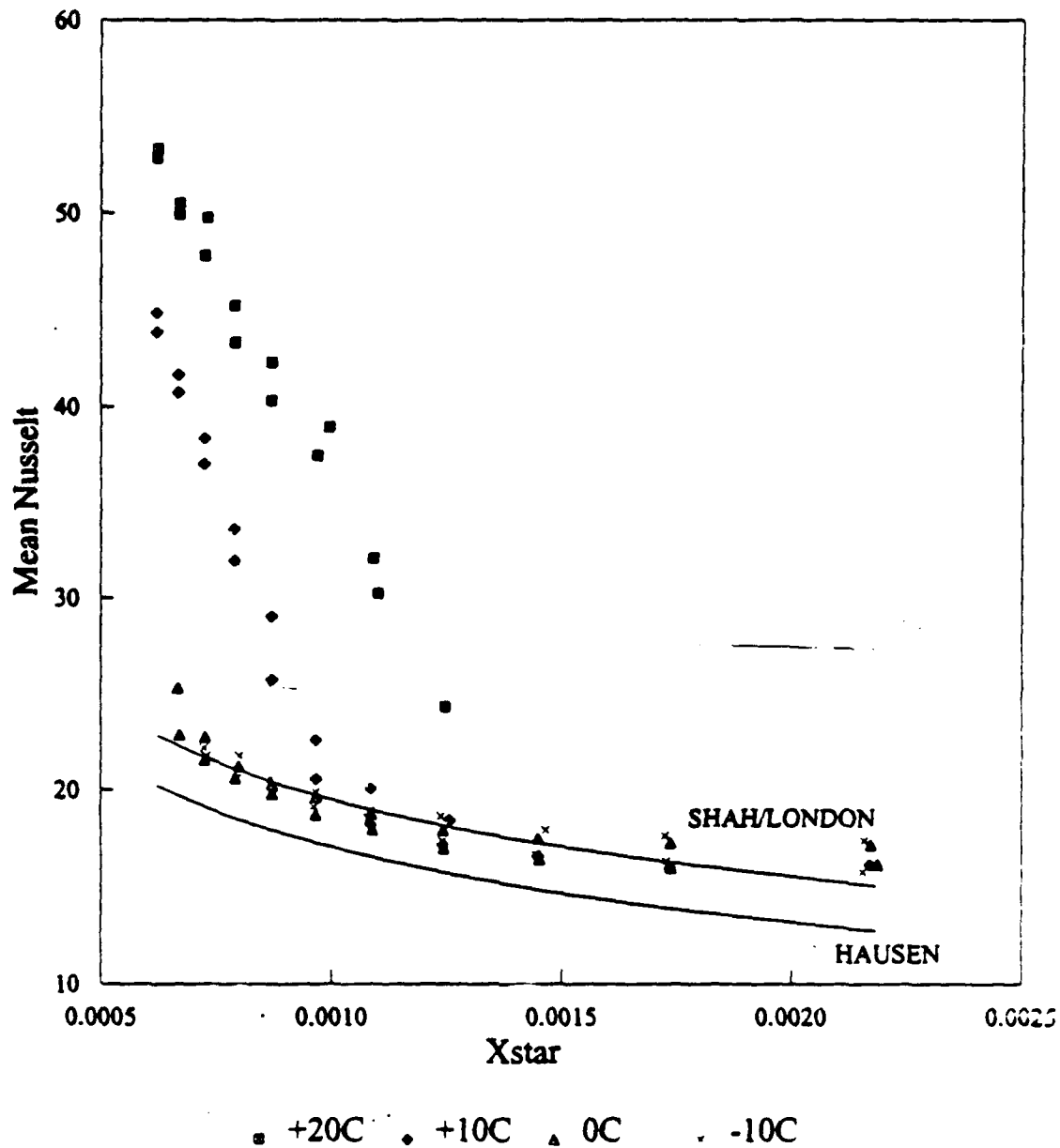
Nu vs Xstar

Figure 6.22 Korodense tube - No insert (Nu_m vs. x^*) results.

KORODENSE TUBE - NO INSERT
LAMINAR FLOW

$Nu = 2.05 Xstar^{-0.326}$

HAUSEN

■ +20C ◆ +10C ▲ 0C . -10C
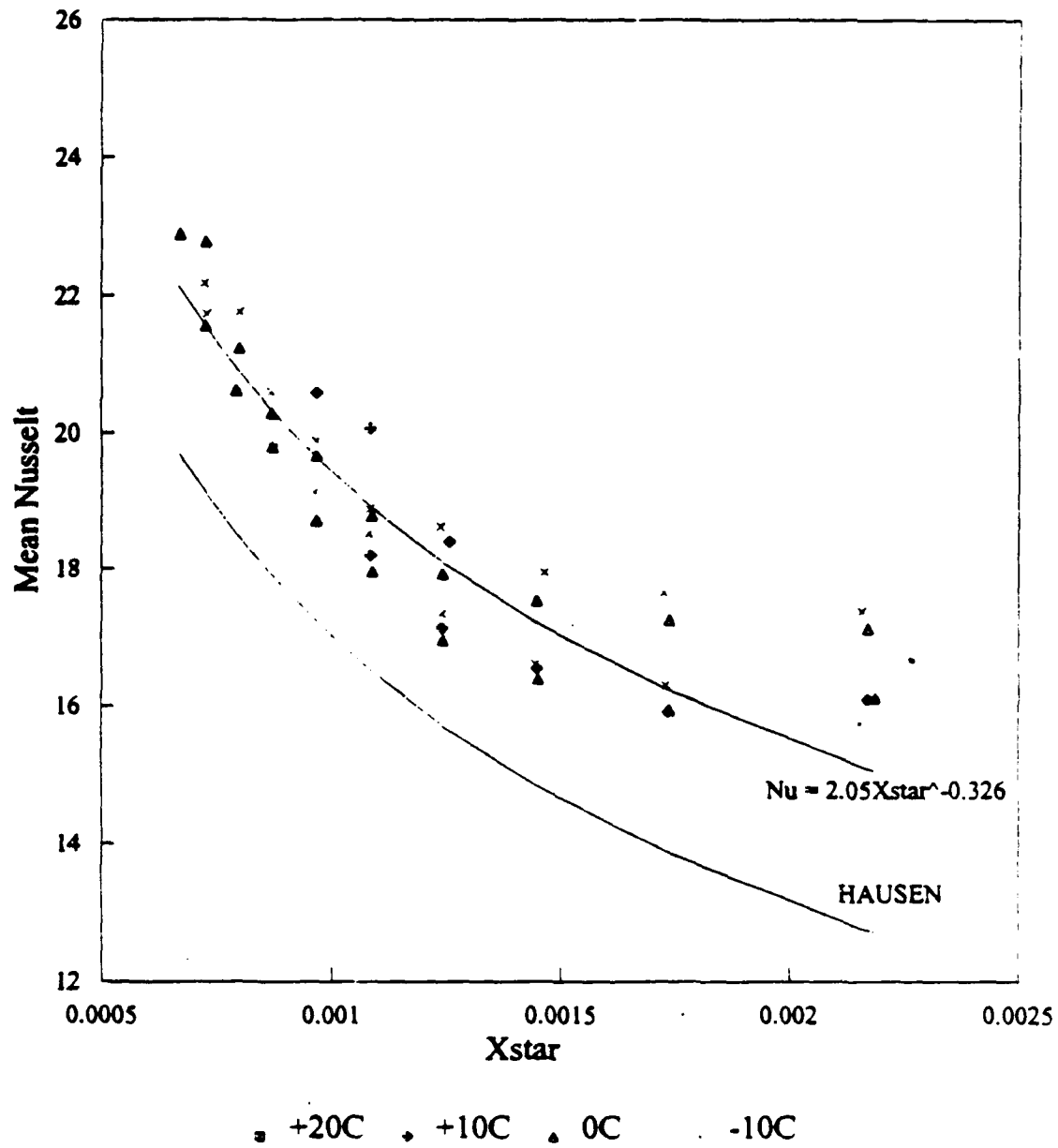
Nu vs Xstar
KDNIXNUL

Figure 6.23 Korodense tube - No insert laminar flow correlation results.

KORODENSE TUBE - TWISTED TAPE
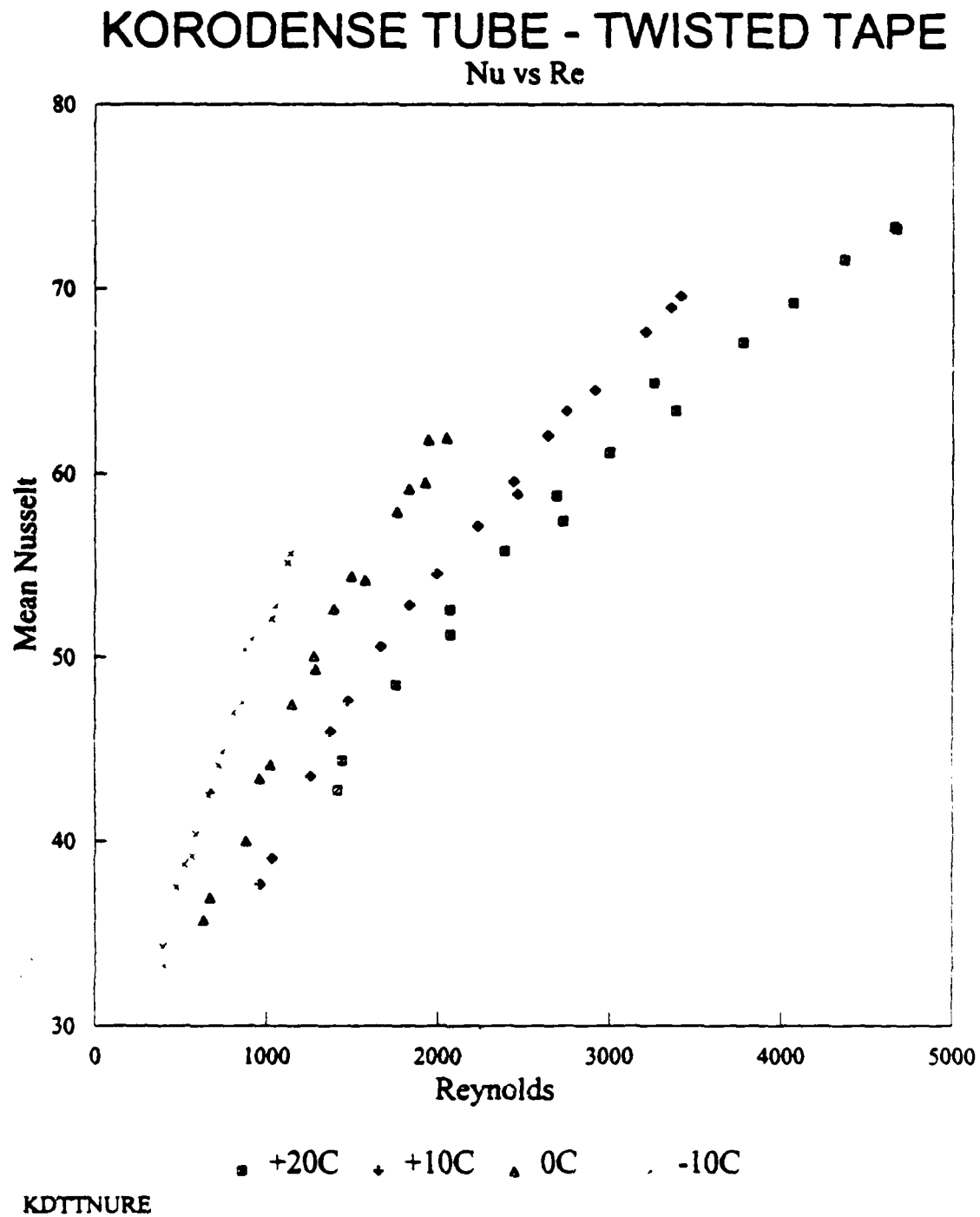
Nu vs Re

Figure 6.24 Korodense tube - Twisted tape (Nu$_m$ vs. Re) results.

92

KORODENSE TUBE- TWISTED TAPE
(Nu/Pr^.35) vs (Res/y)

Nu = 0.383Pr^0.35(Res/y)^0.622

Nu = 0.569Pr^.35(Res/y)^0.498

a +20C   ♦ +10C   ▲ 0C   . -10C

Res = (ṁDi)/(Asμ) , y = H/Di
KDTTNUPR
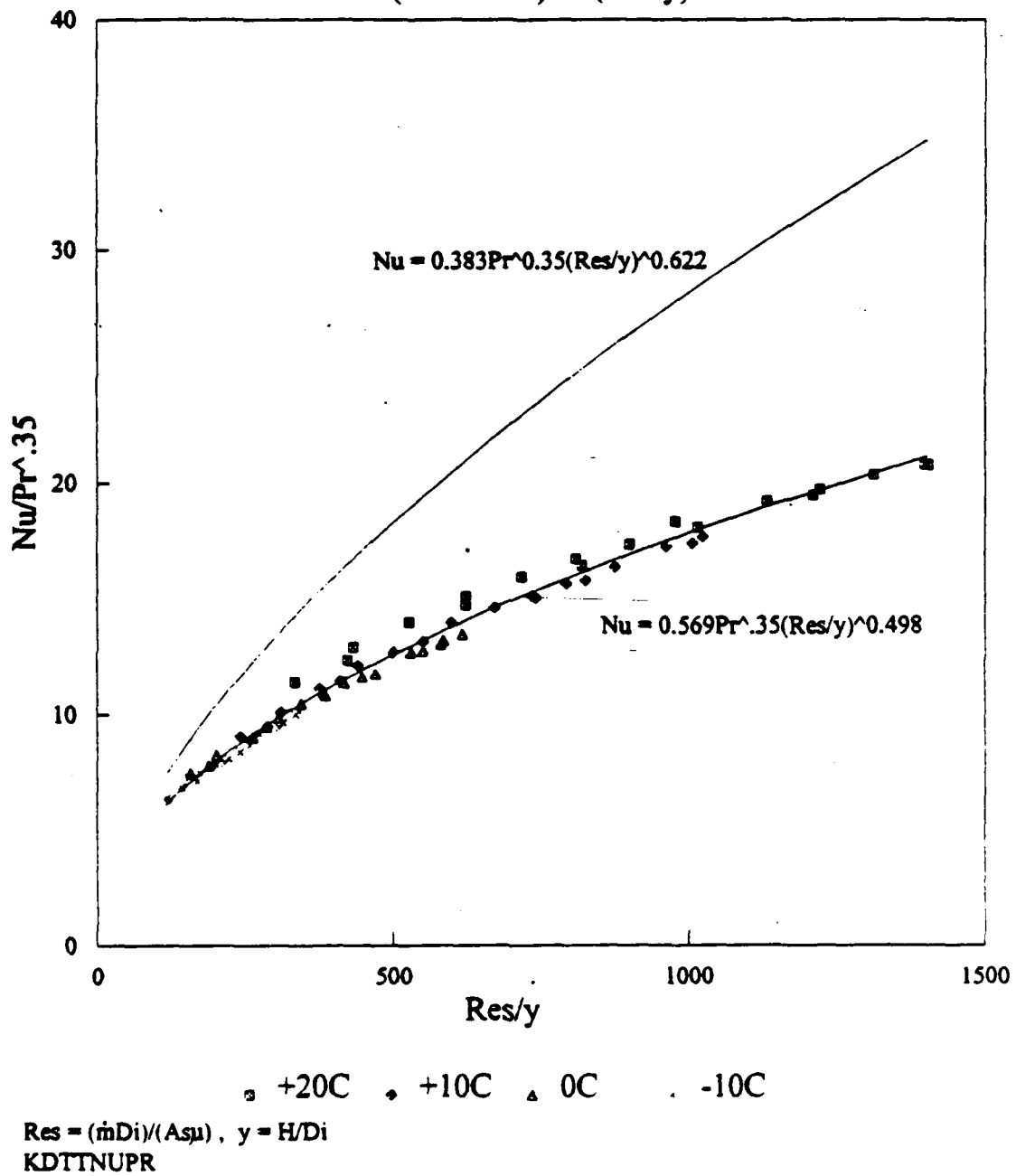
Figure 6.25 Korodense tube - Twisted tape correlation results.
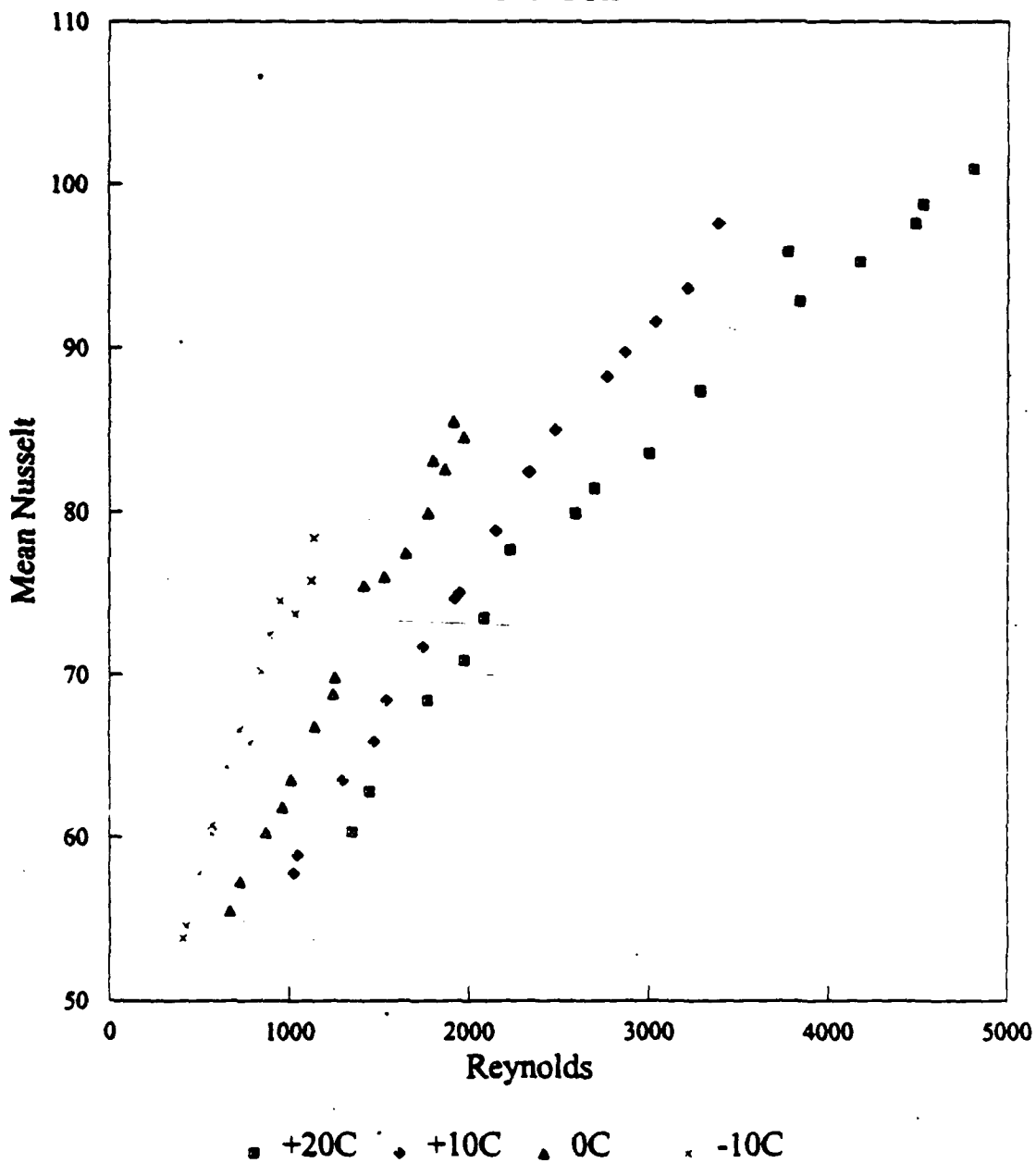
Figure 6.26 Korodense tube - HEATEX (Nu$_m$ vs. Re) results.

94

KORODENSE TUBE - HEATEX

(Nu/Pr^.46) vs Re

Nu = 0.226Pr^0.46Re^0.65

Nu = 0.282Pr^0.46Re^0.499

■ +20C   ◆ +10C   ▲ 0C   × -10C
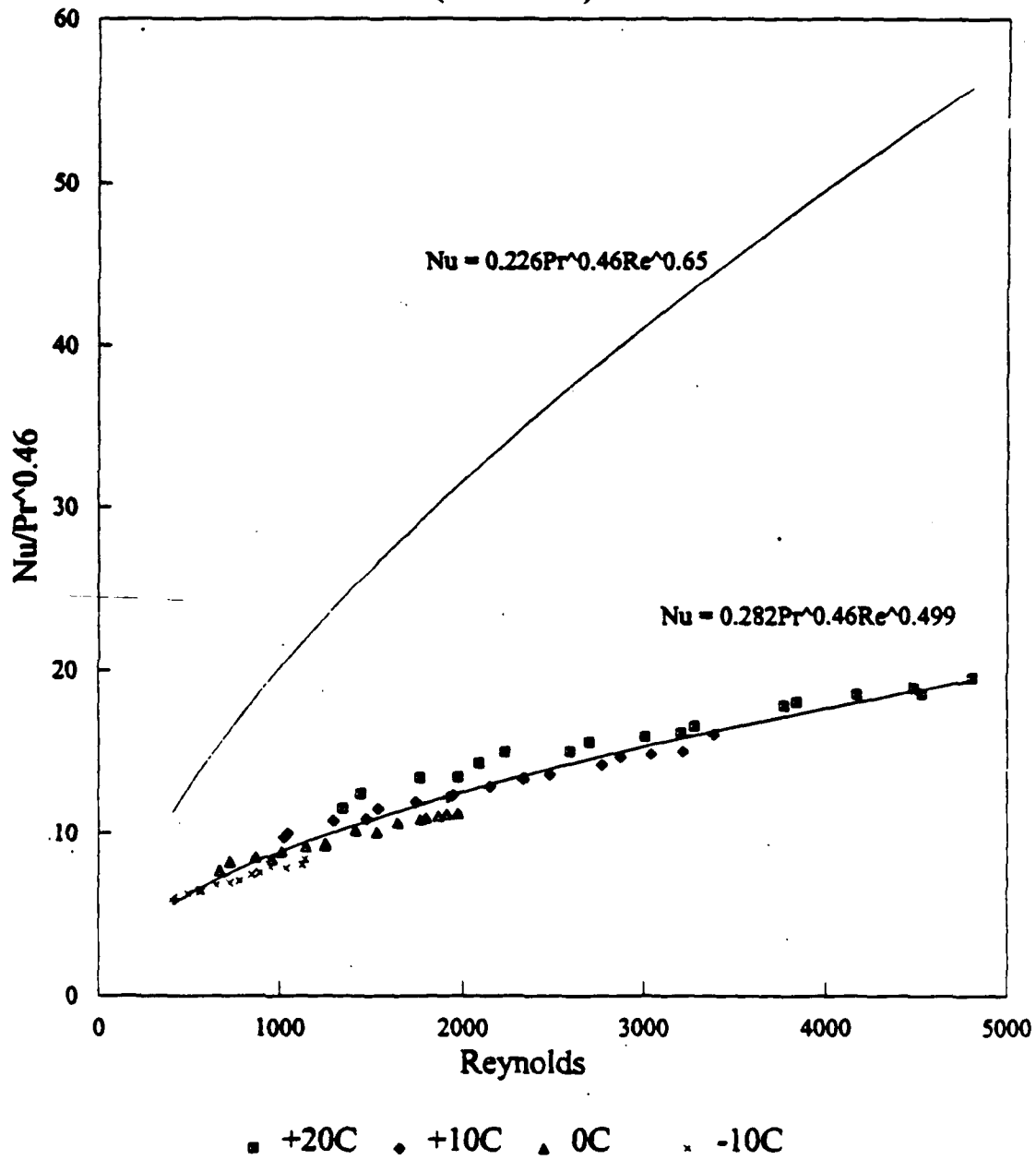
KDHXNURE

Figure 6.27 Korodense tube - HEATEX correlation results.

E. INSERT COMPARISON BETWEEN TUBES

Figures 6.28, 6.29 and 6.30 each compare the three correlations for each tube for no insert, twisted tape, and HEATEX inserts, respectively. It can be seen that with no insert (Figure 6.28), the Korodense correlation is about 10% below the smooth tube data. Although one may expect no increase in the heat transfer with a roped tube under laminar flow conditions, one certainly would not expect to find such a decrease with a similar diameter tube. This difference, therefore, can only be attributed to experimental uncertainty, probably in the wall temperature measurement. The finned tube correlation is lower than both the Korodense ($\approx 5\%$) and smooth tube ($\approx 15\%$) correlations; this tube had a smaller inside diameter and it may be that different induced flow patterns are set up causing a reduction in heat transfer. Experimental uncertainty must also not be ruled out as to the cause of the difference.

Figure 6.29 shows the same three tube correlations, but for the twisted tape insert. The smooth tube again has the highest performance. The finned tube is $\approx 20\%$ below at a high Re number and nearly 40% lower at a low Re number. This could be due to a different twist ratio used for the finned tube due to the smaller inside diameter. The Korodense tube is similar to the finned tube, giving slightly lower heat transfer at high Re number and slightly higher heat transfer at low Re. The reason for this tube being significantly lower than the smooth tube is though to be due to the tape not contacting the inner surface of the tube as well as for the smooth tube,

thereby leaving regions of stagnant flow. These regions would tend to inhibit mixing and lead to a lower heat transfer performance.

For the HEATEX comparison (Figure 6.30), similar conclusions can be made, although the finned tube seems to have better relative performance indicating that the small diameter HEATEX insert used in the small diameter tube is more effective than the twisted tape. The difference between the smooth and Korodense tubes are of similar magnitude to that shown in Figure 6.29 (about 40% at high Re).

NO INSERT COMPARISON
UNDER LAMINAR FLOW
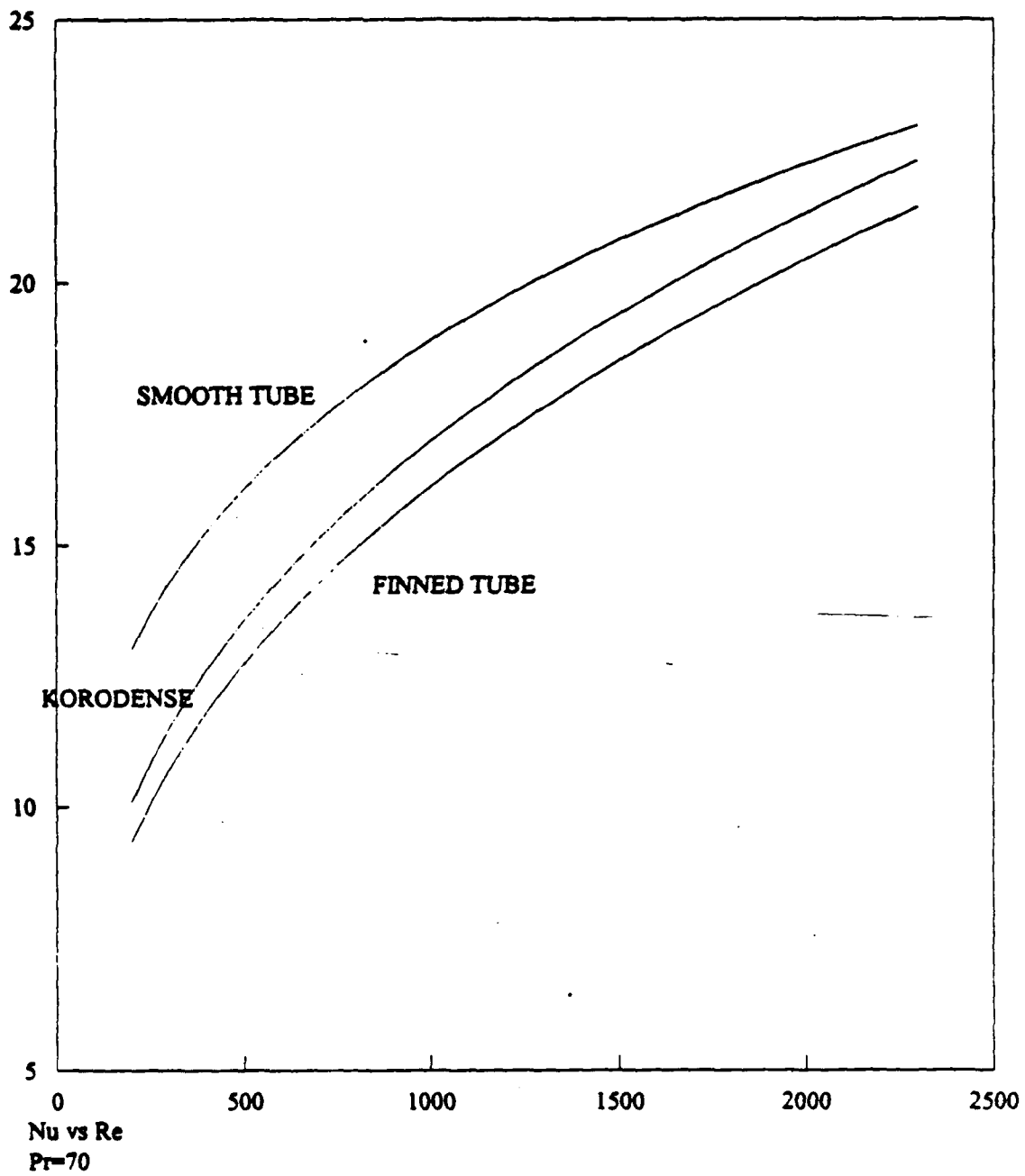
Figure 6.28 No insert comparison under laminar flow for all three tubes.

TWISTED TAPE INSERT COMPARISON
UNDER LAMINAR FLOW

Nu vs Re
Pr ≈ 70
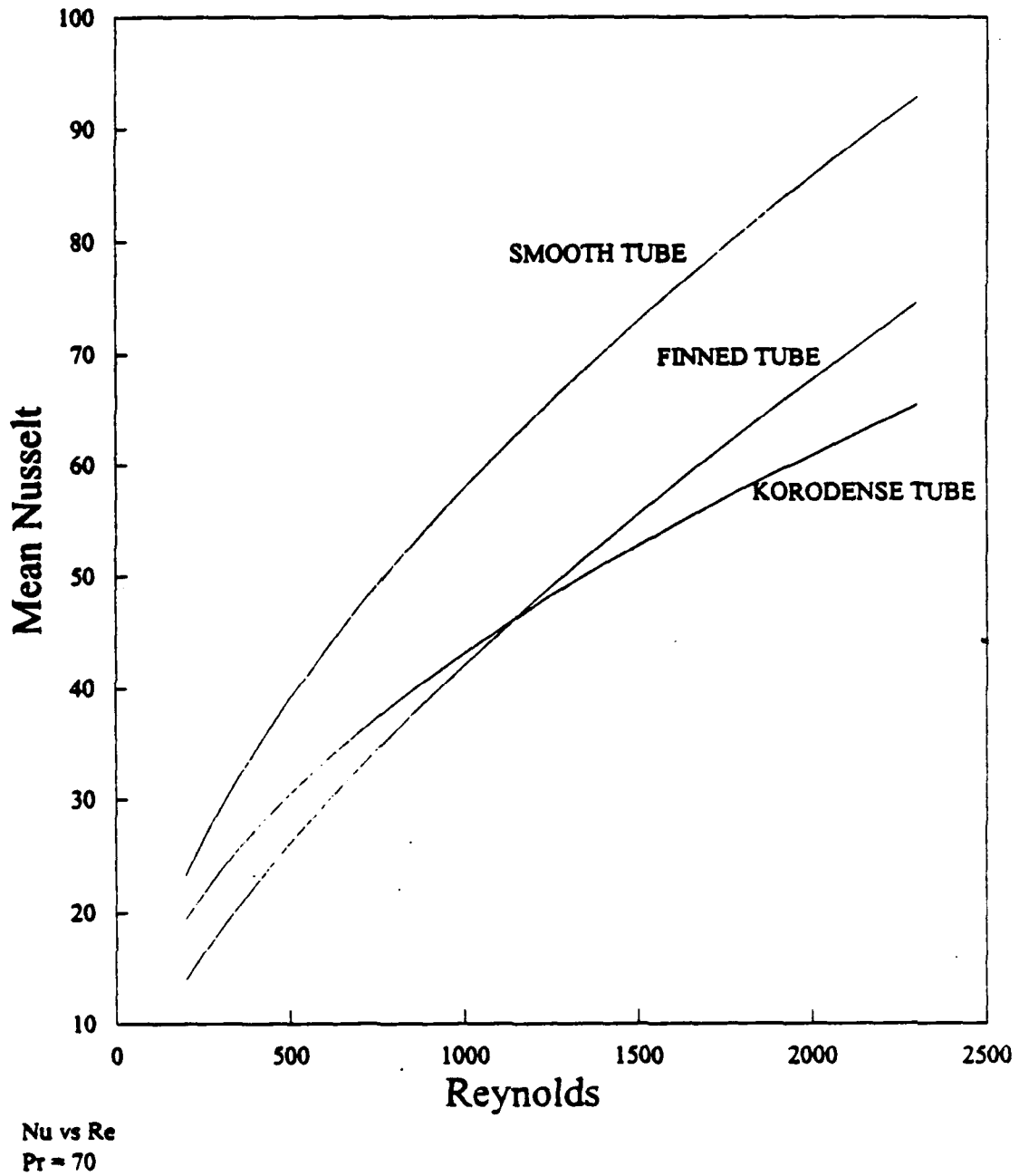
Figure 6.29 Twisted tape insert comparison under laminar flow for all three tubes.

99

Figure 6.30 HEATEX insert comparisons under laminar flow for all three tubes.

F.   LAMINAR FLOW ENHANCEMENT RATIO

The comparisons made in Figures 6.28 through 6.30 are made more complicated by the fact that the uncertainty associated with the wall temperature measurement is unknown and most likely different for each tube. For this reason, it is not known how much of the divergence seen in these figures is due to differences in thermocouple attachment (giving uncertainty to the wall temperature measurement) and how much is an actual flow induced phenomenon. A comparison of the relative effects of the three inserts for a given tube is more accurate, however, due to the fact that any uncertainty for a given tube wall thermocouple attachment combination would be the same.

To determine the degree of tubeside heat transfer enhancement achieved by the use of the twisted tape and HEATEX inserts under laminar flow, an enhancement ratio of the mean Nusselt number for the insert condition (Nu_{insert}) to that for the no insert condition ($Nu_{no\ insert}$) was calculated. The enhancement ratio is therefore defined as:

$$\epsilon = \frac{Nu_{insert}}{Nu_{no\ insert}} \qquad (6.10)$$

Figures 6.31 through 6.33 present mean Nusselt number as a function of Reynolds number under laminar flow conditions for each tube under the three insert conditions. For the purposes of this study, enhancement ratios were calculated at the two extreme Reynolds numbers of 200 and 2300 with a constant Prandtl number of

101

70 using the correlations developed in the previous sections. Table 6.2 summarizes the enhancement ratios for each tube and insert condition.

It is evident from these figures that the greatest enhancement is achieved using the HEATEX insert. An enhancement factor of over seven was achieved for the smooth tube using the HEATEX insert at Re = 2300. This reduced to about 2.6 at low Re. Significantly smaller enhancements were achieved for the twisted tape inset for the smooth tube, indicating that for laminar flow, the stripping and mixing effect of the HEATEX element is considerably more effective than the simple swirl flow effect provided by the twisted tape. It should be mentioned here that HEATEX was developed specifically with laminar flow enhancement in mind. In turbulent flow (Re > 10^4), the enhancements obtained are much smaller (around 1.5 to 2) and both twisted tape and HEATEX elements give similar enhancement values.

TABLE 6.2   SUMMARY OF LAMINAR FLOW ENHANCEMENT RATIOS (defined by equation 6.10)

	SMOOTH TUBE		FINNED TUBE		KORODENSE TUBE	
	TWISTED TAPE	HEATEX	TWISTED TAPE	HEATEX	TWISTED TAPE	HEATEX
Low Re (Re = 200)	1.79	2.66	1.49	2.86	1.92	2.58
High Re (Re = 2300)	4.04	7.19	3.46	6.71	2.93	4.25

For the finned and Korodense tubes, the HEATEX element also provides the highest enhancements. At high Re, the enhancements provided by the twisted tape and HEATEX inserts are lower than those obtained with the smooth tube for the reasons mentioned previously. However, at low Re, the enhancements for the three tubes are about the same for a given insert, indicating the "stagnant" regions mentioned earlier have less of an effect on the total heat transfer.

INSERT CONDITION COMPARISON
LAMINAR FLOW - SMOOTH TUBE
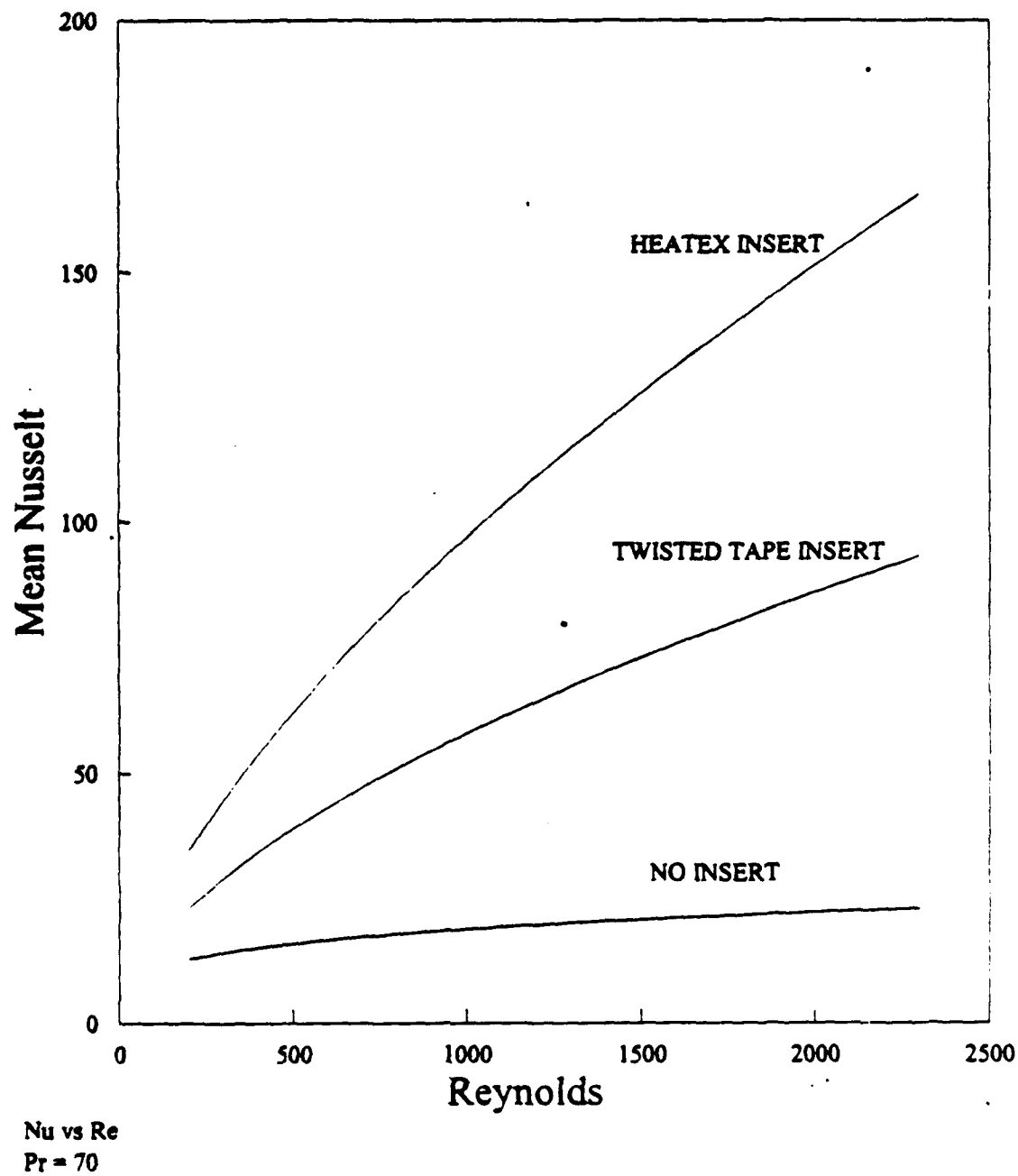
Figure 6.31 Insert condition comparison for laminar flow in a smooth tube.

INSERT CONDITION COMPARISON
LAMINAR FLOW - Cu/Ni FINNED TUBE
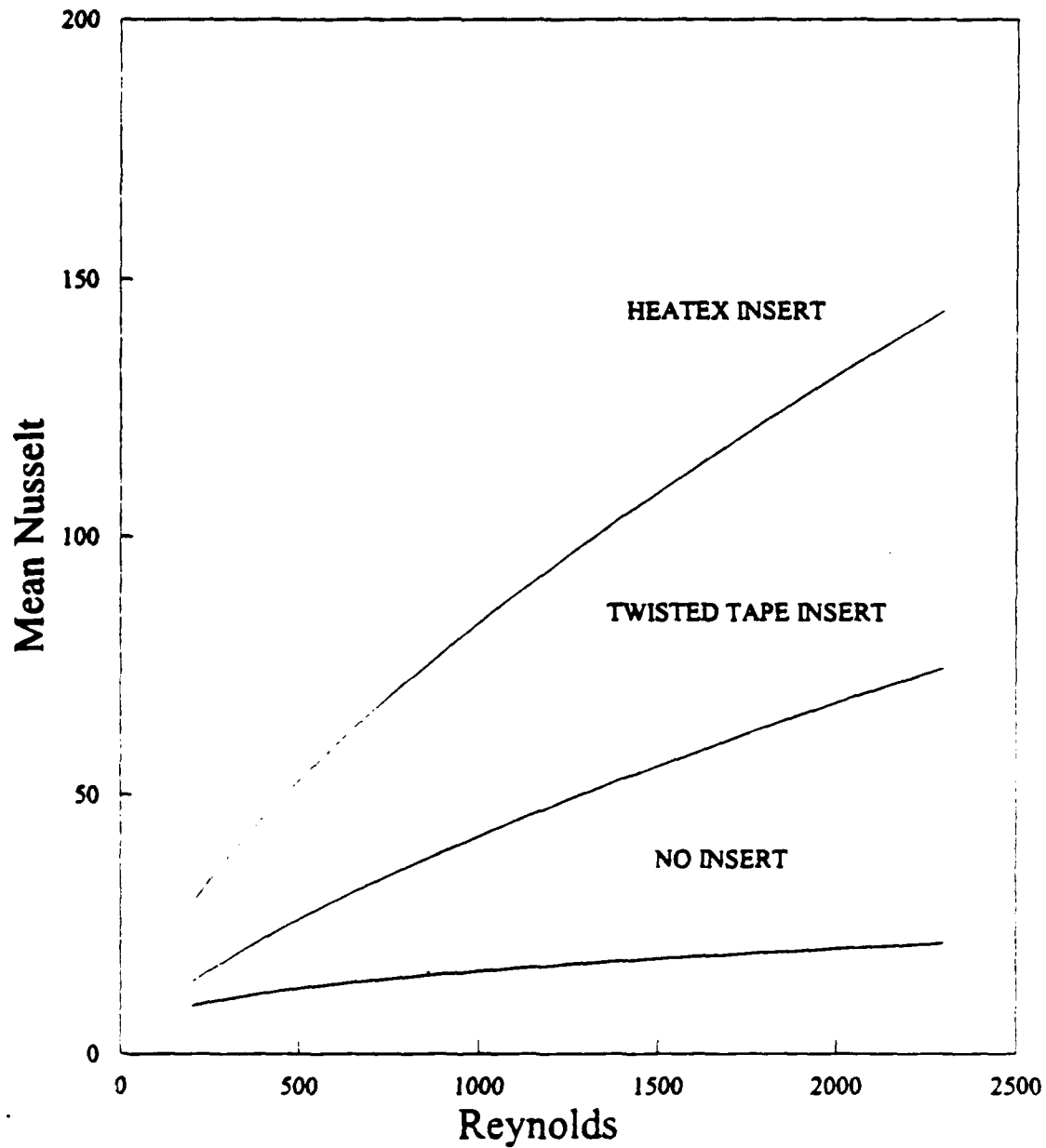
Nu vs Re
Pr = 70

Figure 6.32 Insert condition comparison for laminar flow in a Cu/Ni externally finned tube.

INSERT CONDITION COMPARISON
LAMINAR FLOW - KORODENSE TUBE

HEATEX INSERT

TWISTED TAPE INSERT

NO INSERT

Mean Nusselt

Reynolds

Nu vs Re
Pr = 70
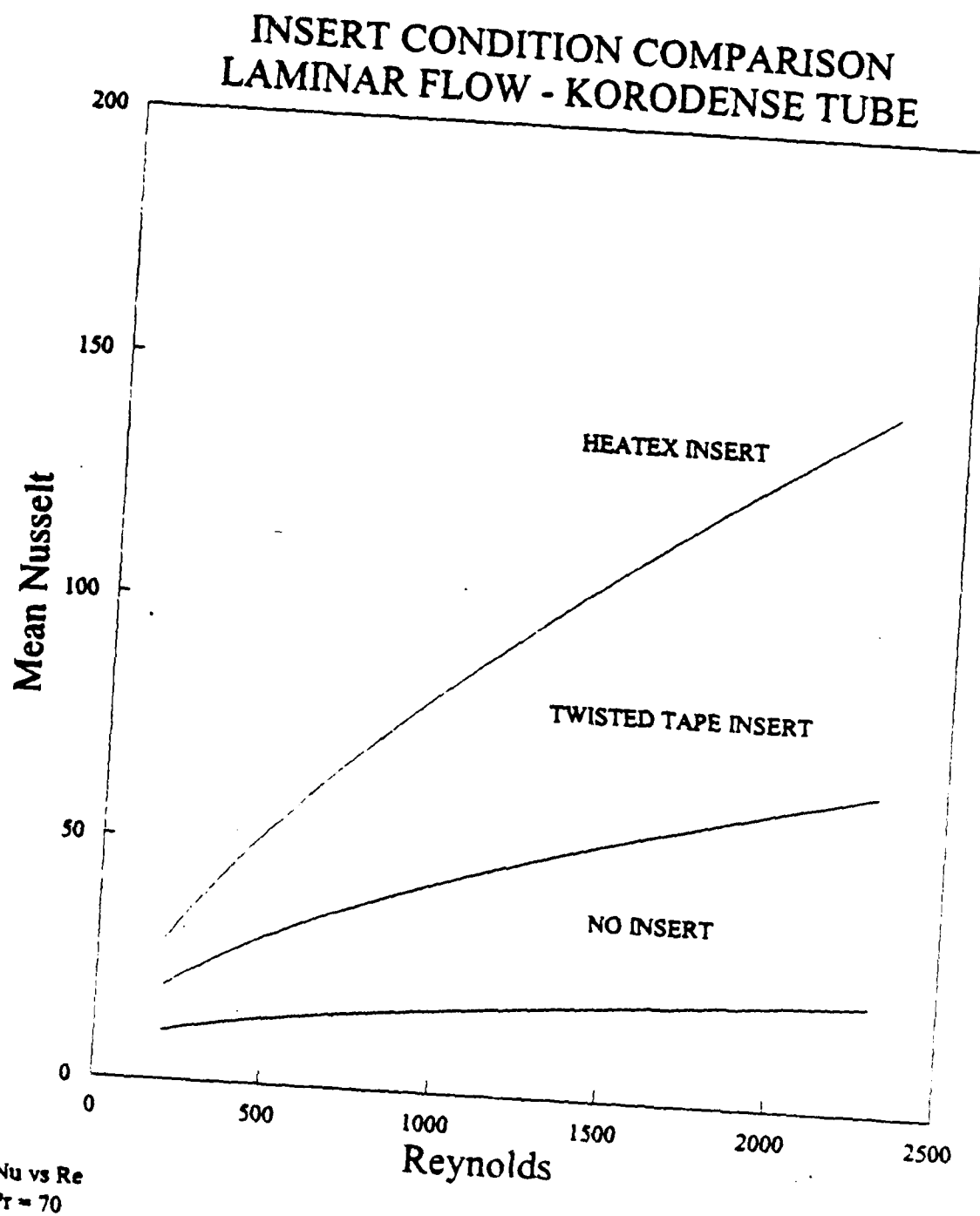
Figure 6.33 Insert condition comparison for laminar flow in a Korodense tube.

106

G. REPROCESSED REFRIGERANT CONDENSATION DATA

Figure 6.34 shows the condensation data of Mazzone [Ref. 6] with the outside heat transfer coefficient recalculated using the present correlations. The data presented are for the top copper smooth tube. Similar recalculations can also be carried out for the other two tubes (Cu/Ni finned and Korodense tubes) as well as for condensation bundle data. The data of Mazzone are reprocessed using the Modified Wilson ' .. 'echnique (see Mazzone [Ref. 6] for details). This technique essentially lets the leading coefficient of the correlation 'float' to try to smooth ou in uncertainty in the correlations being used. As previously stated, the chosen correlation for the no insert condition (even when reprocessing using the Wilson Plot Technique) gave values of inside thermal resistances greater than the measured overall thermal resistance, thereby yielding negative values of the outside heat transfer coefficient, h°. This explains why Figure 6.34 has no data for Mazzone's no insert condition.

It can be seen that by using the present developed correlations for the no insert condition, the calculated values of h_o are significantly improved (i.e. positive values). In addition, for the other two inserts, the new correlations increase h_o by about 10% for the twisted tape insert and nearly 20% for the HEATEX insert. The newly calculated values of h_o when using these inserts are now very close and just above the Nusselt prediction as may be expected for low vapor velocity film condensation. Mazzone commented that his data were below Nusselt by about 10%

107

and thought that this was a consequence of the length of his condenser tubes violating the uniform wall temperature assumption of the Nusselt theory. The fact that these data are so close gives confidence in the new correlations, as the insert itself should have no influence on the magnitude of h_o. By significantly reducing the inside resistance, the insert simply increase the accuracy of h_o. Of course, the no insert condition should also give similar values of h_o. Figure 6.34 shows that they are too high, indicative of the fact that the correlation for the no insert condition, although much improved, is still not ideal. If one recalls the scatter obtained in the present data for the no insert case, together with the fact that the inside resistance is still dominating, then the results shown in Figure 6.34 are not too surprising and still very encouraging. It is recommended, therefore, that all future refrigerant condensation experiments carried out on the bundle facility should be conducted with the inserts using the newly formulated correlations.

One final note is the fact that the present correlations were formulated using a constant wall heat flux, whereas for the condensation experiments, one should ideally use correlations developed under uniform wall temperature conditions. One may expect that the inside heat transfer coefficient would increase slightly under constant wall heat flux conditions, thereby decreasing the outside heat transfer coefficient. However, from Figure 6.34 it is clear that the use of the constant wall heat flux correlations seems to increase h_o. Thus it appears that with the inserts, the inside resistance is so reduced that the boundary condition imposed has little

108

influence. Future investigators should look into this boundary value problem in more detail.

Smooth Tube Condensation Data
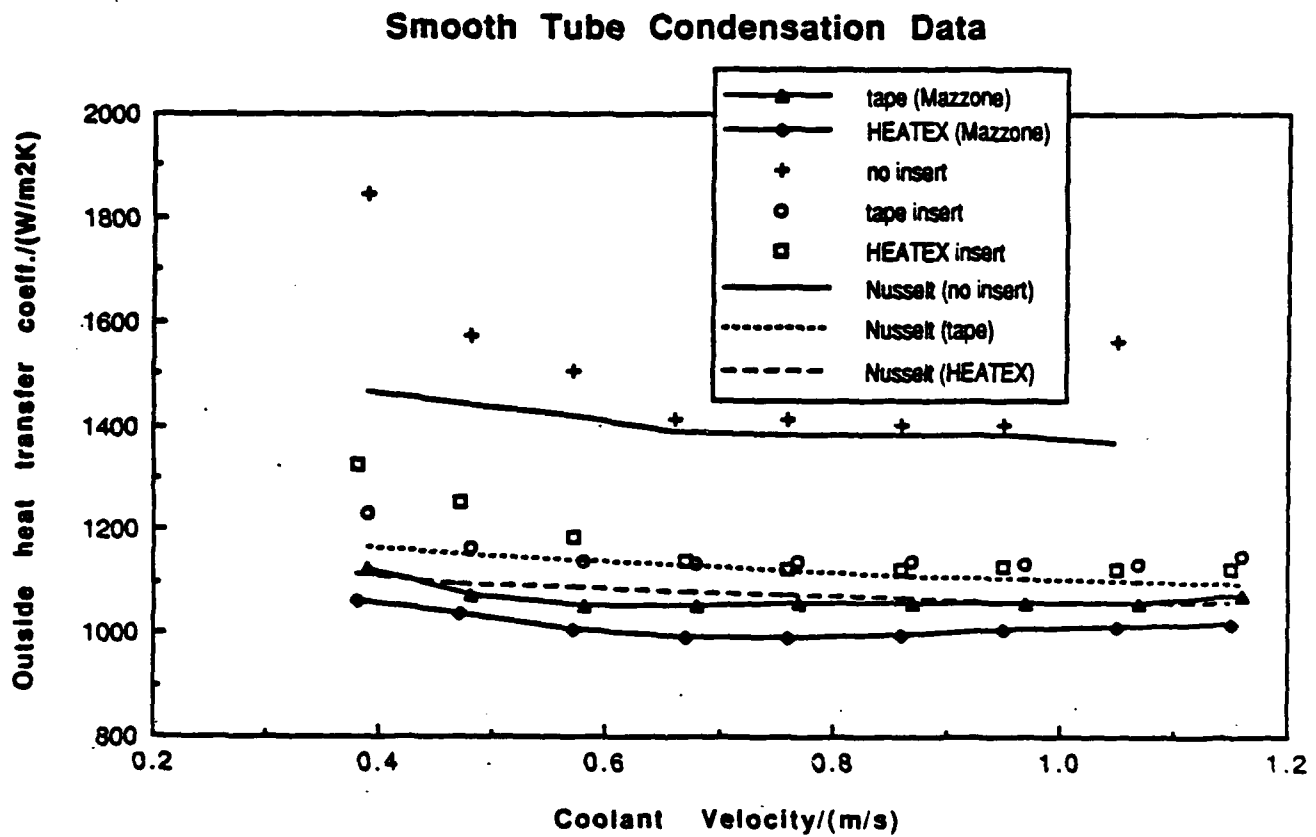
Figure 6.34 Reprocessed refrigerant condensation data using new correlations.

VII. CONCLUSIONS

The following conclusions are based upon results obtained in this study.

A. GENERAL

1. A test apparatus was successfully designed and built to accurately determine inside heat transfer coefficients for the same tubes and insert conditions used in the condensation experiments.

2. Correlations to accurately determine inside heat transfer coefficients under laminar flow conditions both with and without inserts were successfully developed.

3. Reprocessing of Mazzone's [Ref. 6] refrigerant condensation data using these new correlations has yielded more accurate values of the outside heat transfer coefficient. (Note: the name of the program used for the reprocessing is DRPCON7.)

B. SPECIFIC

1. A departure from laminar flow into a transitional flow exists at Reynolds numbers of approximately 2300 for the smooth and Korodense tubes and 2700 for the Cu/Ni finned tube. This contradicts Mazzone's [Ref. 6] assumption of laminar flow up to a Reynolds number of approximately 4000.

2. Laminar flow results for the no insert condition were in close agreement with the Shah and London [Ref. 9] correlation for a constant wall heat flux boundary condition for all three tubes tested.

3. The Hausen [Ref. 10] correlation used by Mazzone [Ref. 6] significantly overpredicted the inside thermal resistance and led to nonsensical results for h_o.

110

4. The smooth tube/twisted tape data were in close agreement with the Hong and Bergles [Ref. 13] correlation. Since this correlation was used by Mazzone [Ref. 6], his results for outside heat transfer coefficient should be fairly accurate for this tube.

5. For the Cu/Ni finned and Korodense tubes with the twisted tape insert, the Hong and Bergles correlation predicted higher inside heat transfer coefficients than the experimental data over the entire Reynolds number range tested. This could have been due to a different twist ratio (for the Cu/Ni finned tube) and stagnant regions (for the Korodense tube).

6. Experimental data for all three tubes using the HEATEX insert yielded results that were well below the correlations developed and used by Mazzone [Ref. 6] over the entire Reynolds number range tested.

7. HEATEX inserts provided the best inside heat transfer enhancement for all three tube. Enhancement ratios of over a factor of seven were found.

VIII. RECOMMENDATIONS

Based on the results of this study, the following recommendations are made:

1. Further refinement of the correlations to better account for different coolant inlet temperatures should be made by optimizing the Prandtl number exponent.

2. These correlations should be used to reprocess all refrigerant condensation data and should be used in future refrigerant condensation experiments conducted at NPS. Note that since these correlations were developed by omitting coolant velocities of 0.2 and 0.3 m/s, then the condensation data should do the same.

3. HEATEX inserts provide the best enhancement of tubeside heat transfer. Due to the data reduction technique used, HEATEX inserts should therefore be used in all tubeside refrigerant condensation experiments to increase the accuracy of the outside heat transfer coefficient.

4. Transitional flow correlations can also be developed for the no insert condition since condensation experiments typically move into this flow region. However, since the transition region is not generally well developed, any developed correlations for this region will be useful only for this particular apparatus.

APPENDIX A. FLOW METER CALIBRATION

The flowmeter used to measure flow through the instrumented tube was initially calibrated at 0°C and 24°C by Mazzone [Ref. 6]. However an additional calibration temperature of -15°C was needed for this study. The flowmeter was calibrated using the same procedure as Mazzone and is summarized as follows.

The outlet of the flowmeter was disconnected from the test section and connected to an empty 55 gallon drum. The drum was placed on a scale with a resolution of 0.5 lbs. The coolant pump was started with the flow through a bypass. The flowmeter was initially opened to maximum flow and then throttled back to 10%. The weight of fluid in the drum was recorded and the timer started. The weight was then recorded at the end of the calibration time. This procedure was repeated in 10% increments up to 100% flow. The calibration run was then repeated from the maximum flow back to 10% flow in 10% increments. The mass flow rate was then calculated in kg/s based on an average of the two readings. The data for the flowmeter calibrations as a function of nominal flow rate are shown in Table A.1.

A least squares linear regression was performed for the flowmeter at each of the three temperatures for which the calibration runs were carried out. The linear regression equation takes the following form:

113

$$\dot{m} = a + bN \qquad \text{(A.1)}$$

where a is the y-intercept in kg/s, b is the slope in kg/s/% and N is the flowmeter

setting in %. The results are shown in Table A.2.

TABLE A.1. MASS FLOW RATE (KG/S) AT -15, 0 AND 24°C

FLOW METER A			
NOMINAL FLOW RATE	MASS FLOW RATE (kg/s)		
(%)	-15°C	0°C	24°C
10	0.0114	0.0149	0.0172
20	0.0295	0.0363	0.0403
30	0.0483	0.0544	0.0621
40	0.0679	0.0794	0.0851
50	0.0866	0.1003	0.1120
60	0.1078	0.1179	0.1339
70	0.1258	0.1388	0.1556
80	0.1453	0.1563	0.1769
90	0.1613	0.1846	0.2028
100	0.1824	0.2019	0.2151

TABLE A-2. FLOWMETER CALIBRATION REGRESSION RESULTS

FLOW METER A			
	-15°C	0°C	24°C
Slope	0.0019	0.00206	0.00225
Y-Intercept	-0.0098	-0.00414	-0.00329

In order to obtain flowrates at any intermediate temperatures, a simple

interpolation procedure was incorporated into the data reduction program

"DRPSING." The results of the calibrations for this flowmeter are shown in Figure

A.1.

FLOWMETER
CALIBRATION @ -15, 0, 24C
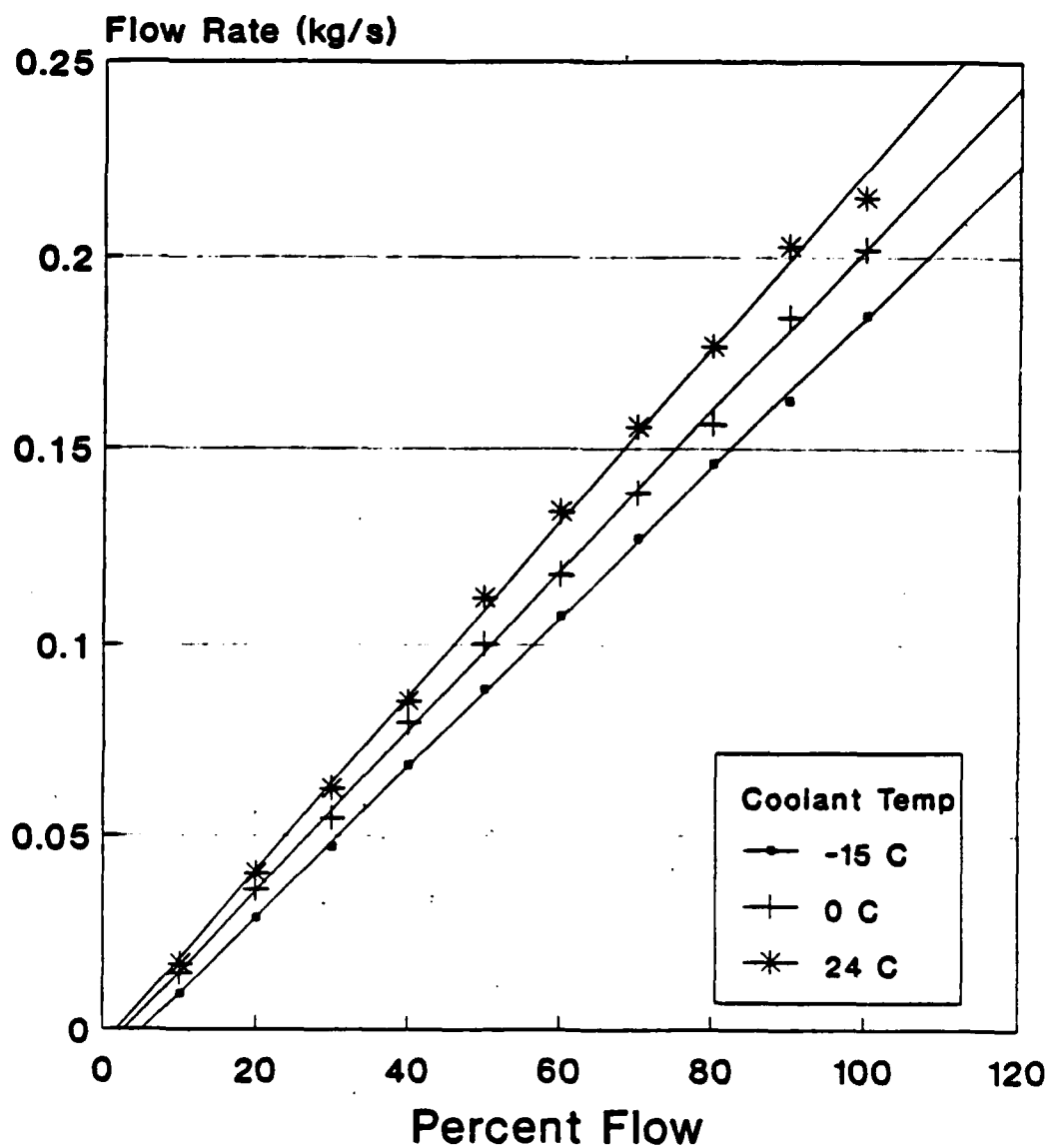
Figure A.1 Flowmeter Calibration.

APPENDIX B. HEAT LOSS TO AMBIENT EXPERIMENT

A series of heat loss experiments were conducted to account for the amount of heat lost to ambient. To accomplish this, the coolant was drained from the test tube and the inlet and outlet capped off to prevent any air flow through the tube. Heater power was set at a desired level and wall temperatures monitored by the DAU. Average wall temperatures were determined every minute for the first 15 minutes and then every four minutes until an equilibrium temperature was reached (after approximately 60 minutes). At that point, any additional heat added could be considered lost to ambient. This procedure was repeated at five nominal power settings, 1W, 3W, 5W, 7W, and 9W. All data were taken at an ambient temperature of 22.0°C.

Figure B.1 is a plot of average wall temperature versus time for the 1W and 7W power settings. It can be seen that an equilibrium average wall temperature was reached after approximately 60 minutes for these two power settings (as it was for the other three power settings.) This graph shows that if the average wall temperature in the experiments reached 46°C or 74°C, then the heat lost to the atmosphere was 1W or 7W, respectively.

Table B.1 shows the data for the equilibrium average wall temperature as a function of the actual power setting ($\dot{q}_{loss}$). The data are shown graphically in Figure B.2. A least squares linear regression was performed and the resulting equation was:

116

$$q_{loss} = \frac{(T_{wi} - 44.15)°C}{4.39\,W/°C} \qquad (B.1)$$

Therefore, for a given average wall temperature, the amount of heat lost to ambient could be determined. Equation B.1 was incorporated into the data reduction program "DRPSING."

TABLE B.1 EQUILIBRIUM AVERAGE WALL TEMPERATURE RESULTS

NOMINAL POWER	ACTUAL POWER (W)	EQUILIBRIUM $\bar{T}_w$ (°C)
1W	0.9412	46.47
3W	3.122	59.23
5W	5.126	67.90
7W	6.790	74.34
9W	9.560	84.85

HEAT LOSS TO AMBIENT
Temperature vs Time
1W and 7W
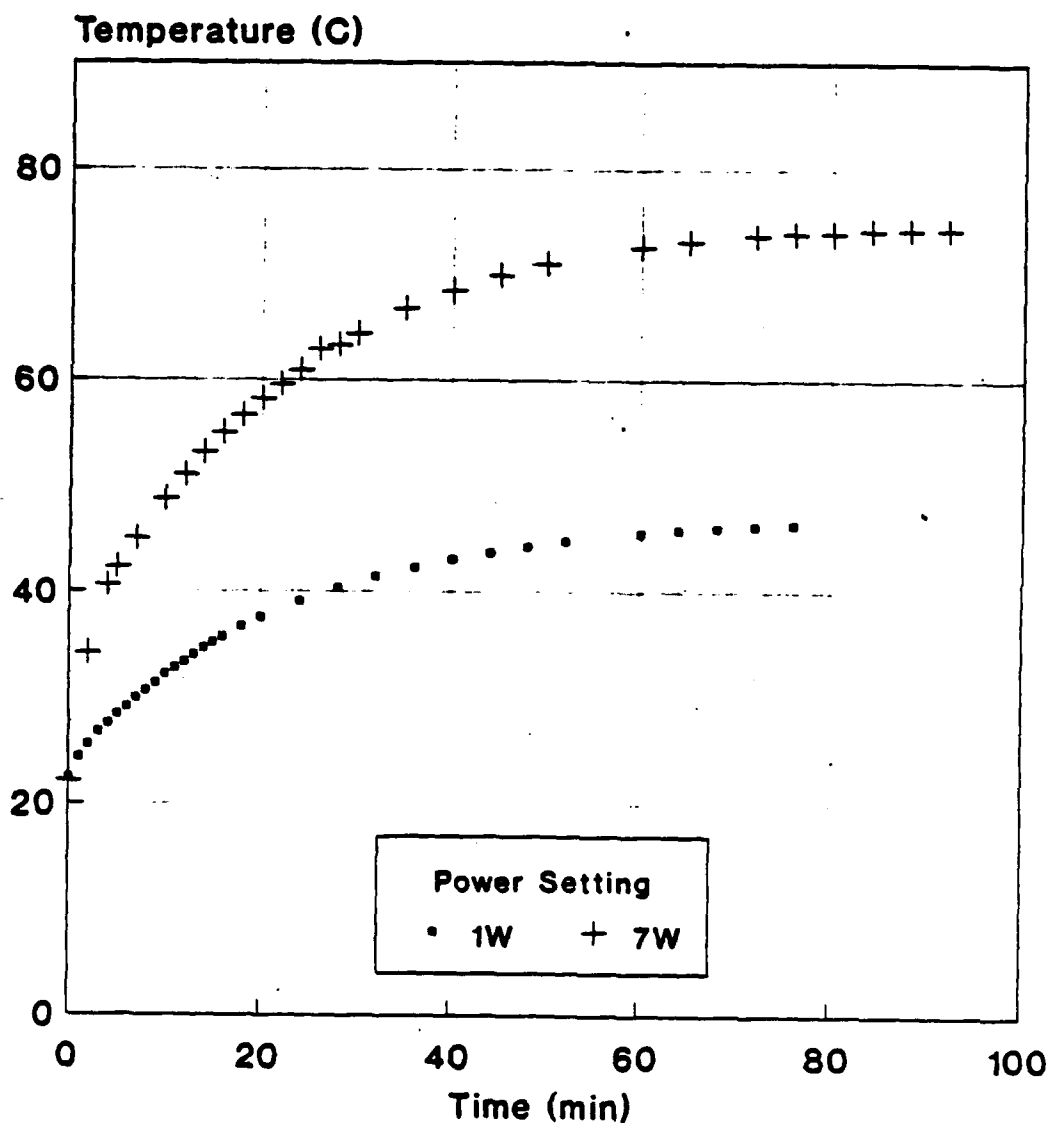
Temperature (C)

Tamb = 22.0

Figure B.1 Heat loss to ambient; Average wall temperature versus time for 1W and 7W.

HEAT LOSS TO AMBIENT
Temperature vs Heat Input

Temperature (C)

Qtape (W)
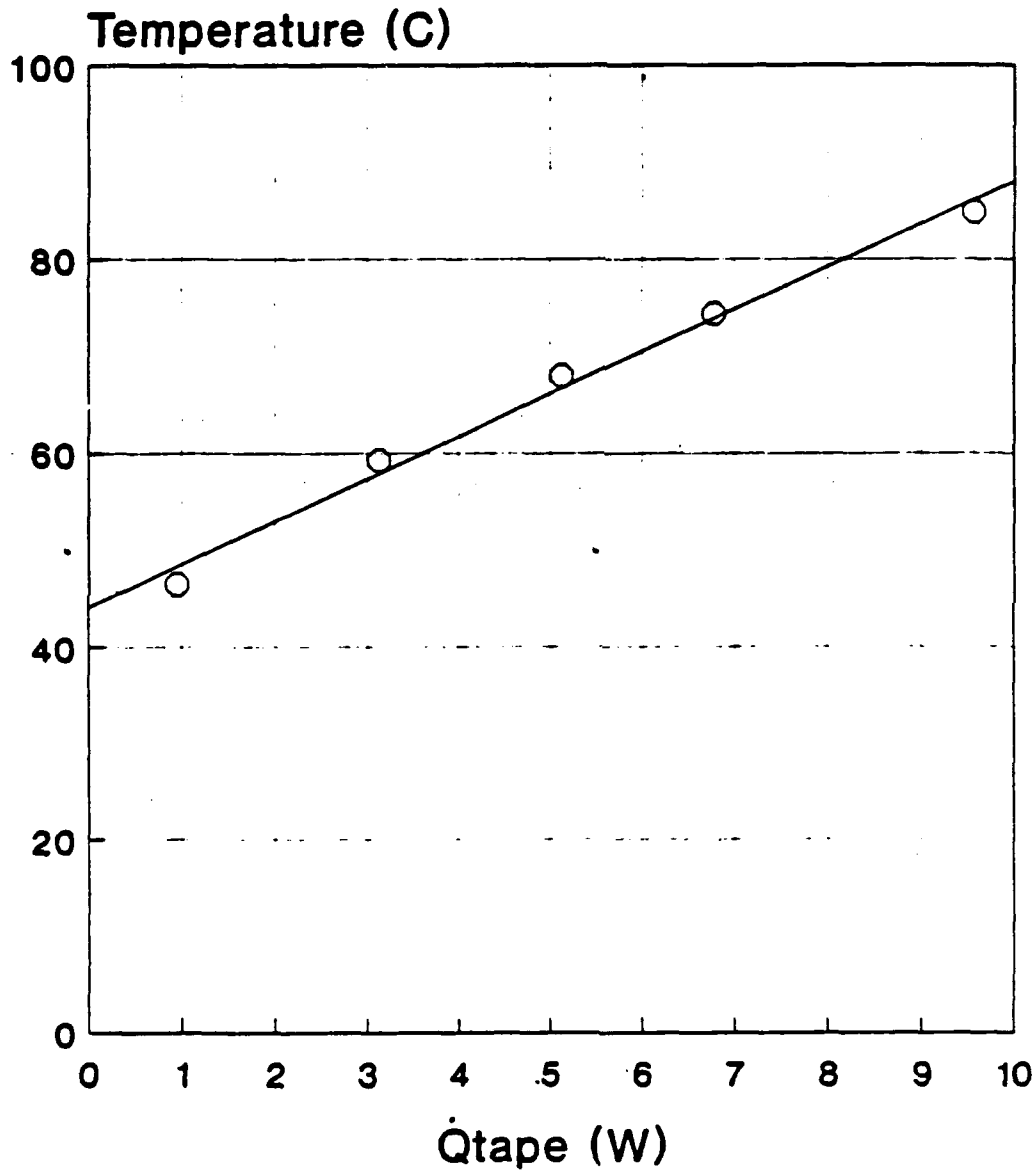
Tamb • 22:0

Figure B.2 Heat loss to ambient; Average wall temperature versus heat input.

119

APPENDIX C. FRICTIONAL/HEAT LEAKAGE EXPERIMENT

As coolant flows through the thermocouple wells/mixing box and along the tube, a small temperature rise results from frictional dissipation. When the coolant inlet temperature drops below ambient, an additional temperature rise can be attributed to heat leakage into the coolant from ambient. Since there was no means available to determine these terms separately, they were considered as one heat leakage term ($\dot{q}_{leak}$).

To determine this heat leakage term, the power to the heating elements was secured and coolant passed through the tube being tested at a given flowmeter setting. Any temperature rise detected was therefore due to frictional effects or heat leakage from ambient. This temperature rise was determined at flowmeter settings of 15% and 100% for each tube and insert condition at all four nominal inlet temperatures.

Data showed that flowmeter setting, tube and insert condition had no substantial effect on the temperature rise and that only the coolant inlet temperature made any difference. It can therefore be concluded that the heat leakage term was primarily due to heat addition from ambient. The results are shown in Table C.1.

TABLE C.1 HEAT LEAKAGE RESULTS

INLET TEMPERATURE	TEMPERATURE RISE
+20°C	0.0°C
+10°C	0.07°C
0°C	0.08°C
-10°C	0.18°C

These corrections were incorporated into the data reduction program "DRPSING" by directly subtracting this temperature rise from the measured outlet temperature.

APPENDIX D. POWER CALIBRATION

Actual heating element power (and therefore heat flux) was based upon the applied voltage and total heating element resistance. To measure voltage and current, the Data Acquisition Unit made use of a voltage and current sensing unit. However, a power factor needed to be applied to these sensed values to determine actual values required for the power/heat flux calculation.

Voltage and current meters were placed in the circuit downstream of the power source and prior to the first heating element as shown in Figure D.1. The voltage rheostat was varied over its entire range and voltage and current sensed by the meters and in the DAU were recorded (Table D.1). For each setting, actual power was calculated by:

$$P = VI \qquad (D.1)$$

and total heating element resistance by:

$$R = \frac{V}{I} = \frac{P}{V^2} \qquad (D.2)$$

In addition, voltage (PF_v) and current (PF_I) power factors were determined by:

$$PF_v = \frac{V_{ACTUAL}}{V_{CH29}} \quad and \quad PF_I = \frac{I_{ACTUAL}}{I_{CH25}} \tag{D.3}$$

where the subscripts "CH25" and "CH29" refer to the DAU sensing unit channel assignments and "actual" to the meter readings. All the above readings and calculations were done for five rheostat settings as shown in Table D.1.

An average heater resistance ($\bar{R}$), current ($\bar{PF}_I$) and voltage ($\bar{PF}_v$) power factors were then calculated. Heater power could then be calculated by one of the following forms of equation:

$$P = (\bar{PF}_I)(\bar{PF}_v) V_{CH29} \, I_{CH25} \tag{D.4}$$

or

$$P = (\bar{PF}_v V_{CH29})^2 / \bar{R} \tag{D.5}$$

The current power factor varied too much to be utilized in a simple calculation. Therefore, it was decided to make use of equation (D.5). The final equation to determine the average heating element power ($\dot{q}_{tape}$ in Watts) for a given rheostat setting was:

$$\dot{q}_{tape} = [59.66 \, V_{CH29}]^2 / 49.6 \tag{D.6}$$

This equation was incorporated into the data reduction program "DRPSING."

123

TABLE D.1 POWER CALIBRATION RESULTS

POWER (W)	V (VOLTS)	I (AMPS)	R (OHMS)	V_{CBS} (VOLTS)	I_{CBS} (AMPS)	PF_v	PF_I
31.31	30.7	0.61	50.32	0.5135	0.0106	59.78	57.50
76.14	61.4	1.24	49.51	1.032	0.0430	59.49	28.80
303.30	122.5	2.48	49.39	2.054	0.1050	59.63	23.60
750.36	192.4	3.90	49.30	3.226	0.1746	59.64	22.30
113.84	234.0	4.76	49.51	3.915	0.2170	59.77	21.90

POWER CALIBRATION
ELECTRICAL SCHEMATIC
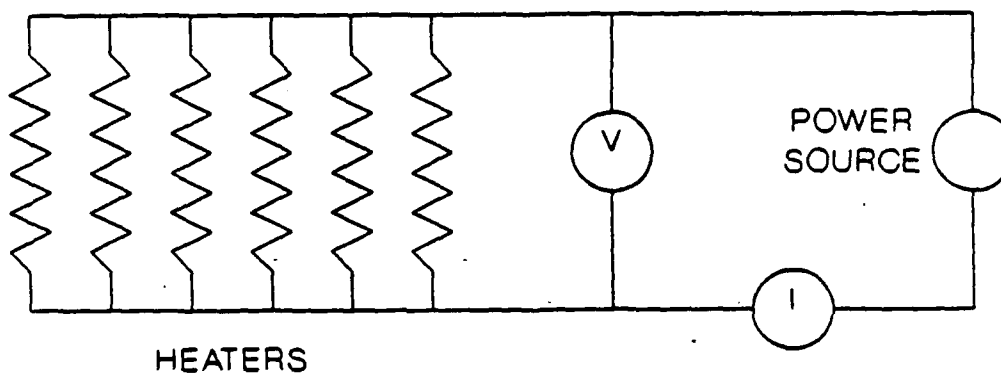
Figure D.1 Electrical schematic of power calibration experiment.

APPENDIX E. TUBE AND INSERT SPECIFICATIONS

TABLE E.1 TUBE CHARACTERISTICS/SPECIFICATIONS

PHYSICAL CHARACTERISTICS	Cu SMOOTH	Cu/Ni FINNED	Cu/Ni KORODENSE
Inside Diameter (D_i)	13.26mm	10.16mm	13.35mm
Outside Diameter (D_o)	15.88mm	14.00mm	15.85mm
T/C Diameter ($D_{t/c}$) t/c	14.36mm	12.62mm	14.53mm
Wall Thickness	1.31mm	1.22mm	1.25mm
Length			
Overall Length (L)	152.4cm	153.7cm	152.7cm
Heated Length (L_H)	140.6cm	143.0cm	142.4cm
Heated Finned Length (L_F)	-	122.3cm	-
Smooth Section Length (L_S)	-	15.7cm	-
T/C Location (1)			
Pos 1	15.2cm	17.8cm	15.6cm
Pos 2	55.9cm	57.2cm	56.2cm
Pos 3	96.5cm	96.5cm	96.8cm
Pos 4	137.2cm	135.9cm	134.5cm
T/C X/D for L_H (2)			
Pos 1	6.77	2.05	7.91
Pos 2	37.41	40.80	38.35
Pos 3	68.06	79.55	68.79
Pos 4	98.71	118.27	96.99
Inside Surface Area for L_H			
A_i	0.0586m^2	0.0340m^2 (3)	0.0600m^2
T/C Attachment Method	Silver Solder	Soft Solder	Tach Weld/ Liquid Metal

(1) measured from tube inlet; (2) measured from start of heated length; (3) for finned heated length.

TABLE E.2 INSERT CHARACTERISTICS/SPECIFICATIONS

TWISTED TAPE	NARROW	WIDE
thickness, δ	0.559mm	0.559mm
width, w	10.16mm	13.26mm
180° pitch, H	3.05cm	5.30cm
twist ratio, y	3	4
material	brass	brass
HEATEX	SMALL	LARGE
diameter	10.16mm	13.26mm
material	stainless steel	stainless steel

APPENDIX F. UNCERTAINTY ANALYSIS FOR THE INSIDE HEAT TRANSFER COEFFICIENT

Data file SMNI03 (smooth tube, no insert, $+10°C/10kW/m^2$),was chosen to conduct an uncertainty analysis of the experimental determination of the inside mean heat transfer coefficient, $\bar{h}_i$. In order to assess the effects of coolant velocity on the uncertainty in the measurement of $\bar{h}_i$, this uncertainty analysis was performed at coolant velocities of 0.4 and 1.4 m/s (for the same data set). The calculations below are shown for the 0.4 m/s coolant velocity. Table F.1 summarizes the results of the uncertainty analysis for both 0.4 m/s and 1.4 m/s coolant velocities.

The uncertainty analysis utilizes the procedure suggested by Kline and McClintock [Ref. 24]. This procedure states that if

$$R = R\ (x_1, x_2, x_3, \ldots\ldots x_n)$$

then the uncertainty in R, namely, δR is given by the equation:

$$\delta R = \left[\left(\frac{\partial R}{\partial x_1} \delta x_1 \right)^2 + \left(\frac{\partial R}{\partial x_2} \delta x_2 \right)^2 + \ldots\ldots + \left(\frac{\partial R}{\partial x_n} \delta x_n \right)^2 \right]^{0.5}$$

where x_n is the measured variable and δx_n is the uncertainty in the measured variable.

The uncertainty in the coolant temperature measurements is due to uncertainty in the voltage measured by the thermocouples. For the thermocouples used, this value was assumed to be 4 microvolts or 0.1°C. The uncertainty in ΔT is found from

127

the uncertainty in the coolant inlet and outlet temperatures, T_{ci} and T_{co}, and can be calculated as follows:

$$T_{co} = \frac{T(14) + T(15)}{2}$$

Taking the partial derivatives we obtain:

$$\frac{\partial T_{co}}{\partial T(14)} = \frac{\partial T_{co}}{\partial T(15)} = \frac{1}{2}$$

The uncertainty in the measurement of T_{co} is thus:

$$\partial T_{co} = \left[\left(\frac{\partial T_{co}}{\partial T(14)} \delta T \right)^2 + \left(\frac{\partial T_{co}}{\partial T(15)} \delta T \right)^2 \right]^{0.5}$$

Based on the thermocouple uncertainty, $\delta T = 0.1°C$, we obtain:

$$\delta T_{co} = 0.071°C$$

The coolant inlet temperature is calculated from a single thermocouple. The uncertainty in this measurement is calculated as:

$$\frac{\partial T_{ci}}{\partial T(13)} = 1$$

128

and

$$\delta T_{ci} = \left[\left(\frac{\partial T_{ci}}{\partial T(13)} \delta T \right)^2 \right]^{0.5} = 0.1°C$$

or,

$$\delta T_{ci} = 0.1°C$$

Since,

$$\left(\frac{\partial T_{co}}{\partial \Delta T} \right) = 1, \quad \left(\frac{\partial T_{ci}}{\partial \Delta T} \right) = -1$$

then the uncertainty in ΔT is calculated from:

$$\delta \Delta T = \left[(\delta T_{co})^2 + (\delta T_{ci})^2 \right]^{0.5}$$

or,

$$\delta \Delta T = 0.1225°C$$

For a measured ΔT of 3.7°C, the uncertainty is therefore:

$$\frac{\delta \Delta T}{\Delta T} = 0.0332 = 3.32\%$$

Coolant velocity is calculated from:

$$V_c = \frac{\dot{m}}{\rho_c A_i}$$

For a coolant velocity 0.4 m/s, $\dot{m}$ was calculated to be 0.05954 kg/s. The uncertainty in the reading of the flowmeter is defined as the scale interpolation. This value corresponds to one-half the value of the smallest marked increment. In this case, the scale interpolation factor, δ_{si}, is 0.5%, which corresponds to 0.00101 kg/s resolution. In addition, a time-wise jitter, δ_{ij}, of 0.5% was noted during the runs. Therefore, the uncertainty in $\dot{m}$ is given by:

$$\frac{\delta\dot{m}}{\dot{m}} = \left[\left(\frac{\delta\dot{m}}{\dot{m}}\delta_{si} \right)^2 + \left(\frac{\delta\dot{m}}{\dot{m}}\delta_{si} \right)^2 \right]^{0.5}$$

For a the measured coolant mass flow rate:

$$\frac{\delta\dot{m}}{\dot{m}} = 0.0239 = 2.39\%$$

The uncertainty in the cross-sectional area of the tubes was estimated from:

$$\frac{\delta A_c}{A_c} = \left[2 \times \left(\frac{\delta D_i}{D_i} \right)^2 \right]^2$$

where δD_i is given as 0.1 mm based on tolerances supplied from the manufacturer.

130

Therefore, for an inside diameter of 13.26 mm,

$$\frac{\delta A_c}{A_c} = 0.0107 = 1.07\%$$

Assuming that the uncertainty in the evaluation of the fluid properties is negligible, the uncertainty in the coolant velocity is now given by:

$$\frac{\delta V_c}{V_c} = \left[\left(\frac{\delta \dot{m}}{\dot{m}}\right)^2 + \left(\frac{\delta A_i}{A_i}\right)^2 \right]^{0.5}$$

or for a coolant velocity of 0.4 m/s,

$$\frac{\delta V_c}{V_c} = 0.0262 = 2.62\%$$

The uncertainty in the calculation of coolant Reynolds number is given by:

$$\frac{\delta Re_c}{Re_c} = \left[\left(\frac{\delta V_c}{V_c}\right)^2 + \left(\frac{\delta D_i}{D_i}\right)^2 \right]^{-0.5}$$

or substituting appropriate numbers we find

$$\frac{\delta Re_c}{Re_c} = 0.0282 = 2.82\%$$

The uncertainty in the calculation of the heat transfer rate to the coolant is related to the uncertainty in the measurements of coolant mass flow rate and coolant

temperature rise where:

$$\frac{\delta \dot{q}}{\dot{q}} = \left[\left(\frac{\delta \dot{m}}{\dot{m}} \right)^2 + \left(\frac{\delta \Delta T}{\Delta T} \right)^2 \right]^{0.5}$$

or

$$\frac{\delta \dot{q}}{\dot{q}} = 0.0409 = 4.09\%$$

The uncertainty in the heat flux is then:

$$\frac{\delta q_i''}{q_i''} = \left[\left(\frac{\delta \dot{q}}{\dot{q}} \right)^2 + \left(\frac{\delta A_s}{A_s} \right)^2 \right]^{0.5}$$

where the uncertainty in A_s is given by:

$$\frac{\delta A_s}{A_s} = \left[\left(\frac{\delta D_i}{D_i} \right)^2 + \left(\frac{\delta L}{L} \right)^2 \right]^{0.5}$$

Here, the uncertainty in the length of the tube, δL, is assumed to be 5 mm while δD_i,

is assumed to be 0.1 mm (again from given manufactures tolerances). Substitution

of the appropriate numbers yields:

$$\frac{\delta q_i''}{q_i''} = 0.0147 = 1.47\%$$

Finally, since $\bar{h}_i$ is given by:

$$h_i = \frac{q_o''}{LMTD}$$

the uncertainty in the LMTD must be calculated. The LMTD is given by:

$$LMTD = \frac{\Delta T}{\ln\left[\dfrac{T_{wi}-T_{ci}}{T_{wi}-T_{c,o}}\right]}$$

In order to calculate the uncertainty in the measurement of the LMTD, the following equations were used:

$$\frac{\partial LMTD}{\partial \Delta T} = \cdot\frac{1}{\ln\left[\dfrac{T_{wi}-T_{ci}}{T_{wi}-T_{co}}\right]}$$

$$\frac{\partial LMTD}{\partial T_{wi}} = \frac{\Delta T[(T_{wi}-T_{co})-(T_{wi}-T_{ci})]}{\left[\ln\left[\dfrac{T_{wi}-T_{ci}}{T_{wi}-T_{co}}\right]\right]^2 (T_{wi}-T_{ci})(T_{wi}-T_{ci})}$$

$$\frac{\partial LMTD}{\partial T_{c,o}} = -\frac{\Delta T}{\left[\ln\left[\dfrac{T_{wi}-T_{ci}}{T_{wi}-T_{co}}\right]\right]^2 (T_{wi}-T_{co})}$$

133

$$\frac{\partial LMTD}{\partial T_{ci}} = \frac{\Delta T}{\left[\ln\left[\frac{T_{wi}-T_{ci}}{T_{wi}-T_{co}}\right]\right]^2 (T_{wi}-T_{ci})}$$

The uncertainty in the LMTD is therefore given by:

$$\delta LMTD = \left[\left(\frac{\partial LMTD}{\partial \Delta T}\delta \Delta T\right)^2 + \left(\frac{\partial LMTD}{\partial T_{wi}}\partial T_{wi}\right)^2 + \left(\frac{\partial LMTD}{\partial T_{co}}\delta T_{co}\right)^2 + \left(\frac{\partial LMTD}{\partial T_{ci}}\delta T_{ci}\right)^2\right]^{\frac{1}{2}}$$

Before the uncertainty in LMTD can be calculated, the uncertainty in the measured average inside wall temperature must be determined. The average inside wall was determined from a total of twelve thermocouples, three at each of the four longitudinal positions. The uncertainty in a single wall temperature measurement is due to the uncertainty in the voltage measurement of the thermocouple ($\delta T = 0.1°C$) and the uncertainty due to the influence caused by the various attachment techniques used. Obviously, the variations seen in the wall thermocouple readings were due to this latter uncertainty and some account has to be made of this as this is by far the dominant uncertainty. If the average temperature at a given longitudinal position is assumed to be the required temperature, then the standard deviation of the three thermocouple readings at that position could be assumed to be this latter uncertainty. Therefore, the uncertainty at a given longitudinal position can be represented by:

134

$$\delta T_{pos(i)} = \frac{\partial T(i)}{\partial T} \delta T$$

where i = 1,2,3,4 for each of the four thermocouple longitudinal locations and

$\frac{\partial T(i)}{\partial T}$ is the standard deviation at each of these locations mentioned above.

Since the average inside wall temperature at each position increases along the length of the tube, the average inside wall temperature for the entire tube must be thought of as the average of the four longitudinal positions' average temperatures ($T_{pos(i)}$). The average inside wall temperature is then determined by:

$$T_{wi} = \frac{T_{pos1} + T_{pos2} + T_{pos3} + T_{pos4}}{4}$$

Taking the partial derivatives gives:

$$\frac{\partial T_{wi}}{\partial T_{pos1}} = \frac{\partial T_{wi}}{\partial T_{pos2}} = \frac{\partial T_{wi}}{\partial T_{pos3}} = \frac{\partial T_{wi}}{\partial T_{pos4}} = \frac{1}{4}$$

Therefore, the uncertainty in the average inside wall temperature measurement is:

$$\delta T_{wi} = \left[\left(\frac{\partial T_{wi}}{\partial T_{pos1}} \delta T_{pos1} \right)^2 + \left(\frac{\partial T_{wi}}{\partial T_{pos2}} \delta T_{pos2} \right)^2 + \left(\frac{\partial T_{wi}}{\partial T_{pos3}} \delta T_{pos3} \right)^2 + \left(\frac{\partial T_{wi}}{\partial T_{pos4}} \delta T_{pos4} \right)^2 \right]^{0.5}$$

Considering position 1, the average inside wall temperature is:

$$T_{pos1} = \frac{T(10) + T(11) + T(12)}{3}$$

For the three thermocouple readings of

$$T(10) = 25.99°C, \quad T(11) = 25.74°C \quad \text{and} \quad T(12) = 26.01°C,$$

the average inside wall temperature for position 1 is

$$T_{pos1} = 25.91°C$$

The standard deviation at this location is given by:

$$S.D. = \delta T_{pos1} = \left(\sum (T_n - T_{avg})^2 / n\right)^{0.5} = 0.123°C$$

Therefore,

$$\frac{\delta T_{pos1}}{\overline{T}_{pos1}} \approx 4.7 \times 10^{-3} = 0.47\%$$

Repeating this for the other three locations gives:

$$\delta T_{pos2} = 0.497°C$$

$$\delta T_{pos3} = 0.634°C$$

$$\delta T_{pos4} = 0.145°C$$

Therefore, the uncertainty in the measurement of average inside wall temperatures is:

$$\delta T_{wi} = \left[\left[(0.25)(0.123)\right]^2 + \left[(0.25)(0.497)\right]^2 + \left[(0.25)(0.634)\right]^2 + \left[(0.25)(0.145)\right]^2 \right]^{0.5} = 0.207$$

After substituting the appropriate values for $\partial LMTD / \partial \Delta T$, $\partial LMTD / \partial \bar{T}_{wi}$, $\partial LMTD / \partial T_{c,o}$ and $\partial LMTD / \partial T_{c,i}$ the uncertainty in the measurement of LMTD is:

$$\delta LMTD = 1.122 °C$$

and

$$\frac{\delta LMTD}{LMTD} = \frac{1.122}{24.13} = 0.0465 = 4.65\%$$

The uncertainty in the overall heat transfer coefficient, U_{ci} is then given by:

$$\frac{\delta \bar{h}_i}{\bar{h}_i} = \left[\left(\frac{\delta q_o''}{q_o''} \right)^2 + \left(\frac{\delta LMTD}{LMTD} \right)^2 \right]^{\frac{1}{2}}$$

or

$$\frac{\delta h_i}{h_i} = \left[(0.0417)^2 + (0.0463)^2 \right]^{\frac{1}{2}}$$

$$\frac{\delta h_i}{\delta h_i} = 0.0625 = 6.25\%$$

137

$$\frac{\delta h_i}{\delta h_i} = 0.0625 = 6.25\%$$

Table F.1 summarizes the results of the uncertainty analysis for the smooth copper tube with no insert for coolant velocities of 0.4 and 1.4 m/s, respectively at a nominal inlet coolant temperature of +10°C.

The uncertainty analysis neglects any uncertainty in the physical properties of the coolant. For the most part, this is probably a reasonable assumption. The exception to this may be the viscosity due to its sensitivity to temperature. Hence, the uncertainty reported here is likely to be conservative.

It is curious that the relative magnitudes of the uncertainty for the low and high coolant velocities are nearly the same. Two different mechanisms dominate in this calculated uncertainty at low and high coolant velocities. In terms of the mass flow rate, the time-wise jitter and scale interpolation terms are the same for both coolant velocities. However, the actual mass flow rate is less at the lower flow rates. Hence, the uncertainty in the mass flow rate calculation is more significant at the lower coolant velocities. At higher coolant flow rates, the uncertainty in the calculation of LMTD becomes the dominant term. This is because the coolant temperature rise is smaller at high coolant velocities but the uncertainty in the temperature measurements remains the same.

138

TABLE F.1 SUMMARY OF RESULTS FOR SAMPLE UNCERTAINTY ANALYSIS

Variable	$V_c = 0.4$ m/s	$V_c = 1.4$ m/s
$\dfrac{\delta T_{ci}}{T_{ci}}$	0.98%	0.87%
$\dfrac{\delta T_{co}}{T_{co}}$	0.51%	0.56%
$\dfrac{\delta \Delta T}{\Delta T}$	3.32%	10.67%
$\dfrac{\delta \dot{m}}{\dot{m}}$	2.39%	0.69%
$\dfrac{\delta A_i}{A_i}$	1.07%	1.07%
$\dfrac{\delta V_c}{V_c}$	2.62%	1.27%
$\dfrac{\delta Re_c}{Re_c}$	2.32%	1.47%
$\dfrac{\delta \dot{q}}{\dot{q}}$	4.09%	10.69%

$\dfrac{\delta T_{wi}}{T_{wi}}$	0.57%	0.71%
$\dfrac{\delta q_o''}{q_o''}$	4.17%	10.72%
$\dfrac{\delta LMTD}{LMTD}$	4.65%	16.32%
$\dfrac{\delta \bar{h}_i}{\bar{h}_i}$	6.25%	19.53%

```
1000 !   FILE:    DRPSING
1005 !   PURPOSE: This program collects and processes single instrumented tube da
ta.
1015 !   CREATED: APRIL 1, 1992 (S. MEMORY)
1030    BEEP
1035    PRINTER IS 1
1040    PRINT USING "4X,""SELECT OPTION"""
1045    PRINT USING "6X,""0  TAKING DATA OR REPROCESING PREVIOUS DATA"""
1065    PRINT USING "6X,""1  PURGE FILES"""
1080    PRINTER IS 701
1085    INPUT Icall
1090    IF Icall=0 THEN CALL Main
1095    IF Icall=1 THEN CALL Purge
1125    END
1130    SUB Main
1135    COM /Cc/ C(7)
1140    COM /Fld/ Ift
1145    COM /Nus/ Iin,Tsat,Qdp1,Hnus,Kf,Rhof,Hfg,Muf,Do,Itube
1150    COM /Will/ Doa(4),Dia(4),Kma(4),Iact,Oroot(4),Ld(3)
1155    COM /Wil2/ Delta,Isat,Nsets,Hod,Cia(4),Alpaa(3)
1160    DIM Emf(17),Tp(4),T(17),Ho(4),Qdp(4),Uo(4),Pc(4),Xstar(4),Nux(4),Nuss(4)
1170    DIM Xxx1(4),Xxx2(4),Xxx3(4),Xxx4(4),Xxx5(4),Xxx6(4)
1180    DIM Num(4),Nueg(4),Ldd(4),Nu(4),Xs(4)
1215    DATA 1.0,5.172,0.226,0.063,5.172
1220    READ Cia(*)
1225    DATA 0.10086091,25727.94369,-767345.8295,78025595.81
1230    DATA -9247486589,6.97688E11,-2.66192E13,3.94078E14
1235    READ C(*)
1240    DATA 0.015875,0.014000,0.015850,0.0159,0.0
1245    DATA 0.013259,0.010160,0.013350,0.01346,0.0
1250    DATA 386.0,42.98,42.98,21.9,0.0
1255    DATA 0.0005588,3
1260    READ Doa(*),Dia(*),Kma(*),Delta,Hod   ! Hod=H/Di
1261    IF Itube=0 THEN
1263    DATA 6.765,37.41,68.06,98.71
1264    READ Ld(*)   !   LENGTH/DIAMETER RATIO FOR 4 T/C LOCS (SMOOTH)
1265    L=1.406    ! Heated length of smooth tube
1266    END IF
1267    IF Itube=1 THEN
1268    DATA 2.05,40.80,79.55,118.29
1269    READ Ld(*)   !   FIN LENGTH/DIAMETER RATIO FOR 4 T/C LOCS (CU/NI FIN)
1270    L=1.223      ! Heated finned length of Cu/Ni fin tube
1271    END IF
1273    IF Itube=2 THEN
1274    DATA 7.908,38.35,68.792,96.987 .
1275    READ Ld(*)   !   LENGTH/DIAMETER RATIO FOR 4 T/C LOCS (KORODENSE)
1276    L=1.422   ! Heated length of Korodense tube
1277    END IF
1283    Jset=0
1284    Okaccpt=1
1285    BEEP
1286    INPUT "ENTER MONTH, DATE AND TIME (MM:DD:HH.MM:SS)",Dtg$
1287    OUTPUT 709;"TO";Dtg$
1290    BEEP
1300    Ihard=1
1310    INPUT "WANT A HARDCOPY PRINTOUT (1-DEF=YES,0=N)",Ihard
1315    BEEP
1325    Iin=1
1345    IF Ihard=1 THEN PRINTER IS 701
1355       BEEP
```

141

```
1360        INPUT "GIVE A NAME FOR THE NEW DATA FILE",Files
1365        CREATE BDAT Files,20
1370        ASSIGN @File TO Files
1375        BEEP
1380        INPUT "ENTER TUBE CODE (0=SMOOTH CU,1=FINNED CU/NI,2=KORODENSE,3=TIT
FIN )",Itube
1383        BEEP
1384        INPUT "0=NO INSERT, 1=TWISTED TAPE (WIDE), 2=HEATEX (L), 3=HEATEX (S)
, 4=TWISTED TAPE (NARROW)",Insert
1385        IF Insert=1 THEN Hod=4
1386        IF Insert=4 THEN Hod=3
1388        BEEP
1389        INPUT "NOMINAL SUMP TEMP. 0=-10 C, 1=0 C, 2=+10 C, 3=+20 C",Itemp
1390        BEEP
1391        Egrat=54
1392        INPUT "ENTER EG CONCENTRATION (WT PERCENT),DEFAULT = 54%",Egrat
1393        BEEP
1395 .      ENTER 709;Otgs
1400        OUTPUT @File;Otgs
1405        OUTPUT @File;Itube,Egrat,Od1,Od2,Od3,Od4,Od5
1430        PRINT USING "10X,""FILE NAME:   "",12A";Files
1435        PRINT
1595     Iout=1
1600     BEEP
1605     INPUT "WANT TO CREATE AN OUTPUT FILE? (1=DEF=YES,0=NO)",Iout
1610     IF Iout=1 THEN
1615   .    BEEP
1620        INPUT "ENTER A NAME FOR OUTPUT FILE",Fouts
1625        CREATE BDAT Fouts,5
1630        ASSIGN @Fout TO Fouts
1635     END IF
1640 '
1646     IF Itube=0 THEN Dtc=.01436        ! DIAMETER TO T/C BURIAL (SMOOTH)
1647     IF Itube=1 THEN Dtc=.0126         ! DIAMETER TO T/C BURIAL (CU/NI FIN)
1649     IF Itube=2 THEN Dtc=.01453        ! DIAMETER TO T/C BURIAL (KORODENSE)
1650     Oo=Ooa(Itube)
1651     Oo1=Ooa(Itube)
1653     O1=O1a(Itube)
1655     Km=Kma(Itube)
1660     Ax=PI*O1^2/4  ! Cross-sectional area
1661     IF Itube=2 THEN Ax=.00014    ! BASED ON WOLVERINE DESIGN DATA
1665     Ao=PI*Oo*L
1666     A1=PI*O1*L
1667     IF Itube=2 THEN Ao=.05*L      ! BASED ON WOLVERINE DESIGN DATA
1668     IF Itube=2 THEN A1=Ao/1.186  ! BASED ON WOLVERINE DESIGN DATA
1670     Perim=PI*O1
1671     Anarea=PI*(Oo^2-O1^2)/4.
1672     Ldd(1)=L/(4.*O1)
1673     Ldd(2)=L/(2.*O1)
1674     Ldd(3)=3.*L/(4.*O1)
1675     Ldd(4)=L/O1
1676     IF Itube=0 THEN
1677     Ulen1=.0627      ! UNHEATED INLET END OF COPPER SMOOTH TUBE ONLY
1678     Ulen2=.0572      ! UNHEATED OUTLET END OF COPPER SMOOTH TUBE ONLY
1679     END IF
1690     IF Itube=1 THEN
1681     Ulen1=.045       ! UNHEATED INLET END OF CU/NI FIN TUBE ONLY
1682     Ulen2=.06        ! UNHEATED OUTLET END OF CU/NI FIN TUBE ONLY
1683     Dcuo=.015875 ! UNHEATED OUTSIDE DIAMETER OF CU/NI FIN TUBE
1684     Dcui=.013259 ! UNHEATED INSIDE DIAMETER OF CU/NI FIN TUBE
```

```
1685    Lcui=.112     ! HEATED INLET SMOOTH END OF CU/NI FIN TUBE
1686    Lcuo=.097     ! HEATED OUTLET SMOOTH END OF CU/NI FIN TUBE
1687    Perim=PI*Ocui
1688    Anarea=PI*(Ocuo^2-Ocui^2)/4.
1689    END IF
1690    IF Itube=2 THEN
1691    Ulen1=.050    ! UNHEATED INLET END OF CU/NI KORODENSE TUBE ONLY
1692    Ulen2=.055    ! UNHEATED OUTLET END OF CU/NI KORODENSE TUBE ONLY
1693    END IF
1694    Hr=50         ! HEATER RESISTANCE
1700 !
1701        PRINTER IS 1
1702        BEEP
1703        INPUT "WHAT IS REQUIRED NOMINAL COOLANT VELOCITY IN m/s (MAX. = 1.4 m
/s)?",Vegst
1704        OUTPUT 709;"AR AF13 AL13 VR5"
1705            OUTPUT 709;"AS SA"
1706            Vsum=0
1707            FOR J=1 TO 5
1708                ENTER 709;E
1709                Vsum=Vsum+E
1710            NEXT J
1711            Emf(13)=Vsum/5
1712            T(13)=FNTvsv(Emf(13))
1713        Tavgl=T(13)
1714        IF Tavgl<-15 OR Tavgl>24 THEN
1715            PRINT "COOLANT TEMP. NOT IN RANGE -15 TO 24 C"
1716            GOTO 1703
1717        END IF
1718        Rhoegl=FNRhoeg(Tavgl,Egrat)
1719        Mdotl=Rhoegl*Ax*Vegst
1720        Pca15=(Mdotl+.0098)/.0019
1721        Pca0=(Mdotl+.00414)/.00206
1722        Pca24=(Mdotl+.00329)/.00225
1723        IF Tavgl<0 THEN
1724            Pc(0)=Pca15+((Tavgl+15)*(Pca0-Pca15))/15
1725        ELSE
1726            Pc(0)=Pca0+(Tavgl*(Pca24-Pca0))/24
1727        END IF
1728        PRINT "SET FLOWMETER READINGS CORRESPONDING TO:"
1729        PRINT USING "6X,""% OF METER A = "",DDD.D";Pc(0)
1730        PRINT
1731        PRINT "HIT CONTINUE WHEN READY"
1733        PAUSE
1734 Repeat:       !
1735 !      PRINTER IS 701
1737        Ido=1
1738        ON KEY 0,15 RECOVER 1734
1739        PRINT USING "4X,""SELECT OPTION """
1740        PRINT USING "6X,""0=TAKE DATA """
1741        PRINT USING "6X,""1=SET Heater Tape Heat Flux (DEFAULT) """
1742        PRINT USING "6X,""2=CHECK FLOWMETER % SETTING """
1744        PRINT USING "4X,""NOTE: KEY 0 = ESCAPE"""
1745 !      Ido = desired option
1746        BEEP
1747        INPUT Ido
1748 !      Set default value for input
1749        IF Ido>2 THEN Ido=2
1750 !      Take data option
1751        IF Ido=0 THEN 1816
```

143

```
1752        IF Ido=2 THEN 1703
1754 !      Loop to set heat flux and check temperatures
1755        IF Ido=1 THEN
1756          INPUT "ENTER DESIRED HEAT FLUX",Qdpwan
1758          PRINT USING "4X,"" Qdp (wanted)   Qdp (actual)   Tin     Delt"""
1759          PRINT USING "4X,""   (W/m^2)        (W/m^2)      (C)     (C) """
1761 !        Read thermocouple voltages
1762          OUTPUT 709;"AR AF1 AL15 VR5"
1764          FOR I=1 TO 15
1765            OUTPUT 709;"AS SA"
1766            Vsum=0
1767            FOR J=1 TO 20
1768              ENTER 709;E
1769              Vsum=Vsum+E
1770            NEXT J
1771            Emf(I)=Vsum/20
1772            T(I)=FNTvsv(Emf(I))
1773          NEXT I
1784 !        Compute average temperature of coolant outlet
1785          Tout=(T(14)+T(15))/2
1789          Delt=Tout-T(13)
1793          OUTPUT 709;"AR AF25 AL25 VR5"
1794            OUTPUT 709;"AS SA"
1795            ENTER 709;Amp
1796          OUTPUT 709;"AR AF29 AL29 VR5"
1797            OUTPUT 709;"AS SA"
1798            ENTER 709;Volt
1799          Qtape=(60*Volt)^2/Hr
1800          Qdptape=Qtape/Ao
1801          PRINT
1803          PRINT USING "4X,5(MZ.3DE,3X)";Qdpwan,Qdptape,T(13),Delt,Qtape
1804          PRINT
1805          PRINT USING "4X,""TEMPS AT POSITION 1"",3(DDD.DD,3X)";T(10),T(11),T
(12)
1806          PRINT
1807          PRINT USING "4X,""TEMPS AT POSITION 2"",3(DDD.DD,3X)";T(7),T(8),T(9
)
1808          PRINT
1809          PRINT USING "4X,""TEMPS AT POSITION 3"",3(DDD.DD,3X)";T(4),T(5),T(6
)
1810          PRINT
1811          PRINT USING "4X,""TEMPS AT POSITION 4"",3( DD.DD,3X)";T(1),T(2),T(3
)
1812          WAIT 2
1913          GOTO 1752
1814        END IF
1815 !      TAKE DATA IF Im=0 LOOP
1816        Twm=0
1818        Twi=0
1819        PRINTER IS 701
1820        OUTPUT 709;"AR AF1 AL15 VR5"
1821        FOR I=1 TO 15
1822          OUTPUT 709;"AS SA"
1823          Vsum=0
1824          FOR J=1 TO 20
1825            ENTER 709;E
1826            Vsum=Vsum+E
1827          NEXT J
1828          Emf(I)=Vsum/20
1829        NEXT I
```

144

```
1840 !
1845 !   DATA ANALYSIS
1850 !
1860    FOR I=1 TO 15
1865        T(I)=FNTvsv(Emf(I))
1870    NEXT I
1871    FOR I=1 TO 12
1872        Twi=Twi+T(I)
1873    NEXT I
1874    Twiav=Twi/12.
1876    Tout=(T(14)+T(15))/2
1880    Delt=Tout-T(13)
1881    Hlc=0.      ! Heat leakage correction
1883    IF Itube=0 THEN
1884    IF Itemp=0 THEN Hlc=.18               ! HEAT LEAKAGE CORRECTION AT -10 C
1885    IF Itemp=1 THEN Hlc=.08               ! HEAT LEAKAGE CORRECTION AT 0 C
1886    IF Itemp=2 THEN Hlc=.07               ! HEAT LEAKAGE CORRECTION AT +10 C
1887    IF Itemp=3 THEN Hlc=0.                ! NO HEAT LEAKAGE CORRECTION AT +20 C
1888    Delt=Delt-Hlc
1890    END IF
1891    Tout=Tout-Hlc
1893        OUTPUT 709;"AS SA"
1894        ENTER 709;Amp
1895    OUTPUT 709;"AR AF29 AL29 VR5"
1896        OUTPUT 709;"AS SA"
1897        ENTER 709;Volt
1898    Qtape=(60*Volt)^2/Hr
1923    Qdptape=Qtape/Ao
1925    Jset=Jset+1
1926    IF Okaccpt=0 THEN Jset=Jset-1
1930    PRINT
1935    PRINT USING "10X,""Data set number  = "",DD";Jset
1940    PRINT
1941    IF Itube=0 THEN PRINT USING "10X,""Smooth tube"""
1942    IF Itube=2 THEN PRINT USING "10X,""Korodense tube"""
1943    IF Itube=1 THEN PRINT USING "10X,""Copper/Nickel fin"""
1945    IF Itemp=0 THEN PRINT USING "10X,""Nominal sump temp. =  -10 C"""
1946    IF Itemp=1 THEN PRINT USING "10X,""Nominal sump temp. =    0 C"""
1948    IF Itemp=2 THEN PRINT USING "10X,""Nominal sump temp. =  +10 C"""
1949    IF Itemp=3 THEN PRINT USING "10X,""Nominal sump temp. =  +20 C"""
1951    IF Insert=0 THEN PRINT USING "10X,""No insert used"""
1952    IF Insert=1 THEN PRINT USING "10X,""Wide twisted tape insert used"""
1953    IF Insert=4 THEN PRINT USING "10X,""Narrow twisted tape insert used"""
1954    IF Insert=2 THEN PRINT USING "10X,""Large HEATEX insert used"""
1955    IF Insert=3 THEN PRINT USING "10X,""Small HEATEX insert used"""
1956    PRINT USING "10X,""Nominal set heat flux  = "",MZ.3DE";Qdptape
1960    PRINT USING "10X,""Nominal set coolant velocity = "",D.D";Vegst
1970    PRINT
1990        Tavg=T(13)+Delt*.5
1996        Rhoeg=FNRhoeg(Tavg,Egrat)
2000        Nuueg=FNNueg(Tavg,Egrat)
2005        Mueg=Nuueg*Rhoeg
2010        Cpeg=FNCpeg(Tavg,Egrat)
2015        Keg=FNKeg(Tavg,Egrat)
2020        Preg=Cpeg*Mueg/Keg
2025        Mdot=FNFmcal(T(13),Pc(0))
2030        Veg=Mdot/(Rhoeg*Ax)
2035        Reeg=Veg*Di/Nuueg
2040        Res=4*Mdot/(PI*Mueg*(Di-4*Delta))
2045        Qdot=Mdot*Cpeg*Delt
```

145

```
2048 '     ITERATE TO FIND INSIDE WALL TEMPERATURES
2049         Tm1=Tw1av
2050         Tm2=Tw1av
2051         Tm1=(Tm1+Tm2)/2.
2052         Ct1=Qdot*LOG(Dtc/D1)/(2.*PI*L*Km)
2053         Tm2=Tw1av-Ct1
2056         IF ABS(Tm2-Tm1)>.001 THEN GOTO 2051
2057         FOR I=1 TO 12
2058           T(I)=T(I)-Ct1
2059           Twm=Twm+T(I)
2060         NEXT I
2061         Twm=Twm/12
2062         Nuuegw=FNNueg(Twm,Egrat)
2063         Muegw=Nuuegw*Rhoeg
2064         Twm1=(T(12)+T(11)+T(10))/3
2065         Twm2=(T(9)+T(8)+T(7))/3
2066         Twm3=(T(6)+T(5)+T(4))/3
2067         Twm4=(T(3)+T(2)+T(1))/3
2068         Twm12=(T(12)+T(11)+T(10)+T(9)+T(8)+T(7))/6
2069         Twm123=(T(12)+T(11)+T(10)+T(9)+T(8)+T(7)+T(6)+T(5)+T(4))/9
2070         Tlm=(Tout-T(13))/LOG((Twm-T(13))/(Twm-Tout))
2071         Qloss=(Twm-44.15)/4.39    ! HEAT LOSS TO ATMOSPHERE
2072         IF Twm<45 THEN Qloss=0
2073         Qtape=Qtape-Qloss
2074         Qdp1=Qdot/A1
2075         Alfa1=Qdp1/Tlm
2076 !     FIN CORRECTION TO ACCOUNT FOR CONDUCTION TO ENDS OF TUBE
2077         Ff1=(Km*Perim*Anarea)^.5
2078         Alfa1l=Alfa1
2079         Alfa12=Alfa1l
2080         Alam1=((Alfa12*Perim)/(Km*Anarea))^.5
2081         Ff3=Ff1*Alfa12^.5*(Twm-T(13))
2082         Ff4=Ff1*Alfa12^.5*(Twm-Tout)
2083         Func6=Ff3*FNTanh(Alam1*Ulen1)
2084         Func7=Ff4*FNTanh(Alam1*Ulen2)
2085         Func8=Alfa12*A1*(Twm-Tavg)
2086         Funcx=Func6+Func7+Func8-Qdot
2087         Dfunc6=(.5*Func6/Alfa12)+2.*Ff3*Ulen1/(1.+FNCosh(2.*Alam1*Ulen1))
2088         Dfunc7=(.5*Func7/Alfa12)+2.*Ff4*Ulen2/(1.+FNCosh(2.*Alam1*Ulen2))
2089         Dfunc8=A1*(Twm-Tavg)
2090         Dfuncx=Dfunc6+Dfunc7+Dfunc8
2091         Alfa1l=Alfa12-Funcx/Dfuncx
2092         IF ABS(Alfa1l-Alfa12)>.05 THEN GOTO 2079
2093         Alfa12=Alfa1l
2095         Cfeg=(Mueg/Muegw)^.14
2096 !       FIND TEMPERATURE INCREASE DUE TO UNHEATED LENGTHS
2097         Deltin=Func6/(Mdot*Cpeg)
2098         Deltout=Func7/(Mdot*Cpeg)
2099         Thlin=T(13)+Deltin
2100         Thlout=Tout-Deltout
2101         Delhl=(Thlout-Thlin)
2105         IF Itube=1 THEN
2106         Heatin=Lcu1*Delhl/(L+Lcu1+Lcuo) ! HEATED SMOOTH INLET SECTION FOR CU
/NI FIN TUBE
2107         Heatout=Lcuo*Delhl/(L+Lcu1+Lcuo) ! HEATED SMOOTH OUTLET SECTION FOR
CU/NI FIN TUBE
2109         Thlin=Thlin+Heatin
2110         Thlout=Thlout-Heatout
2111         Delhl=(Thlout-Thlin)
2114         END IF
```

146

```
2115        Qhl=Mdot*Cpeg*Oelhl
2116        Qdphl=Qhl/Ai
2117        Qdpxx=Func8/Ai
2118        Tcol=Thlin+(Oelhl/4)
2119        Tco2=Thlin+(Oelhl/2)
2120        Tco3=Thlin+(3*Oelhl/4)
2121        Ttc1=T(13)+(Ld(0)*Oi*Oelhl/L)
2122        Ttc2=T(13)+(Ld(1)*Oi*Oelhl/L)
2123        Ttc3=T(13)+(Ld(2)*Oi*Oelhl/L)
2124        Ttc4=T(13)+(Ld(3)*Oi*Oelhl/L)
2126        Tlmall=(Thlout-Thlin)/LOG((Twm-Thlin)/(Twm-Thlout))  ! ALL (1,2,3,4)
2127        Tlm1=(Tcol-Thlin)/LOG((Twm1-Thlin)/(Twm1-Tcol))       ! SECTION 1
2128        Tlm2=(Tco2-Tcol)/LOG((Twm2-Tcol)/(Twm2-Tco2))         ! SECTION 2
2129        Tlm3=(Tco3-Tco2)/LOG((Twm3-Tco2)/(Twm3-Tco3))         ! SECTION 3
2130        Tlm4=(Thlout-Tco3)/LOG((Twm4-Tco3)/(Twm4-Thlout))     ! SECTION 4
2131        Tlm12=(Tco2-Thlin)/LOG((Twm12-Thlin)/(Twm12-Tco2))    ! SECTION 1,2
2132        Tlm123=(Tco3-Thlin)/LOG((Twm123-Thlin)/(Twm123-Tco3))! SECTION 1,2,3
2133        Alpall=Qdphl/Tlmall
2134        Alp1=Qdphl/Tlm1
2135        Alp2=Qdphl/Tlm2
2136        Alp3=Qdphl/Tlm3
2137        Alp4=Qdphl/Tlm4
2138        Alloc1=Qdphl/(Twm1-Ttc1)
2139        Alloc2=Qdphl/(Twm2-Ttc2)
2140        Alloc3=Qdphl/(Twm3-Ttc3)
2141        Alloc4=Qdphl/(Twm4-Ttc4)
2143        Alp12=Qdphl/T!m12
2144        Alp123=Qdphl/Tlm123
2145        Keg1=FNKeg((Tcol+Thlin)/2,Egrat)
2146        Keg2=FNKeg((Tco2+Tcol)/2,Egrat)
2147        Keg3=FNKeg((Tco3+Tco2)/2,Egrat)
2148        Keg4=FNKeg((Thlout+Tco3)/2,Egrat)
2149        Keg12=FNKeg((Tco2+Thlin)/2,Egrat)
2150        Keg123=FNKeg((Tco3+Thlin)/2,Egrat)
2151        Numall=Alpall*Oi/Keg
2152        Nu1=Alp1*Oi/Keg1
2153        Nu2=Alp2*Oi/Keg2
2154        Nu3=Alp3*Oi/Keg3
2155        Nu4=Alp4*Oi/Keg4
2156        Nuloc1=Alloc1*Oi/Keg1
2157        Nuloc2=Alloc2*Oi/Keg2
2158        Nuloc3=Alloc3*Oi/Keg3
2159        Nuloc4=Alloc4*Oi/Keg4
2161        Nu12=Alp12*Oi/Keg12
2162        Nu123=Alp123*Oi/Keg123
2163 !        LOCAL NUSSELT FROM SHAH/LONDON PAGE 128, EQN 240-242
2164 !        CALCULATE XSTAR FIRST FOR EACH THERMOCOUPLE LOCATION
2165 !        DEFINE COOLANT PECLET NUMBER
2166        Peeg=Preg*Reeg
2167        Xs(1)=Ldd(1)/Peeg   ! FOR MEAN VALUES OF h
2168        Xs(2)=Ldd(2)/Peeg
2169        Xs(3)=Ldd(3)/Peeg
2170        Xs(4)=Ldd(4)/Peeg
2171        FOR I=1 TO 4
2172        Xstar(I)=Ld(I-1)/Peeg ! FOR LOCAL VALUES AT T/C POSITIONS
2173           Nux(I)=1.302*Xstar(I)^(-1/3)-.5
2175 !        DEVELOPING HYDRO AND THERMAL BOUNDARY LAYER (S/L P148, EQN. 258)
2176           Xx1=(1+((220/PI)*Xstar(I))^(-10/9))^(3/5)
2177           Xx2=(1+(Preg/.0207)^(2/3))^.5
2178           Xx3=PI/(115.2*Xstar(I))
```

```
2179            Xx4=(1+(Xx3/(Xx2•Xx1))^(5/3))^(3/10)
2180            Xx5=(1+((220/PI)•Xstar(I))^(-10/9))^(3/10)
2181            Nuss(I)=(Xx4•5.364•Xx5)-1
2188         IF Xstar(I)<.00005 THEN
2189            Nux(I)=1.302•Xstar(I)^(-1/3)-1
2190         END IF
2194         IF Xstar(I)>.0015 THEN
2195            Nux(I)=4.364+8.68•(1000•Xstar(I))^(-.506)•EXP(-41•Xstar(I))
2196         END IF
2200         NEXT I
2202         IF Insert=0 THEN
2203         PRINT USING "3X,""              LOCAL NUSSELT VALUES"""
2205         PRINT USING "3X,""   Exp. Nux(TLM)   Exp. Nux(BULK)   Pred. Nux(1)
   Pred. Nux(2)    Xstar(tc)"""
2206         PRINT
2207         PRINT USING "3X,""POS 1 "",5(MZ.3DE,5X)":Nu1,Nuloc1,Nux(1),Nuss(1),X
star(1)
2208         PRINT USING "3X,""POS 2 "",5(MZ.3DE,5X)":Nu2,Nuloc2,Nux(2),Nuss(2),X
star(2)
2209         PRINT USING "3X,""POS 3 "",5(MZ.3DE,5X)":Nu3,Nuloc3,Nux(3),Nuss(3),X
star(3)
2210         PRINT USING "3X,""POS 4 "",5(MZ.3DE,5X)":Nu4,Nuloc4,Nux(4),Nuss(4),X
star(4)
2211         PRINT
2215         ELSE
2216         PRINT USING "3X,""POSITION #  =   Exp. Nux (TLM)    Exp. Nux (BULK)
   Xstar at tc pos."""
2217         PRINT
2218         PRINT USING "3X,""POSITION 1 (LOCAL) = "",3(MZ.3DE,5X)":Nu1,Nuloc1,X
star(1)
2219         PRINT USING "3X,""POSITION 2 (LOCAL) = "",3(MZ.3DE,5X)":Nu2,Nuloc2,X
star(2)
2220         PRINT USING "3X,""POSITION 3 (LOCAL) = "",3(MZ.3DE,5X)":Nu3,Nuloc3,X
star(3)
2221         PRINT USING "3X,""POSITION 4 (LOCAL) = "",3(MZ.3DE,5X)":Nu4,Nuloc4,X
star(4)
2222         END IF
2223         PRINT
2230         FOR I=1 TO 4
2232         IF Insert=0 THEN
2233            Bb1=.0668•Reeg•Preg/Ldd(I)
2234            Bb2=1+.04•(Reeg•Preg/Ldd(I))^.6666
2235            Nueg(I)=3.66+(Bb1/Bb2)
2236         END IF
2237         IF Insert=1 OR Insert=4 THEN
2239            Nueg(I)=Cia(Insert)•(1+5.484E-3•Preg^.7•(Res/Hod)^1.25)^.5
2240           .Nuoth=.383•Preg^.35•(Res/Hod)^.622
2241         END IF
2242         IF Insert=2 THEN
2243            Nueg(I)=Cia(Insert)•(Reeg^.65)•Preg^.46
2244         END IF
2245         IF Insert=3 THEN
2246            Nueg(I)=Cia(Insert)•(Reeg^.76)•Preg^.46
2247         END IF
2248         BEEP
2249'     CALCULATED VALUE OF INSIDE HT. TRANSFER COEFF. FROM CORRELATIONS
2250       Hi=Nueg(4)•Keg/Di
2251'     MEAN NUSSELT NUMBER FROM SHAH/LONDON PAGE 128, EQN 245-246
2254       IF Xs(I)<.03 THEN
2255          Num(I)=1.953•Xs(I)^(-1/3)
```

148

```
2256        F_SE
2258          Num(I)=4.364+(.0722/Xs(I))
2259        END IF
2262        NEXT I
2263        PRINT USING "3X,""POSITION #  =        Exp. mean Nu     Pred. mean Nu
    Xstar at section"""
2264        PRINT
2266        PRINT USING "3X,""POSITION 1 (MEAN) =     "",3(MZ.3DE,5X)";Nu1,Num(1)
,Xs(1)
2267        PRINT USING "3X,""POSITION 12 (MEAN) =    "",3(MZ.3DE,5X)";Nu12,Num(2
),Xs(2)
2268        PRINT USING "3X,""POSITION 123 (MEAN) =   "",3(MZ.3DE,5X)";Nu123,Num(
3),Xs(3)
2269        PRINT USING "3X,""POSITION 1234 (MEAN) = "",3(MZ.3DE,5X)";Numall,Num
(4),Xs(4)
2270            PRINT
2271            PRINT
2272            PRINT USING "10X,""Mass flow rate (kg/s)   = "",MZ.3DE";Mdot
2273'           PRINT USING "10X,""Inside Tube Dia. (m)    = "",MZ.3DE";Dia(Itube)
2274            IF Insert=1 THEN PRINT USING "10X,""180 DEG OVER Dia. (HOD) = "",
MZ.3DE";Hod
2275            PRINT USING "10X,""Inlet temperature (C)   = "",MZ.3DE";T(13)
2276            IF Insert=1 OR Insert=4 THEN
2277            PRINT USING "10X,""DELTA Tape Thickness     = "",MZ.3DE";Delta
2278            END IF
2279            PRINT USING "10X,""DELT  temp  Dif. (C)     = "",MZ.3DE";Delt
2280            PRINT USING "10X,""H. T. to coolant (W)     = "",MZ.3DE";Qdot
2281            PRINT USING "10X,""H. T. from heater tape (W) = "",MZ.3DE";Qtape
2282            PRINT USING "10X,""Prandtl number           = "",MZ.3DE";Preg     ___  _
2283            PRINT USING "10X,""Reynolds number          = "",MZ.3DE";Reeg
2284            IF Insert=1 OR Insert=4 THEN PRINT USING "10X,""Reynolds number H
&& S   = "",MZ.3DE";Res
2285            PRINT USING "10X,""H1 from correl. (W/m^2.K) = "",MZ.3DE";H1
2286            PRINT USING "10X,""H1 from heat bal. (W/m^2.K) = "",MZ.3DE";Alfa1
2
2287            IF Insert=0 THEN PRINT USING "10X,""Nu for no insert (Hausen)   "
"",MZ.3DE";Nueg(4)
2288            IF Insert=1 OR Insert=4 THEN PRINT USING "10X,""Nu for twisted ta
pe (Bergles2)"",MZ.3DE";Nuoth
2289            IF Insert=1 OR Insert=4 THEN PRINT USING "10X,""Nu for twisted ta
pe (Bergles3)"",MZ.3DE";Nueg(4)
2290            IF Insert=2 THEN PRINT USING "10X,""Nu for large Heatex (Mazzone)
"",MZ.3DE";Nueg(4)
2291            IF Insert=3 THEN PRINT USING "10X,""Nu for small Heatex (Mazzone)
"",MZ.3DE";Nueg(4)
2292            IF Insert=0 THEN PRINT USING "10X,""Nu from Shah/London       = "",
MZ.3DE";Num(4)
2293            PRINT USING "10X,""Xstar for heated length = "",MZ.3DE";Xs(4)
2294            PRINT USING "10X,""Experimental Nusselt no.= "",MZ.3DE";Numall
2295            PRINT
2296            PRINT USING "3X,""Wall t/c 12,11,10 (pos. 1) (C) = "",3(000.00,3X
)";T(12),T(11),T(10)
2297            PRINT USING "3X,""Wall t/c 9,8,7    (pos. 2) (C) = "",3(000.00,3X
)";T(9),T(8),T(7)
2298            PRINT USING "3X,""Wall t/c 6,5,4    (pos. 3) (C) = "",3(000.00,3X
)";T(6),T(5),T(4)
2299            PRINT USING "3X,""Wall t/c 3,2,1    (pos. 4) (C) = "",3(000.00,3X
)";T(3),T(2),T(1)
2300            PRINT USING "3X,""Av. inside wall temp (C) = "",MZ.3DE";Twm
2301            PRINT
```

149

```
2302            Nu(1)=Nu1
2303            Nu(2)=Nu12
2304            Nu(3)=Nu123
2305            Nu(4)=Numall
2307            IF Insert=0 THEN
2308            FOR I=1 TO 4
2310            Xxx1(I)=LOG(Nu(I))
2311            Xxx2(I)=LOG(Xs(I))
2312            Xxx3(I)=LOG(Nueg(I))
2313            Xxx4(I)=LOG(Num(I))
2314            NEXT I
2315            PRINT USING "3X,""MEAN VALUES AT          POS 1          POS 1
2       POS 123       POS 1234"""
2317            PRINT USING "6X,""EXP. LOG(Nu)       = "",4(MZ.3DE,4X)":Xxx1(1),X
xx1(2),Xxx1(3),Xxx1(4)
2318            PRINT USING "6X,""COR. LOG(Nu) (H)   = "",4(MZ.3DE,4X)":Xxx3(1),X
xx3(2),Xxx3(3),Xxx3(4)
2319            PRINT USING "6X,""COR. LOG(Nu) (S/L) = "",4(MZ.3DE,4X)":Xxx4(1),X
xx4(2),Xxx4(3),Xxx4(4)
2320            PRINT USING "6X,""LOG(Xstar)         = "",4(MZ.3DE,4X)":Xxx2(1),X
xx2(2),Xxx2(3),Xxx2(4)
2321            END IF
2323            IF Insert=2 OR Insert=3 THEN
2324            FOR I=1 TO 4
2325            Xxx1(I)=LOG(Nu(I)/Preg^.46)
2326            Xxx2(I)=LOG(Reeg)
2327            Xxx3(I)=LOG(Nueg(I)/Preg^.46)
2328            NEXT I
2329            PRINT USING "3X,""MEAN VALUES AT          POS 1          POS 1
2       POS 123       POS 1234"""
2331            PRINT USING "6X,""EXP. LOG(Nu/Pr^.46) = "",4(MZ.3DE,4X)":Xxx1(1),
Xxx1(2),Xxx1(3),Xxx1(4)
2332            PRINT USING "6X,""COR. LOG(Nu/Pr^.46) = "",4(MZ.3DE,4X)":Xxx3(1),
Xxx3(2),Xxx3(3),Xxx3(4)
2334            PRINT USING "6X,""LOG(Re)             = "",4(MZ.3DE,4X)":Xxx2(1),
Xxx2(2),Xxx2(3),Xxx2(4)
2335            END IF
2336            IF Insert=1 OR Insert=4 THEN
2337            FOR I=1 TO 4
2338            Xxx1(I)=LOG(Nu(I)/Preg^.35)
2339            Xxx2(I)=LOG(Res/Hod)
2340            Xxx3(I)=LOG(Nuoth/Preg^.35)
2341            Xxx4(I)=LOG(Nu(I))
2342            Xxx5(I)=LOG(Preg*(Res/Hod)^1.78)
2343            Xxx6(I)=LOG(Nueg(I))
2344            NEXT I
2345            PRINT USING "3X,""MEAN VALUES AT          POS 1          POS 1
2       POS 123       POS 1234"""
2346            PRINT USING "6X,""EXP. LOG(Nu/Pr^.35) = "",4(MZ.3DE,4X)":Xxx1(1),
Xxx1(2),Xxx1(3),Xxx1(4)
2347            PRINT USING "6X,""COR. LOG(Nu/Pr^.35) = "",4(MZ.3DE,4X)":Xxx3(1),
Xxx3(2),Xxx3(3),Xxx3(4)
2348            PRINT USING "6X,""LOG(Res/y)          = "",4(MZ.3DE,4X)":Xxx2(1),
Xxx2(2),Xxx2(3),Xxx2(4)
2349            PRINT
2350            PRINT USING "6X,""EXP. LOG(Nu)        = "",4(MZ.3DE,4X)":Xxx4(1),
Xxx4(2),Xxx4(3),Xxx4(4)
2351            PRINT USING "6X,""COR. LOG(Nu)        = "",4(MZ.3DE,4X)":Xxx6(1),
Xxx6(2),Xxx6(3),Xxx6(4)
2352            PRINT USING "6X,""LOG(Pr(Res/y)^1.78) = "",4(MZ.3DE,4X)":Xxx5(1),
```

150

```
Xxx5(2),Xxx5(3),Xxx5(4)
2353          END IF
2354          IF Insert=0 AND Reeg>2300 THEN
2355          Nutu=.027*Reeg^.8*Preg^.3333*Cfeg
2356          PRINT USING "6X,""TURBULENT S/T CORRELATION = "",4(MZ.3DE,4X)";Nu
tu
2357          Xxx7=LOG(Nutu)
2358          PRINT USING "6X,""TURB. COR. LOG(Nu)   = "",4(MZ.3DE,4X)";Xxx7
2359          END IF
2360      Okaccpt=1
2361      BEEP
2362      INPUT "OK TO ACCEPT THIS SET (1=DEFAULT=YES, 0=NO)?",Okaccpt
2363      IF Okaccpt=1 THEN OUTPUT @File;Pc(*),Emf(*),Tp(*)
2364    IF Im=0 THEN
2365      Okrpt=1
2366      BEEP
2367      INPUT "WILL THERE BE ANOTHER RUN (1=YES=DEFAULT,0=NO)",Okrpt
2368      IF Okrpt=1 THEN 1701
2369    ELSE
2370      IF Jset<Nsets THEN 1701
2371    END IF
2372    ASSIGN @File TO *
2373    IF Iout=1 THEN ASSIGN @File TO *
2374    SUBEND
2375    DEF FNGrad(T)
2376    Grad=-3:877857E-5-2*4.7142857E-8*T
2377    RETURN Grad
2378    FNEND
2379    DEF FNKcu(T)
2380 !  OFHC COPPER 250 TO 300 K
2381    Tk=T+273.15
2382    K=434-.112*Tk
2383    RETURN K
2384    FNEND
2385    DEF FNNueg(Tc,Egr)
2386 !  RANGE OF VALIDITY:  -20 TO 20 DEG C
2387    Tk=Tc+273.15
2388    Nu1=7.1196507E-3-Tk*(7.4863347E-5-Tk*(2.6294943E-7-Tk*3.0833329E-10))
2390    Nu2=4.9237638E-3-Tk*(4.9213912E-5-Tk*(1.6437534E-7-Tk*1.3333331E-10))
2395    Nu3=8.6586293E-3-Tk*(8.8837902E-5-Tk*(3.0495032E-7-Tk*3.4999996E-10))
2400    A2=(Nu3-2*Nu2+Nu1)/200
2405    A1=(Nu2-Nu1-940*A2)/10
2410    A0=Nu1-42*A1-1764*A2
2415    Nu=A0+Egr*(A1+Egr*A2)
2420    RETURN Nu
2425    FNEND
2430    DEF FNCpeg(Tc,Egr)
2435 !  RANGE OF VALIDITY  0 TO 20 DEG C
2440    Tk=Tc+273.15
2445    Cp1=1.6701550E+3+Tk*6.3
2450    Cp2=1.4748125E+3+Tk*6.25
2455    Cp3=9.5800500E+2+Tk*7.3
2460    A2=(Cp3-2*Cp2+Cp1)/200
2465    A1=(Cp2-Cp1-900*A2)/10
2470    A0=Cp1-40*A1-1600*A2
2475    Cp=A0+Egr*(A1+Egr*A2)
2480    RETURN Cp
2485    FNEND
2490    DEF FNRhoeg(T,Egr)
2495    Ro1=1.0607093E+3-T*(3.7031283E-1+T*4.0837183E-3)
```

151

```
2500    Ro2=1.0748272E+3-T*(4.4266195E-1+T*4.0939706E-3)
2505    Ro3=1.0885934E+3-T*(5.7356653E-1+T*6.128140SE-3)
2510    A2=(Ro3-2*Ro2+Ro1)/200
2515    A1=(Ro2-Ro1-900*A2)/10
2520    A0=Ro1-40*A1-1600*A2
2525    Ro=A0+Egr*(A1+Egr*A2)
2530    RETURN Ro
2535    FNEND
2540    DEF FNPreg(T,Egr)
2545    Pr=FNCpeg(T,Egr)*FNNueg(T,Egr)*FNRoeg(T,Egr)/FNKeg(T,Egr)
2550    RETURN Pr
2555    FNEND
2560    DEF FNKeg(Tc,Egr)
2565 !  RANGE OF VALIDITY:  -20 TO 20 DEG C
2570    Tk=Tc+273.15
2575    K1=2.2824708E-1+Tk*(5.5989286E-4+Tk*3.5714286E-7)
2580    K2=2.5846616E-1+Tk*(2.3978571E-4+Tk*7.1428571E-7)
2585    K3=3.2138932E-1-Tk*(3.0042857E-4-Tk*1.4285714E-6)
2590    A2=(K3-2*K2+K1)/200
2595    A1=(K2-K1-900*A2)/10
2600    A0=K1-40*A1-1600*A2
2605    K=A0+Egr*(A1+Egr*A2)
2610    RETURN K
2615    FNEND
2620    DEF FNTanh(X)
2625    P=EXP(X)
2630    Q=1/P
2635    Tanh=(P-Q)/(P+Q)
2640    RETURN Tanh
2645    FNEND
2650    DEF FNTvsv(V)
2655    COM /Cc/ C(7)
2660    T=C(0)
2665    FOR I=1 TO 7
2670        T=T+C(I)*V^I
2675    NEXT I
2680    RETURN T
2685    FNEND
2690    DEF FNBeta(T)
2695    Rop=FNRho(T+.1)
2700    Rom=FNRho(T-.1)
2705    Beta=-2/(Rop+Rom)*(Rop-Rom)/.2
2710    RETURN Beta
2715    FNEND
2720    DEF FNPsat(Tc)
2725 !  0 TO 80 deg F CURVE FIT OF Psat
2730    Tf=1.8*Tc+32
2735    Pa=5.945525+Tf*(.15352082+Tf*(1.4840963E-3+Tf*9.6150671E-6))
2740    Pg=Pa-14.7
2745    IF Pg>0 THEN         ! +=PSIG,-=in Hg
2750        Psat=Pg
2755    ELSE
2760        Psat=Pg*29.92/14.7
2765    END IF
2770    RETURN Psat
2775    FNEND
2905    SUB Purge
2910    BEEP
2915    INPUT "ENTER FILE NAME TO BE DELETED",File$
2920    PURGE File$
```

152

```
2925    GOTO 2910
2930    SUBEND
2935    SUB Wilson
2940    COM /Will/ Doa(4),Dia(4),Kma(4),Iact,Droot(4),Ld(3)
2945    COM /Wil2/ Delta,Isat,Nsets,Hod,Cia(4),Alpaa(3)
2950    DIM Emf(17),T(17),Xa(100),Ya(100),Pc(4),Tp(4)
2955    BEEP
2960    INPUT "PLEASE RE-ENTER NAME OF FILE",File$
2965    ASSIGN @File TO File$
2970    INPUT "0=SMOOTH COPPER TUBE, 1=CUNI FIN, 2=KORODENSE, 3=FIN TITAN",Itube
2975    BEEP
2976    INPUT "0=NO INSERT, 1= TWISTED TAPE INSERT, 2=HITRAN1, 3=HITRAN2",Insert
2977    BEEP
2980    INPUT "GIVE A NAME FOR XY FILE",Xy$
2985    CREATE BDAT Xy$,20
2990    ASSIGN @Xy TO Xy$
2995    L=1.2192
3000    Do=Doa(Itube)
3005    Di=Dia(Itube)
3010    Km=Kma(Itube)
3015    Ax=PI*Di^2/4   ! Cross-sectional area
3020    Ao=PI*Do*L
3025    Rm=Do*LOG(Do/Di)/(2*Km)
3030 !
3035 !  Initial values
3040    Tf=Tsat
3045    Alpa=.655
3046    IF Insert=0 THEN
3050    Ci=1.0.
3051    END IF
3052    IF Insert=1 THEN
3053    Ci=5.172
3054    END IF
3055    IF Insert=2 THEN
3056    Ci=.226
3057    END IF
3058    IF Insert=3 THEN
3059    Ci=.063
3060    END IF
3062    G=9.31
3063    Ibeg=0
3065    Iend=0   'CHANGE TO 4, IF FIVE TUBES IN BUNDLE
3070    IF Iact<10 THEN
3075        Ibeg=Iact
3080        Iend=Iact
3085    END IF
3090 !
3095    FOR I=Ibeg TO Iend
3100        Sx=0
3105        Sy=0
3110        Sxs=0
3115        Sxy=0
3120        Jset=0
3125        ASSIGN @File TO File$
3130        ENTER @File;Otg$,Itube,Egrat,Od1,Od2,Od3,Od4,Od5
3135        ENTER @File;Pc(*),Emf(*),Tp(*)
3140        FOR J=0 TO 17
3145            T(J)=FNTvsv(Emf(J))
3150        NEXT J
3155        Tvap=(T(0)+T(1)+T(2))/3
```

```
3160        Tliq=(T(3)+T(4))/2
3161        Tliql=T(5)
3165        IF Isat=0 THEN
3170            Tsat=Tliql
3175        ELSE
3180            Tsat=Tvap
3185        END IF
3190 !      Grad=FNGrad(T(I+6))
3191        Tout=(T(2*I+10)+T(2*I+11))/2
3195        Delt=Tout-T(I+6)
3200        Tavg=T(I+6)+Delt*.5
3201 !      IF I=Iend THEN
3202 !        Delt=T(10)-T(9)
3204 !        Tavg=(T(10)-T(9))/2
3205 !      END IF
3206 !
3210 !      Water/Ethylene Glycol Mixture Properties
3215        Rhoeg=FNRhoeg(Tavg,Egrat)
3220        Nueg=FNNueg(Tavg,Egrat)
3225        Mueg=Nueg*Rhoeg
3230        Cpeg=FNCpeg(Tavg,Egrat)
3235        Keg=FNKeg(Tavg,Egrat)
3240        Preg=Cpeg*Mueg/Keg
3245 !
3250        Mdot=FNFmcal(I,T(I+6),Pc(I))
3255        Veg=Mdot/(Rhoeg*Ax)
3260        Reeg=Veg*Di/Nueg
3265        Res=4*Mdot/(Mueg*(PI*Di-4*Delta))
3270        Qdot=Mdot*Cpeg*Delt
3275        Qdp=Qdot/Ao
3280        Lmtd=Delt/LOG((Tsat-T(I+6))/(Tsat-T(I+6)-Delt))
3285        Uo=Qdp/Lmtd
3286        IF Insert=0 THEN
3287        Bb1=.0668*(Di/L)*Reeg*Preg
3288        Bb2=1+.04*((Di/L)*Reeg*Preg)^.6666
3289        Omega=3.66+(Bb1/Bb2)
3290        END IF
3291        IF Insert=1 THEN
3293        Omega=(1+5.484E-3*Preg^.7*(Res/Hod)^1.25)^.5
3294        END IF
3295        IF Insert=2 THEN
3296        Omega=(Reeg^.65)*(Preg^.46)
3297        END IF
3298        IF Insert=3 THEN
3299        Omega=(Reeg^.76)*(Preg^.46)
3300        END IF
3302 !
3303 !      R-114/R113 Properties
3305        Hfg=FNHfg(Tsat)
3310        Kf=FNK(Tf)
3315        Rhof=FNRho(Tf)
3320        Muf=FNMu(Tf)
3325 !
3330        F=(Kf^3*Rhof^2*G*Hfg/(Muf*Do*Qdp))^.33333
3335        Ho=Alpa*F
3340        Two=Tsat-Qdp/Ho
3345        Tf=Tsat/3+2*Two/3
3350        Y=(1/Uo-Rm)*F
3355        X=Do*F/(Keg*Omega)
3360 !      PRINT "OMEGA=";Omega;"F=",F,"X=";X;"Y=";Y
```

154

```
3365        Xa(Jset)=X       !   INEFFICIENT (MODIFY LATER)
3370        Ya(Jset)=Y
3375        Sx=Sx+X
3380        Sy=Sy+Y
3385        Sxs=Sxs+X*X
3390        Sxy=Sxy+X*Y
3395        Jset=Jset+1
3400        IF Jset<Nsets THEN 3135
3405        ASSIGN @File TO *
3410        Slope=(Nsets*Sxy-Sx*Sy)/(Nsets*Sxs-Sx^2)
3415        Intcpt=(Sy-Slope*Sx)/Nsets
3420        Cic=1/Slope
3425        Alpac=1/Intcpt
3430        Cerr=ABS((C1-Cic)/Cic)
3435        Aerr=ABS((Alpac-Alpa)/Alpac)
3440        IF Cerr>.001 OR Aerr>.001 THEN
3445           Alpa=(Alpa+Alpac)*.5
3450           C1=(C1+Cic)*.5
3455    !      PRINT "CIC=";Cic;"ALPA=";Alpa
3460           GOTO 3100
3465        END IF
3470        BEEP
3475        BEEP
3480  . .   PRINTER IS 1
3485        PRINT "CIC=";Cic;"ALPA=";Alpa  .
3490        Cia(Insert)=Cic
3495        Alpaa(I)=Alpac
3500        PRINTER IS 701
3505        FOR J=0 TO Nsets-1     .
3510           OUTPUT @Xy;Xa(J),Ya(J)
3515        NEXT J
3520        PRINTER IS 1
3525     NEXT I
3530     ASSIGN @Xy TO *
3535     SUBEND
8270     DEF FNFmcal(T,Pc)
8280        Mdot15=.0019*Pc-.0098
8290        Mdot0=.00206*Pc-.00414
8300        Mdot24=.00225*Pc-.00329
8310     IF T<0 THEN
8311     Mdt=((T+15)*(Mdot0-Mdot15)/15)+Mdot15
8320     ELSE
8470     Mdt=(T*(Mdot24-Mdot0)/24)+Mdot0
8471     END IF
8480     RETURN Mdt
8490     FNEND
8500     DEF FNCosh(X)
8510     P=EXP(X)
8520     Q=EXP(-X)
8530     Cosh=.5*(P+Q)
8540     RETURN Cosh
8550     FNEND
```

LIST OF REFERENCES

1. *Montreal Protocol on Substances that Deplete the Ozone Layer, Final Act,* Montreal, Canada, United Nations Environment Program (UNEP), September 1987.

2. Federal Register, *Protection of Stratospehric Ozone; Final Rule,* 40 CFR Part 82, Vol. 53, No. 156, pp. 30566-30602, Washington, D.C., U.S. Environmental Protection Agency, August 12, 1988.

3. *Montreal Protocol on Substances that Deplete the Ozone Layer, Amendments and Adjustments,* London, England, United Nations Environment Program (UNEP), June 1990.

4. Zebrowski, D.S., *Condensation Heat Transfer Measurements of Refrigerants on Externally Enhanced Surfaces,* M.S. Thesis, Naval Postgraduate School, Monterey, California, September 1987.

5. Mabrey, B.D., *Condensation of Refrigerants on Small Tube Bundles,* M.S. Thesis, Naval Postgraduate School, Monterey, California, December 1988.

6. Mazzone, R.W., *Enhanced Condensation of R-113 on a Small Bundle of Horizontal Tubes,* Master's Thesis, Naval Postgraduate School, Monterey, California, December 1991.

7. Graetz, L., "Uber die Warmeleitungsfahigkeit von Flussigkeitn (On the Thermal Conductivity of Liquids), Part 1," *Ann. Phys. Chem.,* 18, 79-94 (1883); "Part 2," *Ann. Phys. Chem.,* 25, 337-357 (1885).

8. Nusselt, W., "Die Abhangigkeit der Warmeubergangszahl von der Rohrlange (The Dependence of the Heat-transfer Coefficient on the Tube Length)," *VDI Z,* 54, 1154-1158 (1910).

9. Shah, R.K., and London, A.L., *Laminar Flow Forced Convection in Ducts,* Academic Press, New York, 1978.

10. Incropera, F.P., and DeWitt, D.P., *Introduction to Heat Transfer,* 2nd Edition, John Wiley and Sons, New York, pp. 127-133, 1990.

11. Kays, W., and Crawford, M.E., *Convective Heat and Mass Transfer,* 2nd Edition, McGraw Hill Book Company, New York, 1980.

12. Schlichting, H., *Boundary Layer Theory*, 7th Edition, McGraw-Hill Book Company, New York, 1987.

13. Churchill, S.W., and Ozoe, H., "Correlations for Laminar Forced Convection with Uniform Heating in Flow Over a Plate and in Developing and Fully Developed Flow in a Tube," *J. Heat Transfer*, 95, 78-84, 1973.

14. Bergles, A.E., and Joshi, S.D., *Augmentation Techniques for Low Reynolds Number In-Tube Flow, Low Reynolds Number Flow Heat Exchanges*, ed. by Kakac, S., Shah, R.K., and Bergles, A.E., Hemisphere Publishing Company, pp. 695-720, 1983.

15. Hong, S.W. and Bergles, A.E., "Augmentation of Laminar Flow Heat Transfer in Tubes by Means of Twisted Tape Insert," *J. Heat Transfer*, vol. 98, no. 2, pp. 251-256, 1976.

16. Date, A.W., and Singham, J.R., *Numerical Prediction of Friction and Heat Transfer Characteristics of Fully-Developed Laminar Flow in Tube Containing Twisted Tape*, ASME Paper No. 72-HT-17, 1972.

17. Saha, S.K., Gatinoe, U.N., and Date, A.W., *Heat Transfer and Pressure Drop Characteristics of Laminar Flow in a Circular Tube Fitted with Regularly Spaced Twisted Tape Elements*, Experimental Heat Transfer, Fluid Mechanics and Thermodynamics, ed. by Shah, R.K., Ganic, E.N., and Yang, K.T., Elsevier Science Publishing Company, pp. 511-518, 1988.

18. Marner, W.J., and Bergles, A.E., "Augmentation of Tubeside Laminar Flow Heat Transfer by Means of Twisted-Tape Inserts, Static-Mixer Inserts and Internally Finned Tubes," *Heat Transfer 1978*, Proceedings of the Sixth International Heat Transfer Conference, vol. 2, pp. 583-588, Hemisphere Publishing Corp., Washington, D.C., 1978.

19. Gough, M.J., Rodgers, J.V., and Russel, G.M.B, "The Development of a Practical Answer to the Improvement of Tubeside Heat Transfer," *12th HTFS Res. Symposium.*, University of Warwick, United Kingdom, pp. 123-134, 1982.

20. Oliver, D.R., and Aldington, R.W.J., "Heat Transfer Enhancement in Round Tubes using Wire Matrix Turbulators: Newtonian and Non-Newtonian Liquids," *Chem. Eng. Res. Des.*, vol. 66, pp. 555-565, 1988.

21. Wolverine Technical Bulletin No. 4020, *Wolverine Korodense Tube*, Wolverine Tube Company, Decatur, Alabama, 1982.

22. Cragoe, C.S., *Properties of Ethylene Glycol and its Aqueous Solutions*, Cooperative Research Council, New York, Unpublished.

23. Gallant, R.W., *Ethylene Glycols, Physical Properties of Hydrocarbons*, Golf Publishing Co., Houston, Texas, Chapter 13, pp. 109-123, 1968.

24. Kline, S.J., and McClintock, F.A., "Describing Uncertainties in Single Sample Experiments," *Mechanical Engineering*, vol. 78, pp. 3-8, 1953.

INITIAL DISTRIBUTION LIST

No. Copies

1. Defense Technical Information Center   2
   Cameron Station
   Alexandria, Virginia 22304-6145

2. Library, Code 52   2
   Naval Postgraduate School
   Monterey, California 93943-5000

3. Professor Paul J. Marto, Code ME/Mx   2
   Department of Mechanical Engineering
   Naval Postgraduate School
   Monterey, California 93943-5000

4. Professor Stephen B. Memory, Code ME/Mr   1
   Department of Mechanical Engineering
   Naval Postgraduate School
   Monterey, California 93943-5000

5. Department Chairman, Code ME   1
   Department of Mechanical Engineering
   Naval Postgraduate School
   Monterey, California 93943-5000

6. Naval Engineering Curricular Office, Code 34   1
   Department of Mechanical Engineering
   Naval Postgraduate School
   Monterey, California 93943-5000

7. Mr. R. Helmick, Code 2722   1
   Annapolis Detachment, CD
   Naval Surface Warfare Center
   Annapolis, Maryland 21402-5067

8.   Mr. Bruce G. Unkel   1
      NAVSEA (CODE 56Y15)
      Department of the Navy
      Washington, D.C. 20362-5101

9.   LCDR Joseph D. Guido   1
      5846-D Mission Ctr. Rd.
      San Diego, California 92123

10.   Dr. William Guido   1
      9 Sophomore Lane
      Stoney Brook, New York 11790

11.   Mr. William Guido   1
      440 Park Blvd.
      Massapequa Pk., New York 11762

12.   Mr. William Melvin   1
      CMR 451, Box 25
      Shape Education Center
      APO, AE 09708